RAFT microemulsion polymerization with surface-active chain transfer agent

by

Ibrahim Adnan El-Hedok

A dissertation submitted to the graduate faculty

in partial fulfillment of the requirements for the degree of

DOCTOR OF PHILOSOPHY

Major: Chemical Engineering

Program of Study Committee:
Jennifer M. Heinen, Major Professor
Charles E. Glatz
Andrew C. Hillier
Eric W. Cochran
Michael Kessler
Malika Jeffries-EL

Iowa State University

Ames, Iowa

2013

TABLE OF CONTENTS

LIST OF FIGURES

LIST OF TABLES

ACKNOWLEDGEMENTS

I would like to start by thanking the most important people to me, my family. My parents have been always a source of encouragement throughout my entire life. My father has always made sure that I strive to achieve higher goal despite any hardship or pitfalls. I would like to thank my mother for patience and support during the past 9 years away from home. I would like to thank my wife Ihsan Zaatari for her sincere love, support, and motivation throughout these years despite the long hours, stress, and ups and downs that are part of every PhD. I would like to thank her for being an exemplary mother for our two years old daughter Samar. Thank you for being there for me.

I am very grateful to my major professor Jennifer Heinen for her patient mentoring and motivation. She was able to offer guidance while still providing the freedom to pursue my own ideas and learn from my own mistakes. She always tried to provide the opportunity for my professional development and gave multiple advices on choosing my career path. Thank you Dr. Heinen for everything and for the support needed to complete this project.

I would also like to thank all of the past and current members of the Heinen research group that have been wonderful research colleagues and friends. I would like to thank graduate student James Bergman for his useful and entertaining research discussions and his help in managing the labs. I would also like to thank undergraduate student Scott Meester for his assistance with experiments.

Finally, I want to express my thanks and appreciation to Dr. Charles Glatz, Dr. Andrew Hillier, Dr. Eric Cochran, Dr. Michael Kessler, and Dr. Malika Jeffries-EL for being members on my program of study committee.

CHAPTER 1. GENERAL INTRODUCTION

1.1 Motivation and General Background

Polymer nanoparticles (PNP) are becoming increasingly useful in a broad range of applications. Besides the conventional use of polymer latex in coatings and adhesives, PNP are of interest in many other applications such as electronics, drug delivery and pollution control. The field of PNP has attracted many researchers over the past decade. In 2010 alone over 20,000 publications concerning PNP has been published.[1] Researchers have looked into techniques that improve the control of the chemical structure, particle size and microstructure of the PNP. The synthesis of PNP can be done either by dispersing a preformed polymer into the form of nanoparticles or by directly polymerizing monomer in a dispersed system (e.g. heterogeneous techniques). The choice of synthesis route depends on the desired polymer characteristics and application. Microemulsion polymerization has the advantage of forming monodisperse colloidally stable particles in the size range of 10-100nm. The rate of polymerization in microemulsion is very rapid; however the process lacks control over molecular weight.

Reversible addition-fragmentation chain transfer (RAFT), a controlled/living radical polymerization technique, is successful in producing low polydispersity polymers with predetermined molecular weight.[2] The essence of RAFT relies on a chain transfer agent (CTA) which mediates the activity of a polymerizing radical. The CTA has a stable Z group and a cleavable R group. The mechanism of RAFT begins with the reaction of the propagating polymer chain (P•) with the CTA molecule (XR), which forms a dormant polymer (PX) and a new radical (R•),

$$P\bullet + XR \rightarrow PX + R\bullet \qquad (1.1)$$

The R• radical reacts with monomer to initiate an active polymer chain (P•). Active (P•) and dormant (XP) polymer chains react to form a macroRAFT intermediate radical (PX•P) which then fragments to release either chain for further propagation,

$$P_m \bullet + XP_n \leftrightarrow P_m X \bullet P_n \leftrightarrow P_m X + P_n \bullet \quad (1.2)$$

The equilibrium reaction between active and dormant polymers provides an equal opportunity for the chains to grow while minimizing radical-radical termination, which achieves low molecular weight polydispersity index (PDI). The number average molecular weight of the polymers can be predetermined by the ratio of monomer to CTA concentration.

The implementation of RAFT in microemulsion polymerization to produce PNP has been proven to be feasible.[3-6] However, several challenges hinder the degree of RAFT control in microemulsion polymerization. O'Donnell and Kaler [6] have identified the key parameters that determine control in RAFT microemulsion polymerization as the CTA solubility, and the initial CTA per micelle ratio. It has been shown that the diffusion of CTA during polymerization from uninitiated micelles to growing polymer particles causes the particles to have a broad range of RAFT reaction conditions over the course of polymerization and broadens the CTA per particle ratio. Such effects lead to the observed high molecular weight polydispersity index (PDI>1.4).

1.2 Dissertation Organization and Summary

The main goal of this research is to improve control in RAFT microemulsion polymerization in order to achieve predetermined molecular weight with narrow molecular weight polydispersity. The hypothesis is that the use of an amphiphilic CTA (surface-active CTA) will confine the CTA to the surface of the particle and thermodynamically favor partitioning of the CTA between micelles and particles throughout the polymerization. Thus, the

CTA diffusion from micelles to polymer particles would be minimized and the breadth of the CTA per particle distribution would remain low.

The first objective of this research aims to implement the use of a surface-active CTA in the microemulsion polymerization, and identify the critical parameters for achieving good RAFT control. This is done by investigating the performance of a surface-active CTA (B11T) against a similar traditional hydrophobic CTA (B11C). The chemical structure and names of the chain transfer agents are shown in **Figure 1.2.1**. **CHAPTER 2** summarizes the relevant background and literature review pertaining to the RAFT and microemulsion polymerization, while **CHAPTER 3** describes the experimental methods used in this research.

In **CHAPTER 4** the polymerization kinetics, polymer characteristics and latex size in the RAFT microemulsion of n-butyl acrylate (BA) are presented. The polymerization rate decreases as the CTA/micelle ratio increased for both CTAs due to rate retardation caused by higher CTA/particle ratio. The B11T CTA demonstrates superior RAFT control over the B11C CTA, although the polydispersity from the B11T polymerizations remains above 1.4. The molecular weight and PNP size analysis indicate that the B11T remains partitioned between the micelles and polymer particles throughout the polymerization.

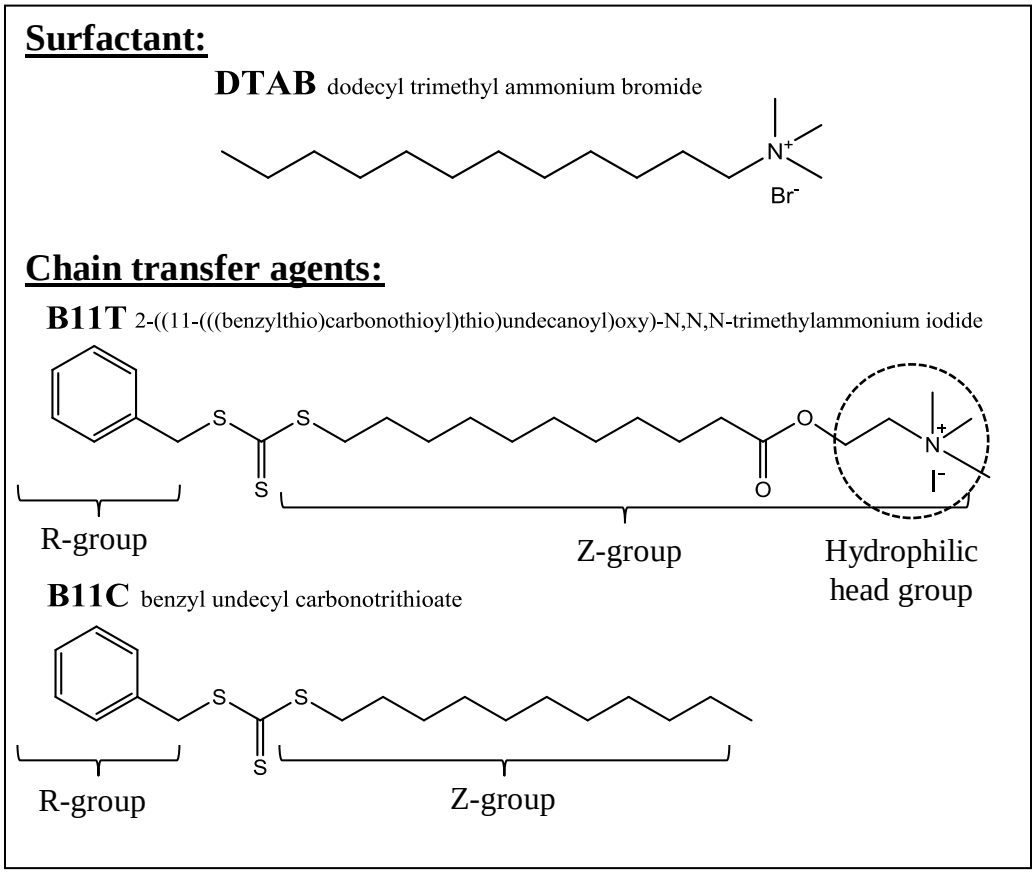

Figure 1.2.1: Chemical structure of the surfactant (DTAB), surface-active chain transfer agent (B11T), and traditional chain transfer agent (B11C).

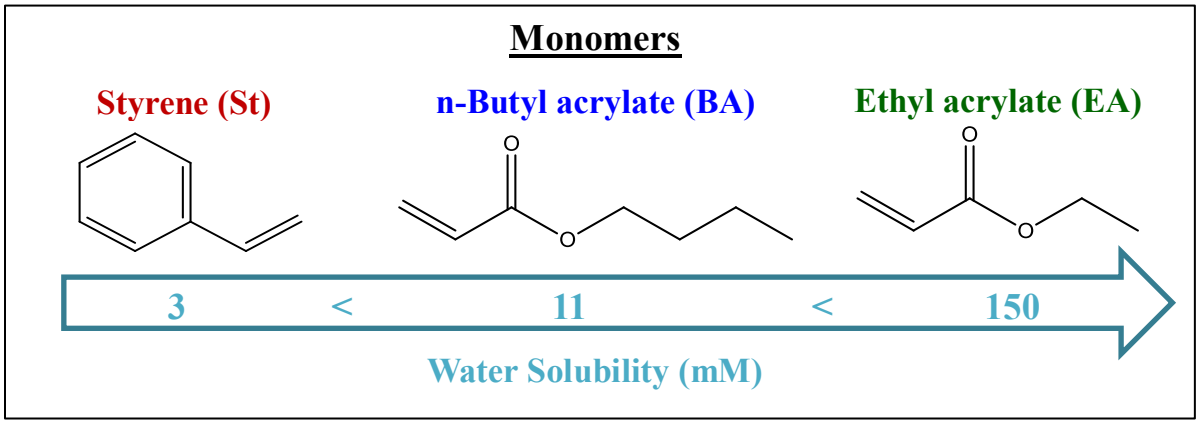

Figure 1.2.2: Chemical structure and water solubility of the monomers used in this research.

CHAPTER 5 examines the effect of the monomer water solubility on the RAFT microemulsion polymerization with B11T and B11C by investigating a more hydrophobic monomer styrene (St) and a more hydrophilic monomer ethyl acrylate (EA). The concentration of larger particles increases with the monomer water solubility and polarity due to coalescence. The degree of rate retardation is proportional to the water solubility of the monomer, due to higher CTA/particle ratio as the water solubility increases. Good RAFT control is achieved for all B11T RAFT microemulsion polymerization, with evidence that the surface-active CTA remains partitioned between micelles and particles. The polydispersity of the poly(St) and poly(EA) is around the desired value of 1.1 at B11T/micelle ratios equal to or greater than 1.1. Hence, monomer solubility dose not adversely affect the polymerization control. The St RAFT microemulsion polymerization with the traditional CTA B11C shows higher molecular weight polydispersity compared to the polymerizations with the surface-active CTA B11T. Whereas in EA RAFT microemulsion polymerization, the B11C lacks control over the polymerizations at lower B11C/micelle ratios (<1.1) and phase separation is observed at higher B11C/micelle ratios.

In **CHAPTER 6**, the polymerization rate of the RAFT microemulsion polymerizations with the traditional and surface-active CTAs (Chapter 4 and 5) are fitted with O'Donnell's kinetic model[7] for RAFT microemulsion polymerization to obtain the RAFT kinetic parameters, i.e. fragmentation and CTA activation rates. The model fits indicates slow fragmentation of the MacroRAFT intermediate radical and demonstrate partial consumption of the surface-active CTA, which corresponds with the experimental findings.

The second objective of this research aims to use the fundamental understandings from the first part to exploit the use of the surface-active CTA in synthesizing core/shell polymer nanoparticles (**CHAPTER 7**). It is expected that the amphiphilic moiety in B11T would restrict

the polymerization growth to the surface of the particle, as illustrated in **Figure 1.2.3**, which provides three main advantages to the use of surface-active CTA in core/shell synthesis:

- Formation of block co-polymers with subsequent second monomer addition instead of discrete homopolymers.
- Polymer propagation is constrained to the corona of the particle facilitating polymer shell formation.
- Prevention of potential phase inversion by introducing an energetic penalty for transferring the surface-active moiety to the core of the particle.

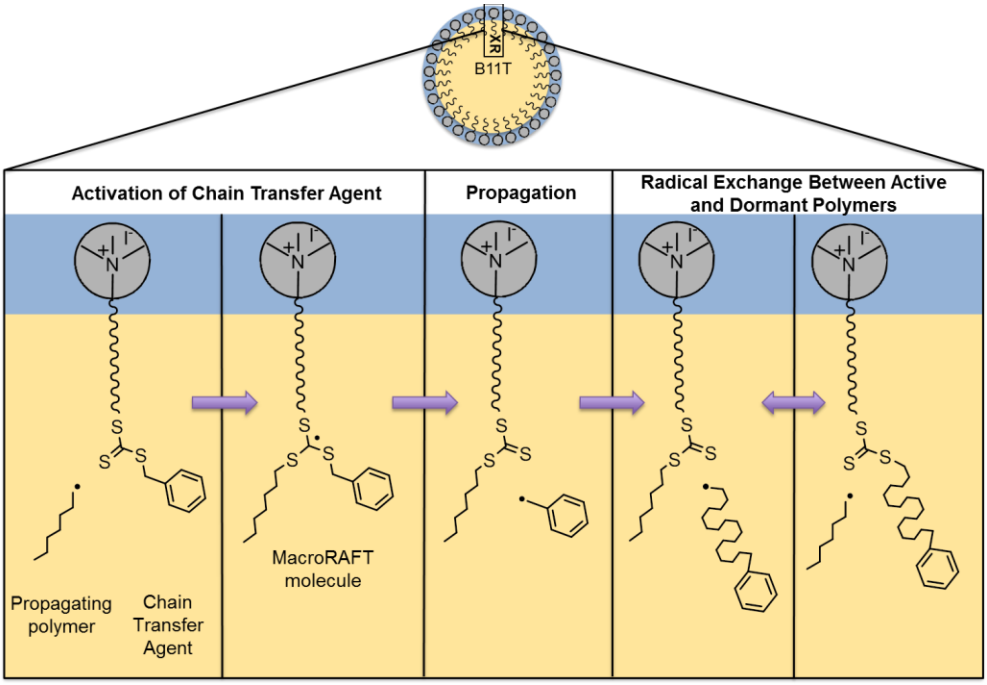

Figure 1.2.3: Reversible fragmentation-addition chain transfer mechanism inside a growing polymer particle.

Such advantages shall permit the production of core/shell polymer of new compositions and structures that can be practical for a desired range of mechanical and chemical properties.

CHAPTER 7 examines the semi-continuous microemulsion polymerization (SCMEP) as a synthesis method for core/shell PNP. The SCMEP begins with a first-stage batch seed polymerization followed by a second-stage continuous second monomer feed. In the first section, the polymerization kinetics and latex characteristics of St/BA & BA/St uncontrolled SCMEP are investigated. The polymerization rate during second-stage reaches steady state under all feed rates studied. The St/BA uncontrolled SCMEP shows an increase in polymerization rate after a critical BA conversion (~23% conversion), which is attributed to the shift in the locus of polymerization from core to shell. The TEM imaging of the latex shows core/shell formation with poly(St) in the core and poly(BA) in shell, regardless of polymerization sequence. In the second section, the St/BA RAFT SCMEP with the surface-active CTA B11T is investigated. The continuously added BA monomer must swell the seed polymer particles and react with the dormant poly(St) chains as opposed to entering empty micelles and activating more chain transfer agents. The effect of BA feed rate on the kinetics, polymer properties and latex characteristics are presented. Under starved monomer feed conditions, the polymerization rate reaches steady state and only shell block copolymers are formed without secondary particle nucleation. The RAFT control was maintained throughout the second-stage polymerization with final polydispersity of 1.1. Therefore, the RAFT SCMEP with B11T is successful in producing well-defined core/shell PNP under the right feeding conditions.

1.3 Bibliography

1. Rao, J. P.; Geckeler, K. E. *Progress in Polymer Science* **2011,** 36, (7), 887-913.

2. Chiefari, J.; Chong, Y. K.; Ercole, F.; Krstina, J.; Jeffery, J.; Le, T. P. T.; Mayadunne, R. T. A.; Meijs, G. F.; Moad, C. L.; Moad, G.; Rizzardo, E.; Thang, S. H. *Macromolecules* **1998,** 31, (16), 5559-5562.

3. Liu, S.; Hermanson, K. D.; Kaler, E. W. *Macromolecules* **2006,** 39, (13), 4345-4350.

4. O'Donnell, J. M. Reversible addition-fragmentation chain transfer in microemulsion polymerizations. Dissertation, University of Delaware, Newark, Delaware, 2007.

5. Hermanson, K. D.; Liu, S.; Kaler, E. W. *Journal of Polymer Science Part A: Polymer Chemistry* **2006,** 44, (20), 6055-6070.

6. O'Donnell, J.; Kaler, E. W. *Macromolecules* **2010,** 43, (4), 1730-1738.

7. O'Donnell, J. M.; Kaler, E. W. *Journal of Polymer Science Part A: Polymer Chemistry* **2010,** 48, (3), 604-613.

CHAPTER 2. BACKGROUND AND LITERATURE REVIEW

2.1 Reversible Addition-Fragmentation Chain Transfer Polymerization

Free radical polymerization is the synthetic pathway of approximately 50% of industrial polymers. The advantage of radical polymerization is the fast chain growth, convenient reaction conditions, and wide production methods (solution, bulk, suspension, dispersion). However, large molecular weight polydispersity is typically obtained in free radical polymerization, mainly due to unavoidable termination reactions. Controlled or "living" radical polymerizations (CLRP) are methods for achieving predetermined molecular weight with near monodispersity.[1] The livingness in CLRP relies on minimizing the chain breaking reactions, i.e. termination and transfer, and simultaneous growth of all chains. This is achieved through the use of dormant species would reversibly react with the growing chains. Common CLRP techniques are atom transfer radical polymerization (ATRP),[2, 3] nitroxide-mediated polymerization (NMP),[4] and reversible addition-fragmentation chain transfer (RAFT).[5]

RAFT has been proven to be a successful controlled/"living" radical polymerization technique that works with a wide range of monomers. Since the first RAFT publication in 1998 by Chiefari et al.,[5] the RAFT method has been investigated for its mechanism, kinetics and applicability.[6] In principle, the RAFT mechanism is believed to have a chain transfer agent activation and equilibration reactions in addition to the ordinary initiation, propagation, and termination reactions that occur in the conventional radical polymerization (**Figure 2.1.1**).

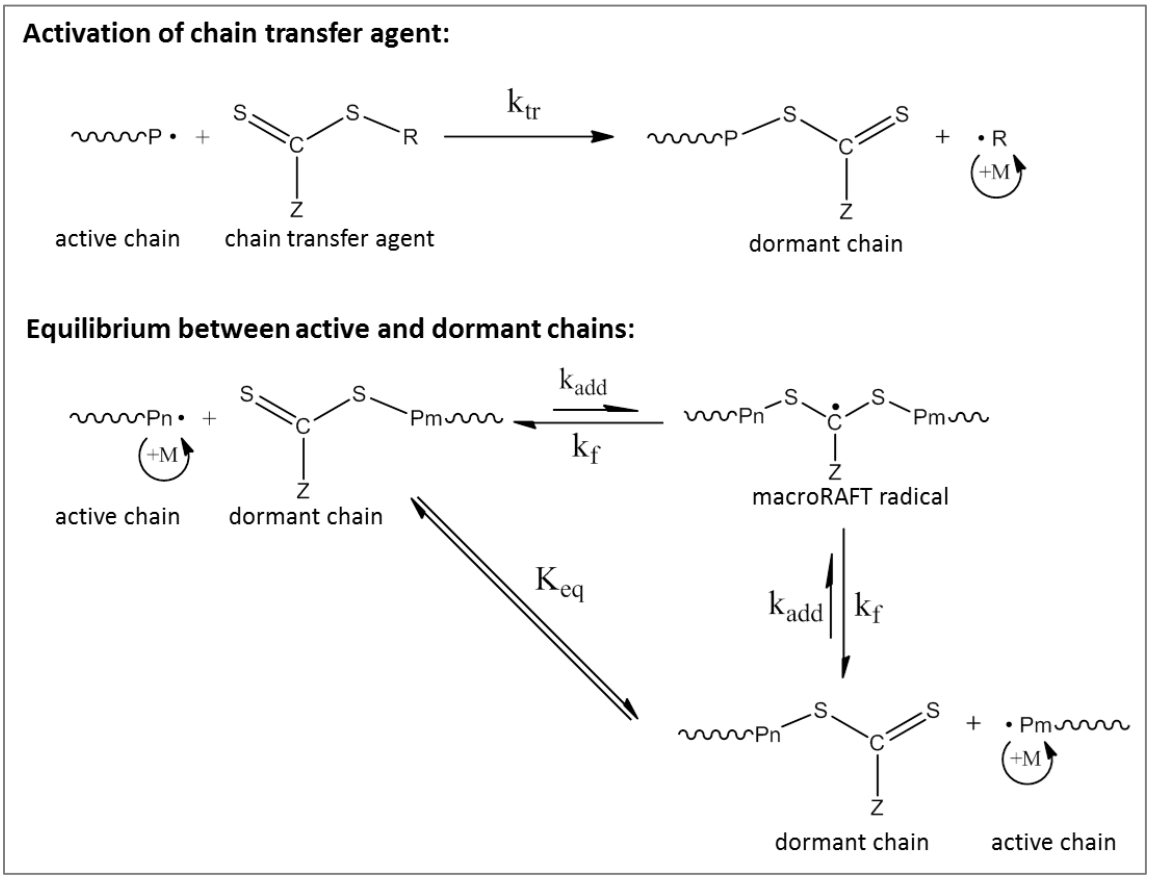

Figure 2.1.1: Mechanism of RAFT polymerization as proposed by Chiefari et al.[5] Reproduced and modified from reference [1].

The RAFT agent, or chain transfer agent (CTA), consists of a reactive thiocarbonyl group (C=S) (i.e. typically a dithioester, trithiocarbonate or xanthates), a R-group, and a Z-group. The requirement for choosing the R-group is that the S-R bond is weaker than the C-Z bond, hence Z-group should be more stable. Moreover, R• should be more stable than P• for the reaction to proceed in the forward direction.[7]

The functionality of the CTA comes from the C=S bond which reacts with the propagating chain. The CTA then fragments into a radical containing R-group and a dormant polymer chain capped with the thiocarbonyl group, also called macro-RAFT. The R-group continues to react with the surrounding monomer forming another propagating polymer chain.

Active and dormant polymer chains react to form a macroRAFT intermediate radical which then fragments to release either chain for further propagation. The equilibrium reaction between active and dormant polymers provides an equal opportunity for the chain to grow while minimizing radical-radical termination, which achieves low molecular weight polydispersity (PDI<1.2).

The number of chain transfer chain agents determines the number of polymer chains. In an ideal RAFT reaction, the number average molecular weight (M_N) increases linearly with conversion according to the following equation:

$$M_N = \frac{C_{mon,o} MW_{mon} f}{C_{RAFT,o}} \qquad \text{(eq 2.1)}$$

where $C_{mon,o}$ is the initial monomer concentration, MW_{mon} is the monomer molecular weight, $C_{RAFT,o}$ is the initial chain transfer concentration, and f is the conversion. This equation is used to predict the final molecular weight of the polymer chains with f = 1, and to confirm control of the polymerization by plotting M_N vs f.

In order for the RAFT process to work effectively, certain parameters are required to be above certain limits. For instance, the concentration of CTA must be higher than the concentration of initiator. A typical CTA/initiator ratio is 10:1. This maintains a high concentration of dormant polymer chain over the propagating chains, which in turns reduces termination reactions and favors constant rate of propagation. Moreover, the activation of the chain transfer agent (k_{tr}) should be relatively rapid in order to capture the radical activity. The guideline for the selection of the proper R and Z groups according to monomer types has been outlined by Moad et al.[6]

In an ideal RAFT polymerization the exchange of radical activity is rapid relative to the rate of propagation so the kinetics are unaffected. However, typical RAFT experiences reduction in the polymerization rate relative to the conventional radical polymerization. There are two main theories on the origin of rate retardation: (1) slow fragmentation (low k_{frag}) of the CTA due to the long-lived intermediate macro-RAFT radicals,[8, 9] and (2) cross-termination of the CTA intermediate radicals.[10, 11] The retardation effect increases significantly with higher CTA concentrations, which is required for obtaining low molecular weight polymers.

2.2 Microemulsion Polymerization

The microemulsion polymerization technique is a useful method to produce colloidally stable polymer nanoparticles (30-100nm). The oil-in-water microemulsion system consists of monomer swollen micelles in a continuous aqueous medium. It differs from the (mini)emulsion techniques by being thermodynamically stable through having a higher surfactant concentration which leads to formation of much smaller monomer-swollen micelles.

Microemulsion is visually characterized as a single phase transparent solution, and it is dependent on the temperature and concentration of the ternary components as characterized by γ and α values where $\alpha=mass_{oil}/(mass_{oil}+mass_{water})\times100$ and $\gamma=mass_{surfactant}/(mass_{surfactant}+mass_{oil}+mass_{water})\times100$. Variation of temperature and α would change the solution from two phases (Φ) to one Φ region as shown in **Figure 2.2.1**.

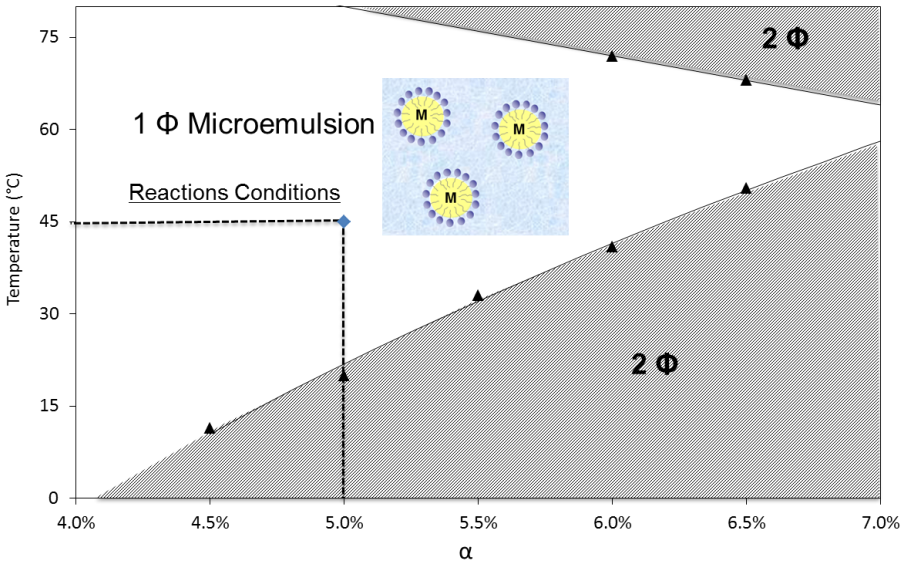

Figure 2.2.1: The phase diagram for n-butyl acrylate/DTAB/H_2O at γ=12%.

The microemulsion polymerization is typically initiated using a thermally decomposing radical initiator. In the case of water-soluble initiator (I), initiation begins in the aqueous medium where I• reacts with the small amount of monomer that is soluble in water. Upon reaching a critical degree of polymerization the chain enters a monomer swollen micelle and forms a particle. Throughout the microemulsion polymerization, the number of micelles is around 1000 times greater than the number of polymer particles. Hence monomer diffusion occurs between the uninitiated micelles and growing polymer particles.

The compartmentalized nature of microemulsion polymerization induces fast polymerization rates due to negligible bi-radical termination and high concentration of monomer inside micelles. Morgan and Kaler[12] developed a simple model to calculate the uncontrolled microemulsion polymerization kinetics using the fundamental second order rate equation:

$$\frac{df}{dt} = \frac{k_p C_{mon}^{(part)} N^*}{M_o} \qquad \text{(eq 2.2)}$$

where k_p is the propagation rate constant, $C_{mon}^{(part)}$ is the concentration of monomer at the locus of polymerization, N* is the concentration of propagating radicals, and M_o is the initial concentration of monomer in microemulsion.

Assuming negligible biradical termination, N* is directly related to the amount of radicals formed by the thermal decomposition of the initiator, which increases linearly with time. Thus,

$$N^* = 2\gamma k_d I_0 t \qquad \text{(eq 2.3)}$$

where γ is efficiency of initiation, k_d is the dissociation constant, I_0 is the initial concentration of initiator in the microemulsion and t is the reaction time.

Monomer partitions between the micelles and polymer particles during microemulsion polymerization in one of two ways; the first possibility is that the monomer depletes from the micelles and swells the polymer particles earlier in the polymerization, whereas the second possibility is that the monomer remains partitioned between the micelles and polymer particles and, hence, diffuses throughout the polymerization. The underlying monomer transport is determined by equilibrium thermodynamics,[13-15] thus if the monomer is fairly soluble in the polymer then swelling the polymer particle at earlier stages would be dominant. On the other hand, if the monomer is less soluble in the polymer, then monomer diffusion over the course of polymerization is maintained and a monomer swelling of the surfactant tails would be formed at the growing polymer particle. In the case of n-butyl acrylate and styrene microemulsion polymerization, it was verified that the monomer diffuses throughout the polymerization using small-angle neutron scattering.[14, 16, 17]

Whichever maybe the case, the concentration of monomer at the locus of polymerization $C_{mon}^{(part)}$ decreases linearly as a function of conversion:

$$C_{mon}^{(part)} = C_{mon,0}^{(part)}(1-f) \qquad \text{(eq 2.4)}$$

where $C_{mon,0}^{(part)}$ is the initial concentration of monomer at the locus of polymerization and *f* is the fractional conversion. With the assumption of negligible biradical termination and linear monomer partitioning (eq 2.3 & 2.4 in eq 2.2), the final Morgan model is:

$$\frac{df}{dt} = \frac{2k_p k_d C_{mon,0}^{(part)}(1-f)I_0 t}{M_o} \qquad \text{(eq 2.5)}$$

The model predicts a maximum conversion rate at 39% conversion irrespective of the rate constants or initial monomer and initiator concentrations. In case a different location of the rate maximum is observed experimentally, this model becomes useful in assessing the above assumptions. Previous studies have shown that a shift to lower conversions may occur due to non-linear monomer partitioning which is semi-empirically described in a modified form of eq 2.4:

$$C_{mon}^{(part)} = C_{mon,0}^{(part)}(1-f)^b \qquad \text{(eq 2.6)}$$

where b is the non-linearity power factor. b is determined to range from 1 (linear) to a maximum value of 1.4, as observed in the hexyl methacrylate, butyl methacrylate and styrene microemulsion polymerizations [14].

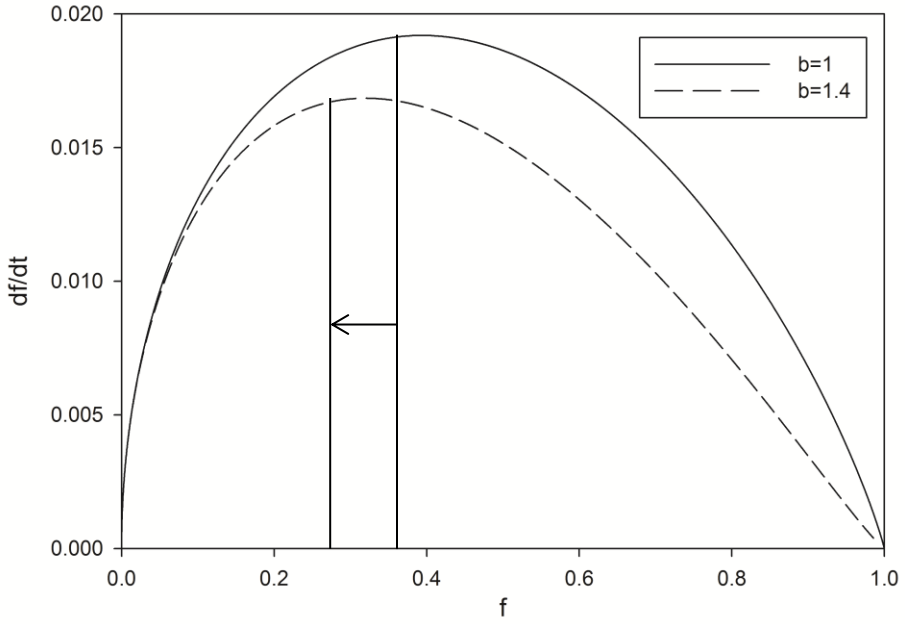

Figure 2.2.2: The effect of non-linearity in monomer partitioning (eq 2.6) on the rate of conversion prediction by the Morgan model. The Morgan model predicted rate maximum at f = 0.39 shifts to a lower f = 0.30 under the effect of non-linearity (b>1).

As shown the in the above figure, the location of the rate maximum may shift downward to as low as 30% conversion due to non-linear monomer partitioning. Biradical terminations have been shown to have a similar effect on shifting the location of the rate maximum to even lower conversions.[15] The biradical terminations were kinetically described by de Vries and coworkers[15] by assuming that instantaneous polymer particle termination occurs when a aqueous phase radical enters an actively propagating polymer particle. The source of the aqueous phase radical can be either initiator-derived (first term in eq. 2.7) or monomer radicals derived from chain transfer to monomer (second term in eq. 2.7), according to the following equation:

$$\frac{dN^*}{dt} = 2\gamma k_d I_o \left(\frac{1 - p_{term}/p_{prop}}{1 + p_{term}/p_{prop}} \right) - 2k_{tr}^{mono} C_{mon}^{(part)} N^* \left(\frac{p_{term}/p_{prop}}{1 + p_{term}/p_{prop}} \right) \qquad \text{(eq 2.7)}$$

where k_{tr}^{mono} is the rate constant for radical transfer from the polymer to the monomer, and the probability of polymer particle termination (p_{term}) is described to be inversely proportional to the characteristic residence time (τ_{res}) of the "typical" aqueous phase radical that causes termination:

$$\frac{p_{term}}{p_{prop}} = \frac{N^*}{\tau_{res} k_p C_{mon}^{(part)} N_{mic}} \qquad \text{(eq 2.8)}$$

where N_{mic} is the concentration of micelles in the microemulsion.

2.3 Reversible Addition-Fragmentation Chain Transfer Microemulsion Polymerization

In RAFT microemulsion polymerization, the monomer and chain transfer agent that are in excess of the aqueous solubility threshold swell the micelles. The proposed RAFT process in microemulsion is outlined in **Figure 2.3.1**.

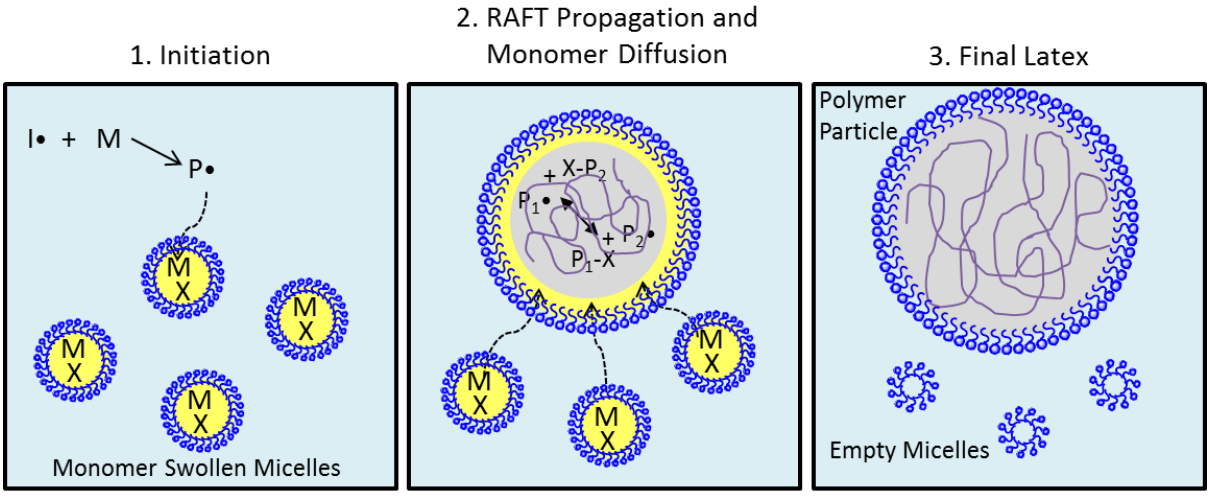

Figure 2.3.1: The proposed RAFT microemulsion polymerization process. M: monomer, X: chain transfer agent, I•: initiator, P•: propagating polymer, XP: dormant polymer.

For initiation, the aqueous initiator reacts with the monomer in the aqueous phase and then diffuses into a micelle upon reaching a critical degree of polymerization. Once the micelle is initiated, the micelle begins to grow as a polymer particle. The propagating chain inside the particle reacts with CTA leading to RAFT activation and subsequent control mechanism within the particle. Over the course of polymerization, the monomer and CTA diffuses from uninitiated micelles to the growing particles. The diffusion of CTA is necessary to activate all the CTA and achieve the predetermined molecular weight. However, since the CTA diffuses continuously, the CTA/particle ratio vary over the polymerization time, which causes the particles to experience a broad range of reaction conditions.[17] At the end of polymerization, the final solution consists of colloidally stable polymer nanoparticles and empty micelles.

Previous research by Liu et al. have shown that the RAFT can be implemented in the microemulsion polymerization of n-hexyl methacrylate.[18] It was observed that the polymerization had good control when the CTA/micelle ratio was above one. Moreover, by increasing the concentration of CTA the conversion rate experienced higher retardation which is typical in RAFT homogenous polymerization. Later on, Hermanson et al.[19] developed a kinetic model for the RAFT microemulsion polymerization. The Hermanson model is a population balance model that accounts for the concentration of all species at all times, which can predict the reaction rates, molecular weight average and polydispersity, and particle size. The Hermanson model was applied for the n-hexyl methacrylate polymerizations of Liu et al., and it was inferred that, at low CTA, the rapid increase in reaction rate at higher conversions is evidence of less controlled polymerization due to the lack of CTA. At higher CTA, the secondary increase in rate effect is diminished as shown by the model[19] and experimentally.[18]

Recent work by O'Donnell has studied the effect of monomer and chain transfer agent solubility on the RAFT control in microemulsion.[16, 17, 20, 21] The RAFT microemulsion polymerization of butyl acrylate and 2-ethylhexyl acrylate monomers have shown good degree of molecular weight control with the chain transfer agent methyl-2-(O-ethylxanthyl)-propionate (MOEP). The polymerizations reached 100% conversions and the final molecular weight was near the predicted values, which indicated activation of all chain transfer agent, whereas the molecular weight polydispersity (PDI) remained high for most of the controlled polymerizations (PDI>1.3). On the other hand, the RAFT microemulsion polymerizations of butyl acrylate with a low aqueous solubility chain transfer agent methyl-2-(O-dodecylxanthyl)-propionate (MODP) have revealed poor molecular weight control showing a multimodal molecular weight distribution [20].

Moreover, O'Donnell's work has shown a shift in the location of the maximum conversion rate toward lower conversion (<30%) as the CTA/micelle increased for the RAFT microemulsion polymerizations with MOEP, whereas the location remained similar for the RAFT microemulsion polymerizations with MODP. O'Donnell [21] has developed a kinetic model to capture to observed kinetic rate profiles, which offer a simpler evaluation of the reaction rate compared to the computationally expensive Hermanson model. The model is based on the introduction of a radical activity fraction (x_{act}) to the fundamental rate equation (eq 2.2):

$$\frac{df}{dt} = \frac{k_p C_{mon}^{(part)} N^* x_{act}}{M_o} \qquad \text{(eq 2.9)}$$

The x_{act} relates the time fraction a radical spends in active propagation, since the radical spends a portion of its lifetime as a dormant (inactive) macroRAFT radical. Hence the value of x_{act} is:

$$\langle x_{act} \rangle = \frac{\langle t_{act} \rangle}{\langle t_{act} \rangle + \langle t_{dorm} \rangle} \quad \text{(eq 2.10)}$$

where < > designates the ensemble average as the value is averaged over the particles in the polymerizing microemulsion, $<t_{act}>$ is the average time that a particle is in that active state and $<t_{dorm}>$ is the average time that a particle remains in the dormant state. The time a particle spends in the dormant state is inversely proportional to the fragmentation rate constant (k_f):

$$\langle t_{dorm} \rangle = \frac{1}{2k_f} \quad \text{(eq 2.11)}$$

and t_{act} is

$$\langle t_{act} \rangle = \frac{N_A \langle V_{part} \rangle}{k_{add} \langle [XP]_{part} \rangle} \quad \text{(eq 2.12)}$$

where $\langle V_{part} \rangle$ is the volume of the locus of polymerization in the particle, k_{add} is addition rate constant, N_A is the Avogadro's number, and $[XP]_{part}$ is the concentration of the macroRAFT in the particle:

$$\langle [XP]_{part} \rangle = \frac{[XR]_0 - [XR]}{[Particles]} \quad \text{(eq 2.13)}$$

where [Particles] is the concentration of particle in the microemulsion which is estimated as the number of initiated radical, and $[XR]$ is the CTA concentration and its consumption is defined by:

$$\frac{d[XR]}{dt} = -k_{tr}[XR]N^* x_{act} \quad \text{(eq 2.14)}$$

O'Donnell model have adjusted the de Vries model[15] for biradical termination in order to include the fraction of active radicals and radical exit due to R-group release:

$$\frac{dN^*}{dt} = 2\gamma k_d I_o \left(\frac{1 - p_{term}/p_{prop}}{1 + p_{term}/p_{prop}} \right) - 2\left(k_{tr}^{mono} C_{mon}^{(part)} + k_{tr} C_{XR}^{(part)}\right) N^* x_{act} \left(\frac{p_{term}/p_{prop}}{1 + p_{term}/p_{prop}} \right) \quad \text{(eq 2.15)}$$

where $C_{XR}^{(part)}$ is the concentration of the chain transfer agent in the particle, and

$$\frac{p_{term}}{p_{prop}} = \frac{N^* x_{act}}{\tau_{res} k_p C_{mon}^{(part)} N_{mic}} \qquad \text{(eq 2.16)}$$

The advantage of the O'Donnell model is that kinetic data can be fit by adjusting only k_f and rate of diffusion. The summary of the effect of the k_f and CTA diffusion is presented in the following table.

Table 2.3.1: The change in the magnitude and location of the rate maxima as the CTA/micelle increases, as predicted by the O'Donnell model for the BA RAFT microemulsion polymerization with MOEP.[21]

	Reaction-limited CTA activation	Diffusion-limited CTA activation
Slow fragmentation, k_f	Decreasing No shift, ~50% conversion	Decreasing No shift, ~30% conversion
Fast fragmentation, k_f	Decreasing Shift to higher conversions	Decreasing Shift to lower conversions

Aided with data from small-angle neutron scattering,[22] O'Donnell have fit the model for the experimental kinetic data of the BA RAFT microemulsion polymerizations with MOEP and was able to capture the observed shift in the location of the rate maxima to lower conversions as the MOEP/micelle increases.[21] According to the model, this confirms that the shift in the location of rate maxima is as a result of the CTA diffusion during polymerization from uninitiated micelles to growing polymer particles. Due to CTA diffusion, the RAFT rate retardation effect increases over time which leads to longer reaction times and maximum conversion rate at lower conversions. This was apparent with the more soluble CTA, MOEP, which fully diffuses during polymerization, whereas the low solubility CTA, MODP, partially diffuses.

Although the chain transfer agent diffusion is necessary to activate all the CTA and reach the predetermined molecular weight value, the diffusion process during the polymerization brings a variation in reaction conditions inside the growing polymer particle which leads to higher molecular weight polydispersity.[17]

2.4 Surface-Active Chain Transfer Agent in RAFT Emulsion Polymerization

In the literature, there are few examples of surface-active chain transfer agent application for RAFT emulsion polymerization.[23-28] The surface-active CTAs in all of the reported cases have been used to improve the RAFT control, by localizing the polymerization growth, and enhance the colloidal stability of the latex, by replacing all of the surfactant with the surface-active CTA. Shim et al.[23] have used a UV-initiated dithiobenzoyl surface-active CTA, having a benzoic hydrophobic compound and a carboxylate as the hydrophilic entity. This CTA has demonstrated linear molecular weight increase with methyl methacrylate at conversions above 50% (molecular weight below 50% conversion was not obtained), which indicates living-radical polymerization. However, the molecular weight polydispersity was relatively high (PDI= 1.21 to 1.43), which was attributed to RAFT agent degradation over time due to UV radiation.

Ferguson et al.[27, 28] and Rieger et al.[26] have applied the surface-active CTA in emulsion polymerization. The polymerization consisted of two steps; the first step is the reaction of the CTA with a more hydrophilic monomer which then forms micelle structure; and the second step is the continuous feed of a hydrophobic monomer to grow the micelle under RAFT conditions. Both studies have shown good linear molecular weight growth as a function of conversion. Ferguson et al. have used five acrylic acid monomer units as the hydrophilic block with the CTA to form the micelle structure, and then further added butyl acrylate or methyl methacrylate monomer for particle growth. The polydispersity increased with the conversion of the added

monomer until it reach high polydispersity (PDI= 1.50-2.61). Ferguson et al. attributed the PDI increase to the transfer of the inactivated CTA in the aqueous phase and coagulation of particles at early stages.[27]

Rieger et al.[26] used a much larger hydrophilic block (47 ethylene oxide monomer units) to form the initial micelle structure and then added butyl acrylate or styrene. The polymerizations have shown excellent RAFT control with linear molecular weight growth and near predicted molecular weight values. Moreover, the polydispersity of styrene (1.16) was lower than that of BA (1.21-1.41). Although this method achieved favorable RAFT control features, the use of a long PEO chain may be undesired as it alters the desired properties of the polymer particle. In addition, the particle size obtained with this method is at least 200 nm, thus not suitable for producing smaller particles.

The above reported studies have attached the surface-active moiety to the R-group of the CTA which leads to chain propagation toward the particle core. Z-group attachment of the surface-active moiety, as selected in this research, would be desired to maintain the polymer chain growth at the corona of the particle with the fresh monomer diffusion during microemulsion polymerization. Moreover, the location of the CTA at the particle's surface permits added post-functionalization.

2.5 Bibliography

1. Matyjaszewski, K., Radical Polymerization. In *Controlled and Living Polymerizations*, Müller, A. H. E.; Matyjaszewski, K., Eds. Wiley-VCH Verlag GmbH & Co. KGaA: Weinheim, 2009; pp 103-166.

2. Wang, J.-S.; Matyjaszewski, K. *J Am Chem Soc* **1995,** 117, (20), 5614-5615.

3. Kato, M.; Kamigaito, M.; Sawamoto, M.; Higashimura, T. *Macromolecules* **1995,** 28, (5), 1721-1723.

4. Georges, M. K.; Veregin, R. P. N.; Kazmaier, P. M.; Hamer, G. K. *Macromolecules* **1993,** 26, (11), 2987-2988.

5. Chiefari, J.; Chong, Y. K.; Ercole, F.; Krstina, J.; Jeffery, J.; Le, T. P. T.; Mayadunne, R. T. A.; Meijs, G. F.; Moad, C. L.; Moad, G.; Rizzardo, E.; Thang, S. H. *Macromolecules* **1998,** 31, (16), 5559-5562.

6. Moad, G.; Rizzardo, E.; Thang, S. H. *Aust. J. Chem.* **2009,** 62, (11), 1402-1472.

7. Coote, M. L.; Krenske, E. H.; Izgorodina, E. I. *Macromolecular Rapid Communications* **2006,** 27, (7), 473-497.

8. Feldermann, A.; Coote, M. L.; Stenzel, M. H.; Davis, T. P.; Barner-Kowollik, C. *J Am Chem Soc* **2004,** 126, (48), 15915-15923.

9. Barner-Kowollik, C.; Quinn, J. F.; Morsley, D. R.; Davis, T. P. *J. Polym. Sci. Pol. Chem.* **2001,** 39, (9), 1353-1365.

10. Wang, A. R.; Zhu, S. *Journal of Polymer Science Part A: Polymer Chemistry* **2003,** 41, (11), 1553-1566.

11. Monteiro, M. J.; de Brouwer, H. *Macromolecules* **2001,** 34, (3), 349-352.

12. Morgan, J. D.; Lusvardi, K. M.; Kaler, E. W. *Macromolecules* **1997,** 30, (7), 1897-1905.

13. Co, C. C.; Kaler, E. W. *Macromolecules* **1998,** 31, (10), 3203-3210.

14. Co, C. C.; de Vries, R.; Kaler, E. W. *Macromolecules* **2001,** 34, (10), 3224-3232.

15. de Vries, R.; Co, C. C.; Kaler, E. W. *Macromolecules* **2001,** 34, (10), 3233-3244.

16. O'Donnell, J.; Kaler, E. W. *Macromolecular Rapid Communications* **2007,** 28, (14), 1445-1454.

17. O'Donnell, J. M. Reversible addition-fragmentation chain transfer in microemulsion polymerizations. Dissertation, University of Delaware, Newark, Delaware, 2007.

18. Liu, S.; Hermanson, K. D.; Kaler, E. W. *Macromolecules* **2006,** 39, (13), 4345-4350.

19. Hermanson, K. D.; Liu, S.; Kaler, E. W. *Journal of Polymer Science Part A: Polymer Chemistry* **2006,** 44, (20), 6055-6070.

20. O'Donnell, J.; Kaler, E. W. *Macromolecules* **2010,** 43, (4), 1730-1738.

21. O'Donnell, J. M.; Kaler, E. W. *Journal of Polymer Science Part A: Polymer Chemistry* **2010,** 48, (3), 604-613.

22. O'Donnell, J.; Kaler, E. W. *Macromolecules* **2008,** 41, (16), 6094-6099.

23. Shim, S. E.; Shin, Y.; Jun, J. W.; Lee, K.; Jung, H.; Choe, S. *Macromolecules* **2003,** 36, (21), 7994-8000.

24. Shim, S. E.; Shin, Y.; Lee, H.; Choe, S. *Polym Bull* **2003,** 51, (3), 209-216.

25. Shim, S. E.; Shin, Y.; Lee, H.; Jung, H. J.; Chang, Y. H.; Choe, S. *J Ind Eng Chem* **2003,** 9, (6), 619-628.

26. Rieger, J.; Stoffelbach, F.; Bui, C.; Alaimo, D.; Jerome, C.; Charleux, B. *Macromolecules* **2008,** 41, (12), 4065-4068.

27. Ferguson, C. J.; Hughes, R. J.; Nguyen, D.; Pham, B. T. T.; Gilbert, R. G.; Serelis, A. K.; Such, C. H.; Hawkett, B. S. *Macromolecules* **2005,** 38, (6), 2191-2204.

28. Ferguson, C. J.; Hughes, R. J.; Pham, B. T. T.; Hawkett, B. S.; Gilbert, R. G.; Serelis, A. K.; Such, C. H. *Macromolecules* **2002,** 35, (25), 9243-9245.

CHAPTER 3. EXPERIMENTAL MATERIALS AND METHODS

3.1 Materials

Monomers: n-Butyl acrylate (BA), and styrene (S) were purchased from Sigma-Aldrich. n-Butyl acrylate (99%) was distilled under vacuum to remove the inhibitor and stored in the freezer for less than 1 week prior to use. Styrene (99%) was purified by running through a DTR-7 packed column, from Scientific Polymer Products Inc., and stored in the freezer for less than 1 week prior to use. **Initiator:** 2,2-azobis[2-(2-imidazolin-2-yl)propane] dihydrochloride (VA-044) from Wako Pure Chemical Industries was used as received. **Surfactant:** Dodecyltrimethylammonium bromide (DTAB) was obtained from TCI America, having 98% purity, and was used as received.

Chain Transfer Agent Synthesis: The traditional chain transfer agent benzyl undecyl carbonotrithioate (B11C) was synthesized based on the procedure reported by Ting et al. [1] using chemicals from Sigma-Aldrich. 1-undecanethiol (10.0 g, 0.052 mol) was dissolved in distilled water (100 mL) and cooled in an ice bath. Potassium hydroxide (3.34 g, 0.052 mol) was slowly added to the ice-cold solution. An excess of carbon disulfide (10.4 mL, 0.173 mol) was then added dropwise which forms a yellow solution. Benzyl bromide (9.1 g, 0.052 mol) was then slowly added, after which the reaction was set to run at 80 °C for 12 h. After cooling, the aqueous phase was separated from the organic phase and washed with methylene chloride (3 × 50 mL). The combined organic phases were dried over anhydrous magnesium sulfate, filtered, and the solvent was removed under high vacuum, yielding a bright yellow oil (16.9 g, yield 92%). The purity of B11C was confirmed by ^{1}H NMR (400 MHz, $CDCl_3$). δ: 0.88 (t, 3H, CH_3-

CH_2), 1.48 – 1.15 (m, 16H, -$(CH_2)_8$-), 1.80 – 1.62 (m, 2H, S-CH_2-$\underline{CH_2}$), 3.37 (t, 2H, S-$\underline{CH_2}$-CH_2), 4.61 (s, 2H, Φ-CH_2-S), 7.39 – 7.22 (m, 5H, aromatic =CH-).

The surface-active chain transfer agent, with a positively charged Z-group, 2-((11-(((benzylthio)carbonothioyl)thio)undecanoyl)oxy)-N,N,N-trimethylammonium Iodide (B11T) was prepared according to the synthesis reported by Samakande et al [2]. The purity of B11T was confirmed by ^{1}H NMR,(400 MHz, $CDCl_3$). δ: 1.43 – 1.22 (m, 12H, , -$(CH_2)_6$-), 1.76 – 1.58 (m, 4H, S-CH_2-$\underline{CH_2}$ and $\underline{CH_2}$-CH_2-COO), 2.43 – 2.33 (m, 2H, CH_2-COO), 3.37 (t, 2H, S-CH_2), 3.56 (s, 9H, $N^+(CH_3)_3$), 4.24 – 4.08 (m, 2H, CH_2- N^+), 4.69 – 4.51 (m, 4H, O-CH_2 and Φ-CH_2-S), 7.38 – 7.23 (m, 5H, aromatic =CH-).

3.2 Methods

Reaction Calorimetry, Polymerization Kinetics: A Mettler Toledo RC1e reaction calorimeter, with RTCal option, was used to measure the reaction heat release during the polymerization. The calorimeter is equipped with a 500 mL jacketed reactor, metal stirrer, temperature probe, calibration heater, and a horizontal sensor band. The heat evolved during polymerization is directly related to the heat of polymerization. Hence, the instantaneous conversion is calculated based on the heat evolved as a function of time.

The horizontal band sensor measures the heat flux passing through the vessel wall (Q_f), that is between the reaction solution and the reactor jacket. The temperature of the reactor (T_r) is monitored and heat provided by calibration heater and the flow rate of cooling waer to the jacket are altered to maintain T_r. The summation of the heat flux (Q_f) and heat accumulation (Q_a) gives the total differential heat of reaction (Q_r)

$$Q_r = Q_f + Q_a = A.Q_{s0} + m.C_p \frac{\mathrm{d}T_r}{\mathrm{dt}} \qquad \text{(eq 3.1)}$$

where A is the effective heat exchange area between the reactor wall and the reactor solution, Q_{s0} is the specific heat flow through the horizontal sensor band, m is the total mass of the reactor solution and C_p is the heat capacity of the reactor solution. The heat capacity of the solution is determined using the standard calibration procedure provided with the software before and after the polymerization. The RCe1 software calculates the instantaneous Q_r and plots it over time. At the end of polymerization, a baseline (Q_b) and integration interval is manually defined between the start and end time of the polymerization (**Figure 3.2.1**).

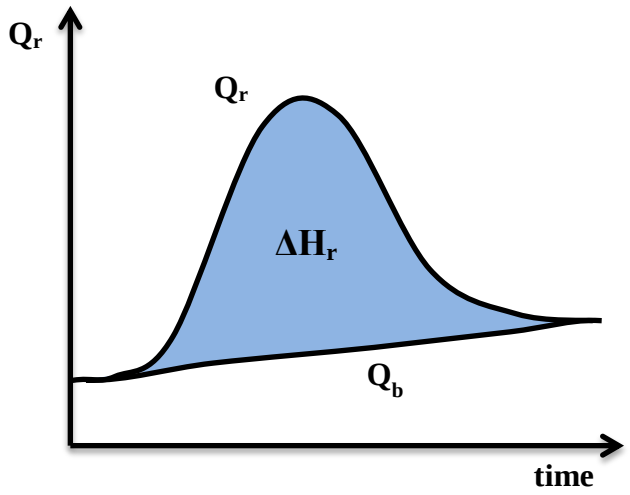

Figure 3.2.1: The reaction enthalpy, ΔHr, is determined by integrating the area under the peak of the heat generation rate between the start and end point

The software then outputs the relative conversion of monomer (f) as a function of time

$$f_{(t)} = \frac{\int_0^t (Q_r - Q_b).dt}{\int_0^{final} (Q_r - Q_b).dt} \qquad \text{(eq 3.2)}$$

The calculation of conversion is based on the assumption that the polymerization reaches complete conversion, which needs to be verified gravimetrically at the end of the polymerization

reaction. In the case the polymerization does not reach full conversion; the relative conversion, $f_{(t)}$, is multiplied by the final gravimetric conversion, f_{grav}, to obtain the true conversion.

Size exclusion chromatography (SEC), Molecular Weight: Polymer solution samples were dried at 70 °C overnight in a vacuum oven, which removes the water and remaining monomer. To remove the surfactant, the dried samples were dissolved in tetrahydrofuran (THF) and centrifuged so that the surfactant pelletize. The polymer containing THF supernatant was decanted, and fresh THF was added to the centrifuge tube to dissolve remaining polymer in the surfactant and then centrifuged. The washing-centrifuging cycle was repeated three times. The combined polymer containing THF solutions were dried to obtain the purified polymer. For molecular weight analysis, the polymer is dissolved in HPLC-grade THF at ~10mg/ml concentration and filtered using low protein binding Durapore® 0.22 μm filters.

Size exclusion chromatography (SEC) with multi-angle laser light scattering (MALLS) and refractive index (RI) detection was used to determine the number average molecular weight (M_N) and polydispersity index (PDI, M_W/M_N) of each polymer sample. The SEC system consisted of an isocratic pump, a solvent degasser and an autosampler. Separation was performed by four PLgel 7.5 mm ID SEC columns purchased from Varian Inc., in the following order: 50 mm guard column, 300 mm 100 Å column, 300mm 500 Å column, and 300 mm 104 Å column. A DAWN HELEOS II MALLS detector together with an Optilab T-rEX RI detector, set at 658nm wavelength, was used for detection. A flow rate of 0.50 ml/min was used. The Astra 5.3.4 software by Wyatt Technology was used to evaluate the collected data.

The refractive index increment (dn/dc), is important in the calculation of molecular weights from light scattering data. dn/dc represents how much the refractive index of a solution varies for a given increment in concentration, expressed as ml/g. dn/dc is dependent on polymer

composition, solvent and detector wave length. Therefore, the dn/dc was determined in this study for poly(butyl acrylate), poly(styrene) and poly(ethyl acrylate). Five samples of each polymer were prepared at different concentrations in THF. The measurements were conducted by injecting the samples incrementally, using a sample injector, before the Optilab T-rEX RI detector, that is set at 25°C. The Astra software was used for calculating the dn/dc values. The amount of CTA has an effect on the determined dn/dc value. The following table shows the average values obtained and used for the set of RAFT microemulsion polymerization experiments.

Table 3.2.1: The refractive index increment (dn/dc) values in ml/g for the polymer samples from the RAFT microemulsion polymerizations.

Monomer	CTA/micelle ≤ 2.3	CTA/micelle ≥ 3.5
Poly(St)	0.164	0.132
Poly(BA)	0.055	0.088
Poly (EA)	0.066	0.071

Dynamic Light Scattering (DLS), Particle Size: The polymer particle size was determined using DLS on a Malvern Instruments Nano ZS90 Zetasizer equipped with a He-Ne laser (633 nm). A sample of polymer latex was diluted with milli-Q water to a DTAB concentration of 120mM, which is 10 times the critical micelle concentration of DTAB. The sample was then placed in a cuvette at 25°C and irradiated by a 4.0mW He-Ne laser light at 90° angle. The scattered light was detected by an Avalanche photodiode detector. The autocorrelation function was fit using a second order cumulant fit to calculate the average hydrodynamic diameter. The numbers presented are the volume-weighted average particle diameter.

Nuclear Magnetic Resonance (NMR): 1H NMR spectra were determined with a Varian VXR-400 spectrometer in deuterated chloroform ($CDCL_3$) solutions at room temperature.

Transmission Electron Microscopy (TEM): The polymeric latex solution was diluted at a 1:50 ratio with deionized water, and 3 µl of the diluted sample was deposited on a carbon grid. After couple minutes, a 3 µl of 2 wt% of uranyl acetate (UAc) was placed on the grid to negatively stain the sample and left to dry for 10 min. Negative staining helps to enhance the contrast between the particles edges and the grid. The sample was then positively stained to enhance the contrast between the poly(St) and poly(BA). This was done by placing the grid in a petri dish above ruthenium tetroxide (RuO_4) solution and vapor staining the sample for 15 min. RuO_4 reacts with poly(St) and not the acrylate due to the benzyl ring in poly(St). Under TEM microscope the RuO_4 stained regions in a particle are dark. The TEM used was JEOL 2100 (200 kV) scanning and transmission electron microscope (STEM) with a Thermo Fisher Noran System 6 elemental analysis. A JEOL specimen holder was used for standard viewing. All measurements were done in room temperature.

3.3 Microemulsion Polymerization

The microemulsion polymerizations were performed in the RC1e Reaction calorimeter. Typically, a total reaction solution volume of 125 ml is chosen for the experiments. Initially, the solid contents of the reaction (surfactant and the CTA) were loaded into the RC1e 500 ml reactor vessel. The vessel was then sealed and purged with argon for 10 minutes. Milli-Q Water was purged with argon in a separate round bottom flask, and then transferred to the purged reactor using syringe pump. The reactor contents were stirred (200 rpm), and the temperature of the solution was raised to 42°C. Argon purged monomer was then added to the reactor using a syringe pump. The heat capacity was measured using the RC1e software procedure, which raised

the temperature by 3°C to 45°C. Once the temperature was stabilized at 45°C, the polymerization was started by adding 1 ml of purged water containing VA044 initiator for a VA044 concentration of 2 wt% with respect to monomer. The reactor was maintained at 45°C throughout the polymerization and the heat evolved during the polymerization was monitored by the RC1e software. During the polymerization, 2 mL sample is extracted at chosen intervals to check for gravimetric conversion and perform size exclusion chromatography analysis. After the polymerization reaction ended, the heat capacity of the latex was measured. The monomer conversion as a function of time was calculated with standard RC1e software, and the final conversion was confirmed gravimetrically.

3.4 Bibliography

1. Ting, S. R. S.; Gregory, A. M.; Stenzel, M. H. *Biomacromolecules* **2009,** 10, (2), 342-352.

2. Samakande, A.; Sanderson, R. D.; Hartmann, P. C. *Synthetic Communications* **2007,** 37, (21), 3861-3872.

CHAPTER 4. IMPROVING RAFT IN MICROEMULSION POLYMERIZATION BY USING A SURFACE-ACTIVE CHAIN TRANSFER AGENT

Modified from a paper submitted for publication in *Macromolecules*. Unpublished work

Ibrahim A. El-Hedok[1,2], Jennifer M. Heinen[1,3]

Abstract

Microemulsion polymerizations are attractive for producing colloidally stable polymer nanoparticles. The implementation of reversible addition-fragmentation chain transfer (RAFT) controlled/living polymerization in microemulsion polymerization provides good control over the molecular weight. However, achieving low molecular weight polydispersity is hindered due to the continuous diffusion of the hydrophobic chain transfer agent (CTA) from monomer-swollen micelles to the locus of polymerization. In this work, the use of a surface-active CTA (B11T) is investigated in the RAFT microemulsion polymerizations of n-butyl acrylate (BA). The polymer properties and polymerization kinetics are analyzed and compared to BA RAFT microemulsion polymerizations with a similar traditional chain transfer agent (B11C). The CTA diffusion was found to be successfully minimized through the use of a surface-active CTA. Polymerizations with the surface-active CTA B11T demonstrate good molecular weight control with moderate polydispersity, and produce polymer nanoparticles of 15-35 nm in diameter, whereas polymerizations with the traditional CTA B11C resulted in a bimodal molecular weight distribution.

[1] Graduate student and Assistant Professor, respectively, Department of Chemical and Biological Engineering, Iowa State University.
[2] Primary researcher and author
[3] Corresponding author

4.1 Introduction

The field of polymer nanoparticles (PNPs) has attracted many researchers over the past decade. In 2010 alone over 20,000 publications concerning PNPs were published.[1] Besides the conventional use of polymer latex in coatings and adhesives, PNPs are becoming of interest in many other applications such as electronics, drug delivery, and environmental control. Researchers have looked into techniques that improve the control of the chemical structure, particle size, and microstructure of PNPs. Microemulsion polymerization is a PNP synthesis method that has the advantage of forming monodisperse, colloidally stable particles with diameter of 10-100 nm. Microemulsion polymerization begins with a high concentration of thermodynamically stable, monomer-swollen micelles. Upon the introduction of an initiator, a fraction of the micelles are initiated to form rapidly growing polymer particles, while monomer diffuses from the remaining uninitiated micelles.[2] At the end of the polymerization, the solution contains surfactant-stabilized polymer particles and empty micelles. Despite the advantage of microemulsion in forming colloidally stable PNPs at a rapid rate, the process lacks control over molecular weight. Utilizing a controlled/living radical polymerization technique, such as reversible addition-fragmentation chain transfer (RAFT),[3] in microemulsion has been proven to produce PNP with predetermined molecular weight, however low molecular weight polydispersity was unattainable.[4-6]

RAFT utilizes a chain transfer agent (CTA) containing a stable Z group and a cleavable R group. The mechanism of RAFT, as proposed by Chiefari et al.,[3] begins with the reaction of the propagating polymer chain (P•) with the CTA, which forms a dormant polymer and a new radical (R•) (Scheme 1). The new R• radical reacts with monomer to initiate a new active polymer chain (Pn•). Active and dormant polymer chains react to form a macroRAFT

intermediate radical which then fragments to release either chain for further propagation. The equilibrium reaction between active and dormant polymers provides an equal opportunity for the chains to grow while minimizing radical-radical termination, which achieves low molecular weight polydispersity.

Scheme 1. The RAFT mechanism as proposed by Chiefari et al., reproduced and modified from reference [7].

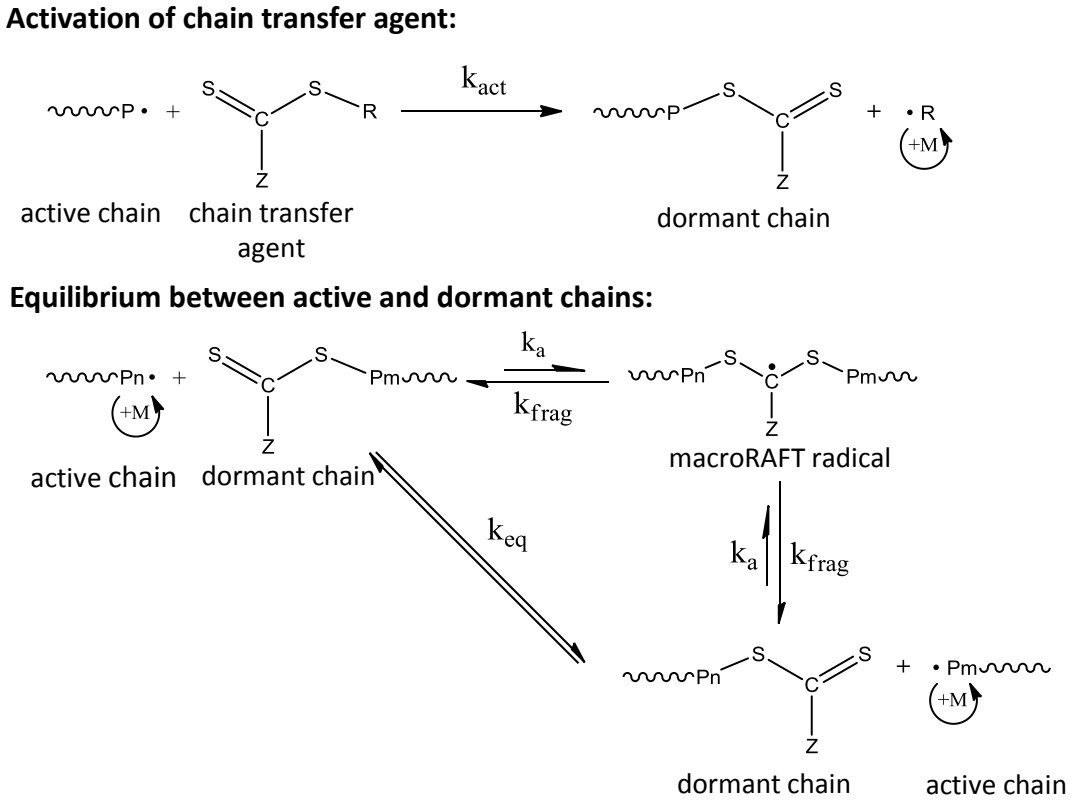

In an ideal RAFT polymerization the exchange of radical activity is rapid relative to the rate of propagation so the kinetics are unaffected. However, typical RAFT polymerizations

experience rate retardation due to the long residence time of the macroRAFT radical[8, 9] or its termination with oligomers.[10]

When RAFT is implemented in microemulsion polymerization, the CTA partitions into the micelles along with the hydrophobic monomer (**Figure 4.1.1-1**). Polymer particles are formed when oligomeric radicals enter micelles from the aqueous domain (**Figure 4.1.1-1**). Thus, the RAFT reaction occurs within the growing polymer particles, with monomer and CTA diffusing into the particles from uninitiated micelles (**Figure 4.1.1-2**). O'Donnell and Kaler[4] have identified the key factors for achieving control in RAFT microemulsion polymerization as the CTA aqueous solubility, and the initial CTA per micelle ratio. It has been shown that while the diffusion of CTA during polymerization from uninitiated micelles to growing polymer particles is necessary for complete activation of the CTA, this causes the particle to experience a broad range of reaction conditions over the course of polymerization and the CTA per particle ratio broadens.[4] Such effects lead to the observed high molecular weight polydispersity index (PDI>1.4).

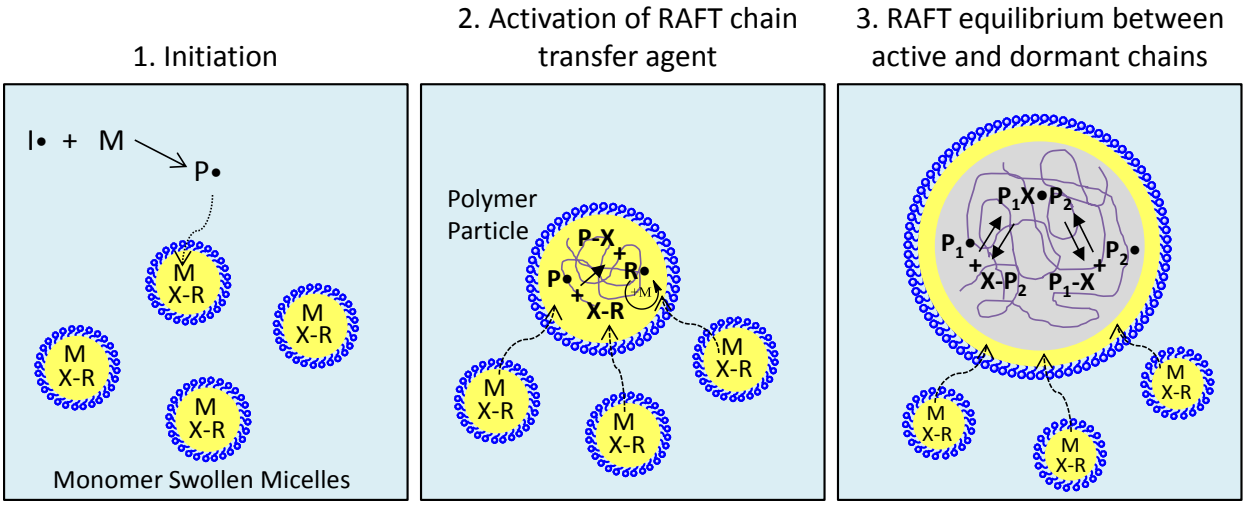

Figure 4.1.1: The proposed RAFT microemulsion polymerization process. M: monomer, X-R: chain transfer agent, I•: water soluble initiator, P•: propagating polymer, X-P: dormant polymer, PX•P: macroRAFT radical.

This work seeks to minimize the rate of CTA diffusion by attaching an amphiphilic moiety to the CTA, which confines the CTA to the surface of the micelles and particles. This causes the surface-active CTA to thermodynamically favor partitioning between micelles and particles throughout the polymerization. The surface-active chain transfer agent, 2-((11-(((benzylthio)carbonothioyl) thio)undecanoyl)oxy)-N,N,N-trimethylammonium iodide (B11T), was synthesized for this work. B11T was selected because it has a surface-active moiety similar to the surfactant dodecyltrimethylammonium bromide (DTAB), which is used to formulate the initial n-butyl acrylate (BA) in water microemulsion. The microemulsion polymerization of BA was selected for the initial studies since it has been previously studied with traditional chain transfer agents.[2, 4, 11, 12] For proper comparison, a traditional hydrophobic chain transfer agent, benzyl undecyl carbonotrithioate (B11C), which has similar R and Z groups to B11T, was also synthesized (Scheme 2). The reaction rate profiles were examined at a range of CTA/micelle ratios (0.3-4.6) for both chain transfer agents to evaluate the difference in polymerization

kinetics. The number average molecular weight was obtained at different monomer conversions to assess the degree of RAFT control. Final polymer molecular weight and particle diameter were also measured at each CTA/micelle ratio.

Scheme 2. The structure of the surface-active chain transfer agent, B11T, and the traditional chain transfer agent, B11C.

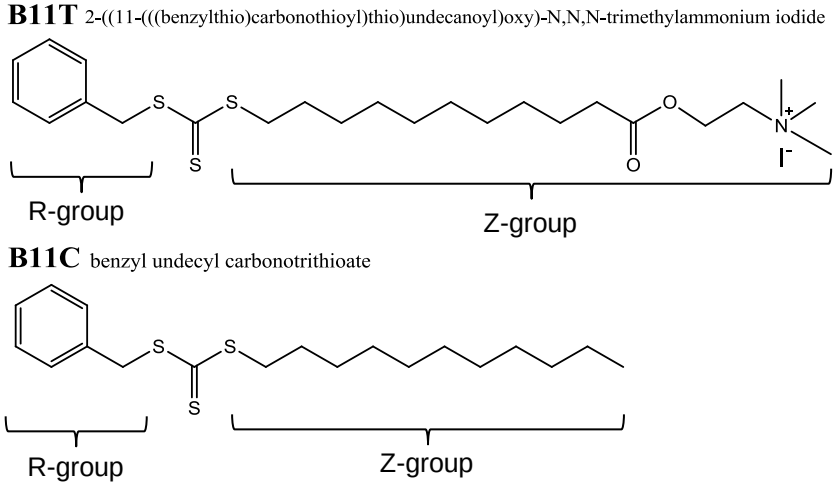

4.2 Materials and Methods

RAFT solution polymerization with B11C. BA solution polymerization was done in 1,4-dioxane at 1M monomer concentration. The required amount of B11C chain transfer agent (13 mM) was first added to 12 ml of 1,4-dioxane in a round flask bottom . Then, the flask was sealed with a rubber septum and purged with argon for ten minutes. BA was purged with argon in a separate round flask bottom then transferred to the dioxane solution using syringe pump. The monomer containing solution was then immersed in an oil bath, and heated to 60ºC. Once the temperature was stabilized, the polymerization reaction was started by adding 1ml of purged 1,4-

dioxane containing AIBN initiator for an AIBN concentration of 2 wt% with respect to BA. Samples were taken at intermediate conversions, dried, and analyzed by size exclusion chromatography to determine polymer molecular weight and polydispersity.

RAFT microemulsion polymerizations with B11C and B11T. Oil-in-water microemulsion of BA stabilized by DTAB was prepared at α=5.0% and γ=12.0% were used, where $\alpha = mass_{monomer}/(mass_{monomer} + mass_{water}) \times 100$ and $\gamma = mass_{surfactant}/(mass_{surfactant} + mass_{monomer} + mass_{water}) \times 100$. The polymerization was performed at 45°C and initiated by injecting VA044 (2 wt % with respect to monomer) solubilized in 1 ml of Milli-Q water. Reaction calorimetry was used to measure the monomer conversion along with sampling over time to check for gravimetric conversion and perform molecular weight analysis. The RAFT microemulsion polymerizations of BA were done at the following CTA per micelle ratios: 0.3, 0.6, 1.1, 2.3, 3.5 and 4.6. The calculation of the CTA/micelle ratio is based on O'Donnell's calculation procedure which is outlined in Appendix A.[11] In the case of surface-Active CTA B11T, the amount of DTAB was replaced by the respective number of added B11T molecules.

4.3 Results and Discussion

4.3.1 Molecular Weight and Polydispersity

RAFT solution polymerization with traditional CTA, B11C The traditional chain transfer agent, B11C, has never been investigated before in RAFT polymerization. Hence, solution polymerization of BA (1M in 1,4-dioxane) was performed with B11C to confirm the effectiveness of the CTA. The polymerization reached 91% conversion after two hours. **Figure 4.3.1** shows the SEC analysis results of the solution polymerization compared to the

theoretical prediction of the number-average molecular weight (M_N^{theo}), which was calculated according to eq.4.1:

$$M_N^{theo} = \frac{C_{mon,o} \cdot MW_{mon} \cdot f}{C_{CTA,o}} \qquad \text{(eq 4.1)}$$

where $C_{mon,o}$ is the initial monomer concentration, MW_{mon} is the monomer molecular weight, $C_{CTA,o}$ is the initial chain transfer concentration, and f is the fractional monomer conversion.

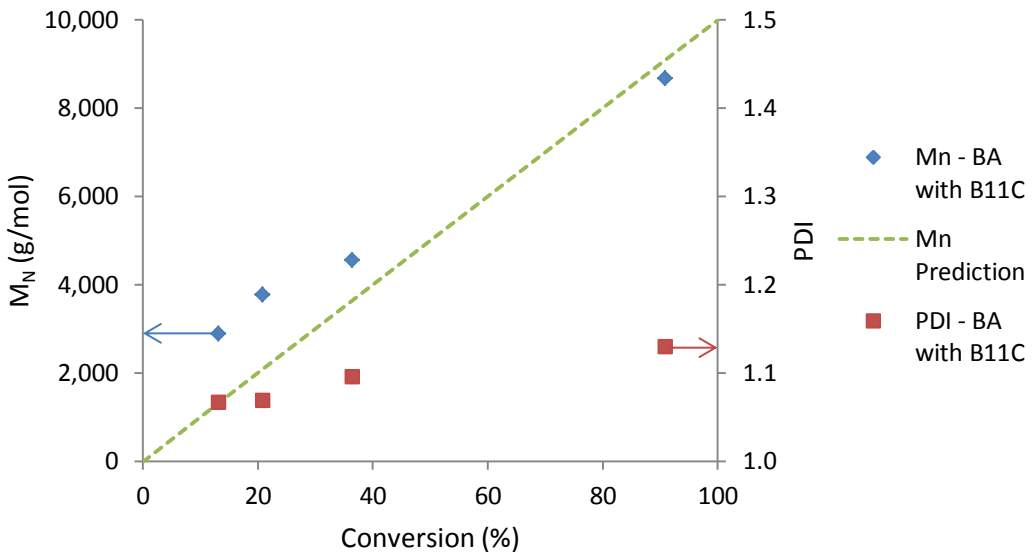

Figure 4.3.1: Number-average molecular weight (M_N) and polydispersity (PDI) as a function conversion for poly(BA) from solution RAFT polymerization with B11C.

The experimental M_N increases linearly with conversion, but deviates from the predicted M_N at low conversion. The polydispersity index (PDI) remains low throughout the polymerization and had a value of 1.13 at 91% conversion. The M_N and PDI indicate that the R and Z groups of the CTA are appropriate to control BA polymerization. However, activation of the B11C is slow, which causes greater than predicted M_N at low conversion.

RAFT microemulsion polymerization with traditional CTA, B11C. The SEC traces of polymers produced by BA RAFT microemulsion polymerizations with the traditional CTA, B11C, show bimodal polymer populations at all of the B11C/micelle ratios (**Figure 4.3.2**).

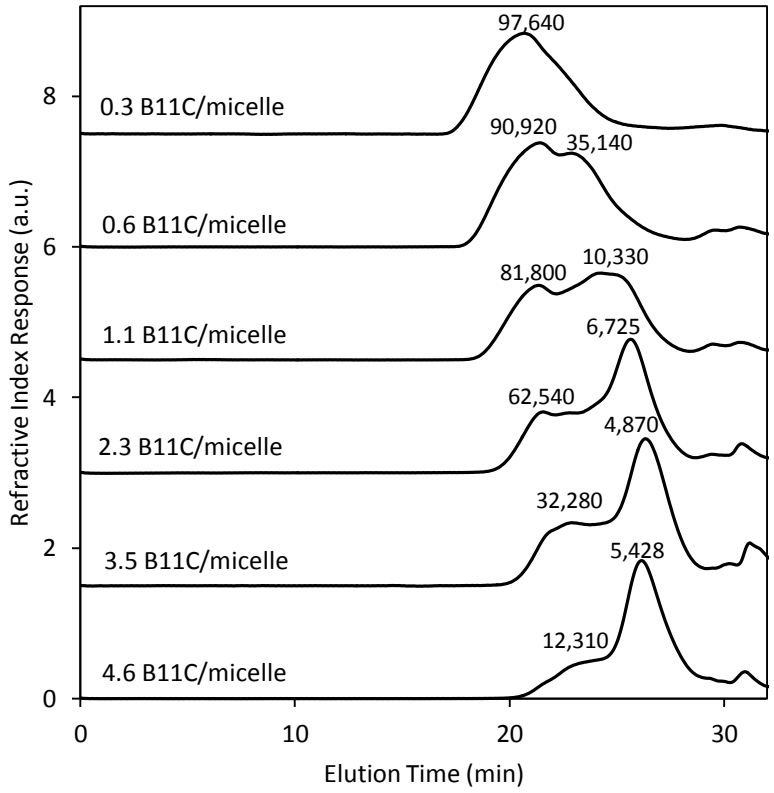

Figure 4.3.2: SEC traces of poly(BA) at full conversion for RAFT microemulsion polymerizations with traditional chain transfer agent, B11C. The number above each peak designates the peak molecular weight in g/mol.

At a B11C/micelle ratio of 0.3, the SEC traces show a peak with a low molecular weight shoulder. As the B11C/micelle ratio increases, the concentration of low molecular weight polymers increases, and high molecular weight polymers decreases. Given that B11C produced controlled monomodal in solution polymerization of BA, the appearance of bimodal polymer populations in microemulsion polymerization must be a result of the distribution of the B11C

between uninitiated micelles and polymer particles. Similar results have been observed with the hydrophobic CTA, methyl-2-(O-dodecylxanthyl)-propionate (MODP).[4]

RAFT microemulsion polymerization with surface-active CTA, B11T. RAFT microemulsion polymerizations with the surface-active CTA B11T produce monomodal polymer populations for B11T/micelle ratios less than 4.6 (**Figure 4.3.4-left**). Examination of M_N as a function of monomer conversion shows a linear increase (**Figure 4.3.3**), which demonstrates that B11T provides good control of the polymerization.

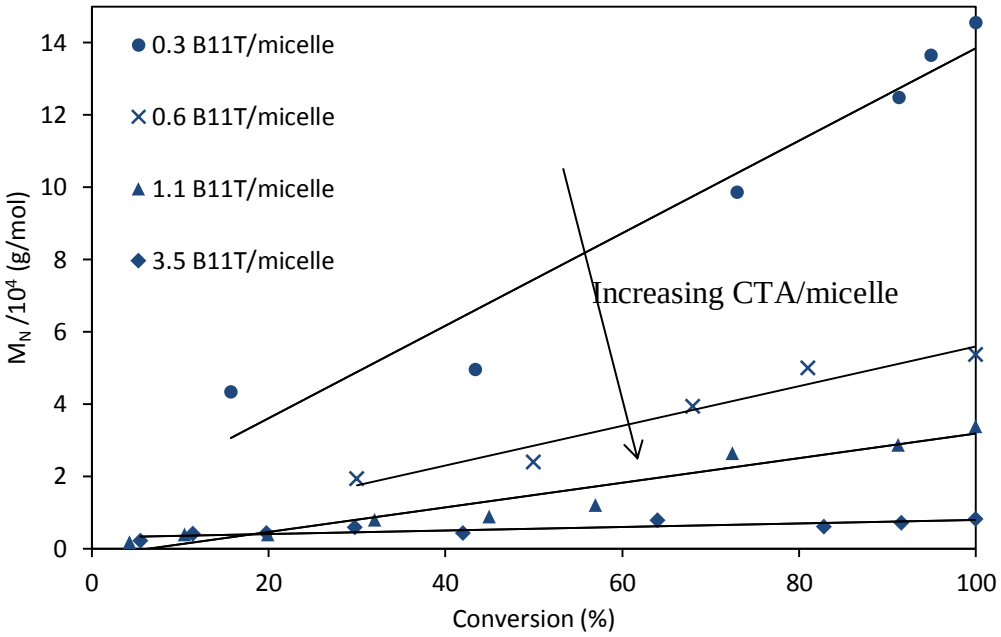

Figure 4.3.3: Number average molecular weight (M_N) of poly(BA) at B11T/micelle ratios of 0.3, 0.6, 1.1, and 3.5. The lines are least-squares linear fits to the data.

The linear least-square fits to the data have an intercept of approximately zero, so the slow activation of B11T does not result in high molecular weight polymer at low conversion, as observed for solution polymerization with B11C. This improvement in molecular weight control

likely results from the confinement of the B11T to the micelle and polymer particles, which causes a greater local concentration of B11T than would exist in solution.

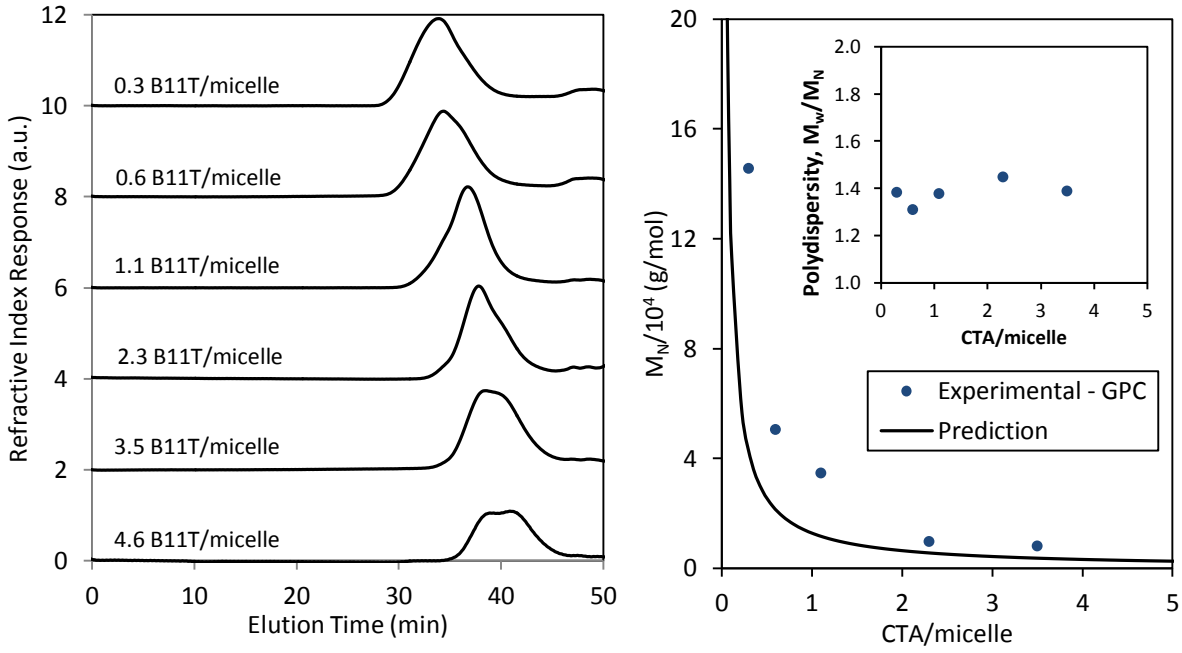

Figure 4.3.4: Left: Gel permeation chromatography traces of poly(BA) at full conversion with B11T CTA. Right: Number average molecular weight (M_N) and polydispersity index M_W/M_N (inset) of poly(BA) at full conversion for RAFT microemulsion polymerization with B11T. The prediction is from equation 4.1.

The final number-average molecular weight (M_N) decreases as the CTA/micelle ratio increases, as expected (**Figure 4.3.4-right**). However, the polydispersity index (Figure 5-inset) is approximately 1.4. Similar polydispersity has been observed in the RAFT microemulsion of BA with methyl-2-(O-ethylxanthyl)-propionate (MOEP).[4] In the case of MOEP, all of the CTA diffuses into the polymer particles and is activated, as demonstrated by the correspondence between the experimental and theoretical M_N. The diffusion of the CTA increases the breadth of the CTA/particle distribution, and thus the polydispersity.[4] The surface-active B11T produces

polymers with a final molecular weight greater than the predicted value, which indicates that not all of the CTA is activated, so the polydispersity is expected to be less than 1.4. The fraction of B11T that is activated (ε) can be calculated from equation 4.2:

$$M_N^{exp} = \frac{C_{mon,o} \cdot MW_{mon} \cdot f}{C_{CTA,o} \cdot \varepsilon^{exp}} \qquad \text{(eq 4.2)}$$

where M_N^{exp} is the experimental number-average molecular weight. The percentage of B11T activated ranges from 29% to 57%, and no clear trend is observed with respect to B11T/micelle ratio (**Figure 4.3.5**). Partial activation indicates that the B11T remains partitioned between uninitiated micelles and polymer particles.

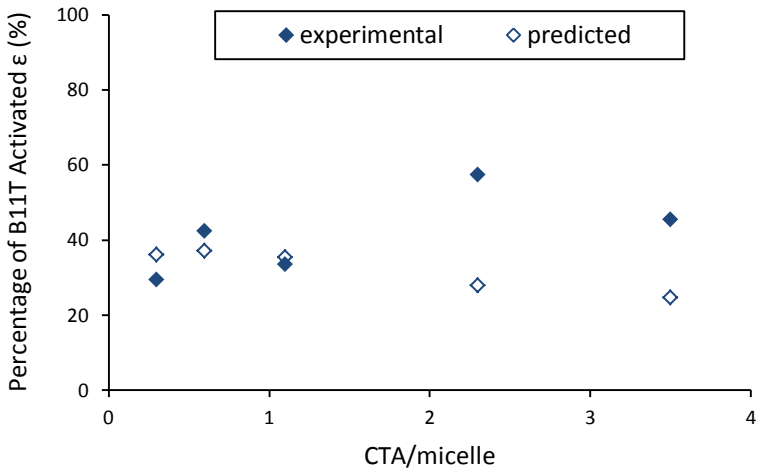

Figure 4.3.5: Percentage of surface-active CTA B11T activated (ε) for the BA RAFT microemulsion polymerizations. The experimental value is obtained from eq 4.2, and the predicted value is obtained from eq 4.3.

The ratio of initial number of monomer-swollen micelles ($N_{mic,i}$) to the final number of polymer particles ($N_{part,f}$) ranges between 110 and 380 for the RAFT microemulsion polymerizations (Appendix B), which means that less than 1% of the monomer-swollen micelles are initiated and converted to polymer particles. However, the percentage of B11T activated (ε^{exp}

> 29%) is much higher than the percentage of micelles initiated, which indicates that some of the B11T diffuses to the initiated micelles. The surface-active CTA can adsorb and desorb to/from a micelle or particle surface, and once the CTA is activated it is expected to remain attached to the particle surface due to the polymer chain growth on its hydrophobic tail. As the polymer particle grows the surface requires more surfactants, i.e. more DTAB and B11T. Hence, the fraction of surface-active CTA activated is expected to be proportional to the surface area expansion. The ε can then be predicted as the fraction of initiated micelles ($N_{part,f}$ / $N_{mic,i}$) multiplied by the ratio of the change in surface area:

$$\varepsilon^{predicted} = \frac{N_{part,f}}{N_{mic,i}} \times \frac{A_{part}}{A_{mic}} \qquad \text{(eq 4.3)}$$

where A_{part} and A_{mic} are the surface areas of the final polymer particle and initial micelle, respectively. The $\varepsilon^{predicted}$ is calculated for each of the CTA/micelle ratio by using particle size measurements from DLS to find $N_{part,f}$ and A_{part}, and assuming an initial micelle diameter of 2.5 nm (**Figure 4.3.5**). There is a close match between the experimental and predicted ε at CTA/micelle ratios less than and equal to 1.1. However, at higher CTA/micelle ratios, the ε^{exp} is significantly higher than $\varepsilon^{predicted}$. This could be due to the fact that coalescence occurs at higher CTA/micelle ratios polymerizations and, as a result, the calculated fraction of micelles converted to particles ($N_{part,f}$ / $N_{mic,i}$) would be underestimated in equation 4.3.

4.3.2 Polymerization Kinetics

All of the BA RAFT microemulsion polymerizations with B11C and B11T reach 100% conversion, which was verified gravimetrically. The increase of CTA/micelle ratio has a significant effect on the polymerization time ranging from fifteen minutes at the lowest CTA/micelle to more than two hours at the highest ratio (**Figure 4.3.6**). The observed increase in

polymerization time is typical of RAFT polymerizations due to the rate retardation caused by the long-lived intermediate macroRAFT radical.[13] The rate retardation effect is magnified in microemulsion polymerization relative to solution polymerization due to the compartmentalization effect. Similar effects on the rate of polymerization have been observed in RAFT polymerizations in other dispersed systems.[4, 14, 15]

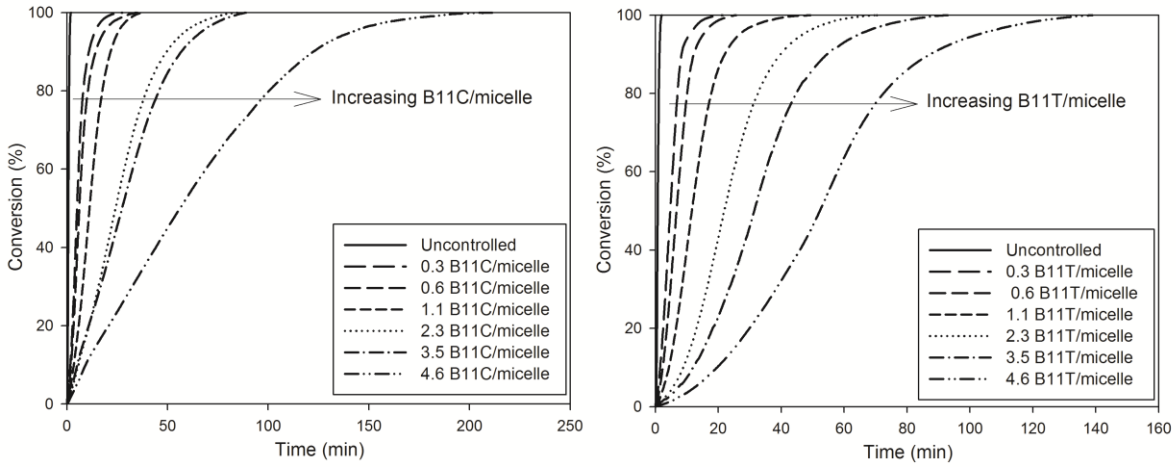

Figure 4.3.6: Conversion of butyl acrylate as a function of time for RAFT microemulsion polymerization: (left) with B11C CTA, (right) with B11T CTA.

Figure 4.3.7 shows the rate of polymerization as a function of monomer conversion, calculated from the data shown in **Figure 4.3.6**. In RAFT microemulsion polymerization, the rate monomer conversion (df/dt) depends on the propagation rate constant (k_p), the monomer concentration the locus of polymerization (C_{mon}^{part}), the total concentration of propagating radicals (N*), and the fraction of active radicals (x_{act}):

$$\frac{df}{dt} = \frac{k_p C_{mon}^{part} N^* x_{act}}{M_o} \qquad \text{(eq 4.4)}$$

where M_o is the initial concentration of monomer in the microemulsion.[12] The theoretical rate profile depends on the relative rate of activation of the CTA and rate of propagation, and the rate

of fragmentation of the intermediate macroRAFT radical. The location of the rate maximum and the shift of the location of the rate maximum provide information about the rate of CTA diffusion to the locus of polymerization.

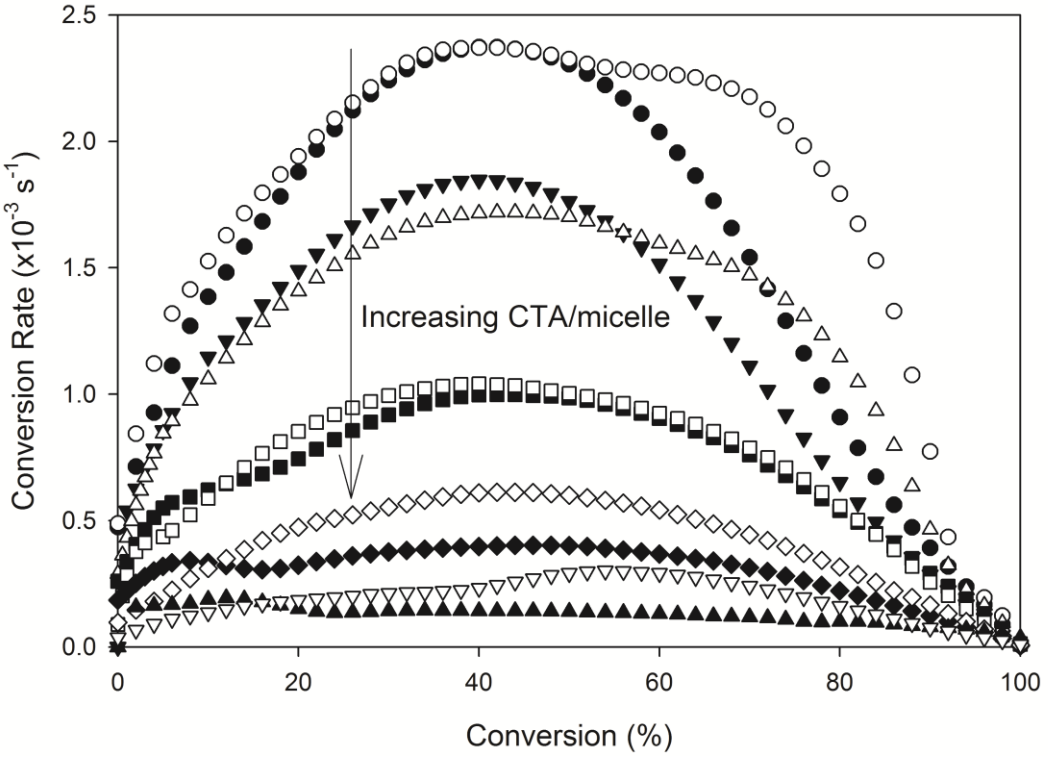

Figure 4.3.7: Rate of conversion of butyl acrylate as a function of conversion for RAFT microemulsion polymerization with traditional CTA, B11C, (filled symbols) and surface-active CTA, B11T (open symbols) at CTA/micelle ratios of 0.3, 0.6, 1.1, 2.3 and 4.6.

At CTA/micelle ratios less than or equal to 1.1, the RAFT microemulsion polymerizations with the traditional chain transfer agent B11C have a rate maximum at ~39% monomer conversion. The location of the rate maximum corresponds to the value predicted by the Morgan model, which assumes negligible biradical termination and linear monomer partitioning between micelles and polymer particles.[16]

At B11C/micelle ratios greater than or equal to 1.1, the RAFT microemulsion polymerizations with the traditional chain transfer agent B11C show an unexpected distinctive rate peak at conversions less than 20% and a second peak at ~39%. The decrease in monomer conversion rate at such early stage likely results from a decrease in the number of propagating radicals due to an increase in B11C/particle. The subsequent increase in rate leading to a secondary peak could result from an increase in the concentration of propagating radical as the thermal initiator continues to decompose, or an increase in the monomer concentration at the locus of polymerization. Previous small-angle neutron scattering studies have shown that BA does not swell the polymer particles,[2] so an increase in propagating radical concentration is more likely.

A distinct difference in the rate profiles for the B11T and B11C polymerizations was observed. The B11T polymerization show two distinct rate maxima at B11T/micelle ratio less than 1.1 and equal to 4.6. The first rate maximum occurs at ~39% conversion and the second occurs at conversions greater than 50%. The secondary increase in the rate of monomer conversion can be due to either a decrease in the reaction rate between propagating polymers and dormant polymers, or an increase in radical concentration by continued decomposition of the thermal initiator. The polymer particle diameter increases around tenfold from the time of initiation, hence the particle surface area becomes significantly larger and the surface-active CTA per surface area decreases. As a result, the probability of interaction between the propagating radical and the surface-active CTA decreases, which could result in a higher monomer conversion rate. This effect is more expected at high conversions and in lower CTA/micelle ratio polymerizations.

4.3.3 Polymer nanoparticle size

RAFT microemulsion polymerization produces more polymer particles in comparison to uncontrolled microemulsion polymerization due to nucleation of more particles by the continual thermal decomposition of the initiator. This results in a significantly smaller particle diameter upon addition of small amounts of CTA compared to the uncontrolled polymerization.[4] In addition, latex size is expected to decrease as the CTA/micelle ratio increases, since more particles would be initiated with longer reaction times. However, the data shows an initial decrease in particle diameter upon addition of CTA followed by an increase in particle diameter as the CTA/micelle ratio increases (**Figure 4.3.8**). This observation is attributed to particle-particle/particle-micelle coalescence that is facilitated by long polymerization times.

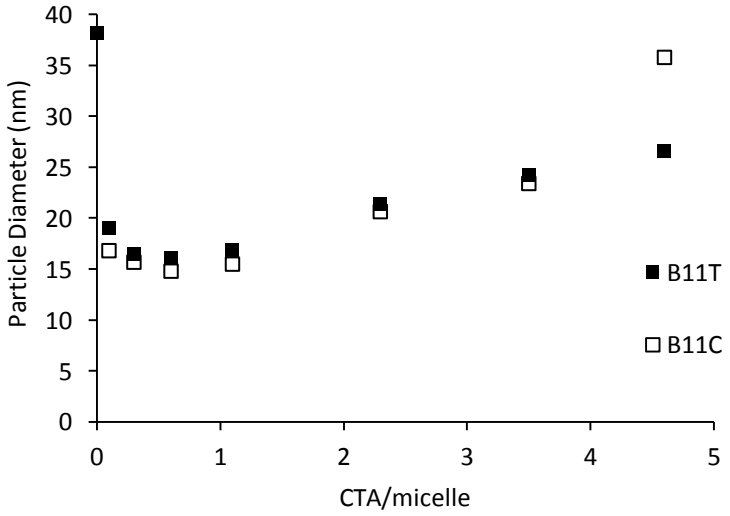

Figure 4.3.8: Volume-average latex particle diameter of poly(BA) as a function of CTA/micelle, measured by dynamic light scattering.

The effect of coalescence may introduce several complications to the polymerization. For instance, particle-micelle coalescence could result in activation of more chain transfer agents in a

growing polymer particle at a later stage of polymerization, which in turn leads to a broader range of polymerization conditions and increased molecular weight polydispersity. Moreover, particle-particle coalescence may lead to bi-radical termination which would decrease the overall rate of polymerization.

4.4 Conclusions

Colloidally stable poly(n-butyl acrylate) nanoparticles 15-35 nm in diameter were successfully synthesized by RAFT microemulsion polymerization using a surface-active chain transfer agent, B11T, and a traditional chain transfer agent, B11C. The B11T chain transfer agent provides good molecular weight control, and produces a more uniform molecular weight distribution than the B11C chain transfer agent. However, the molecular weight polydispersity of the poly(BA) from B11T microemulsion polymerizations (PDI~1.4) is still above the desired PDI value of 1.1 or less. The final number-average molecular weight indicates less than 60% of the B11T is activated, which shows that, as desired, the surface-active CTA does not rapidly diffuse to the locus of polymerization. The kinetic analysis shows that the microemulsion polymerizations with B11T have two distinct rate regions, which is attributed to the location of B11T at the surface of the particle.

4.5 Bibliography

1. Rao, J. P.; Geckeler, K. E. *Progress in Polymer Science* **2011,** 36, (7), 887-913.

2. O'Donnell, J.; Kaler, E. W. *Macromolecular Rapid Communications* **2007,** 28, (14), 1445-1454.

3. Chiefari, J.; Chong, Y. K.; Ercole, F.; Krstina, J.; Jeffery, J.; Le, T. P. T.; Mayadunne, R. T. A.; Meijs, G. F.; Moad, C. L.; Moad, G.; Rizzardo, E.; Thang, S. H. *Macromolecules* **1998,** 31, (16), 5559-5562.

4. O'Donnell, J.; Kaler, E. W. *Macromolecules* **2010,** 43, (4), 1730-1738.

5. Liu, S.; Hermanson, K. D.; Kaler, E. W. *Macromolecules* **2006,** 39, (13), 4345-4350.

6. Hermanson, K. D.; Liu, S.; Kaler, E. W. *Journal of Polymer Science Part A: Polymer Chemistry* **2006,** 44, (20), 6055-6070.

7. Matyjaszewski, K., Radical Polymerization. In *Controlled and Living Polymerizations*, Müller, A. H. E.; Matyjaszewski, K., Eds. Wiley-VCH Verlag GmbH & Co. KGaA: Weinheim, 2009; pp 103-166.

8. Feldermann, A.; Coote, M. L.; Stenzel, M. H.; Davis, T. P.; Barner-Kowollik, C. *J Am Chem Soc* **2004,** 126, (48), 15915-15923.

9. Barner-Kowollik, C.; Quinn, J. F.; Morsley, D. R.; Davis, T. P. *J. Polym. Sci. Pol. Chem.* **2001,** 39, (9), 1353-1365.

10. Monteiro, M. J.; de Brouwer, H. *Macromolecules* **2001,** 34, (3), 349-352.

11. O'Donnell, J. M. Reversible addition-fragmentation chain transfer in microemulsion polymerizations. Dissertation, University of Delaware, Newark, Delaware, 2007.

12. O'Donnell, J. M.; Kaler, E. W. *Journal of Polymer Science Part A: Polymer Chemistry* **2010,** 48, (3), 604-613.

13. Moad, G.; Rizzardo, E.; Thang, S. H. *Aust. J. Chem.* **2009,** 62, (11), 1402-1472.

14. Cunningham, M. F. *Progress in Polymer Science* **2008,** 33, (4), 365-398.

15. Luo, Y.; Wang, R.; Yang, L.; Yu, B.; Li, B.; Zhu, S. *Macromolecules* **2006,** 39, (4), 1328-1337.

16. Morgan, J. D.; Lusvardi, K. M.; Kaler, E. W. *Macromolecules* **1997,** 30, (7), 1897-1905.

CHAPTER 5. EFFECT OF MONOMER SOLUBILITY ON THE RAFT MICROEMULSION POLYMERIZATION USING SURFACE-ACTIVE CHAIN TRANSFER AGENT

5.1 Introduction

The water solubility of the monomer is one of the critical parameters that affects the performance of water based microemulsion polymerization due to the partitioning of the monomer.[1-7] Monomers of higher water solubility have higher concentration in the aqueous domain compared to more hydrophobic monomers. Hence, higher monomer water solubility increases the extent of polymerization in the aqueous domain and the critical degree of polymerization that must be reached before a chain enters a micelle to form a particle. In addition, the probability of monomer/oligomer radical exit from a particle and entering another becomes higher with increasing water solubility, which results in a higher chance of biradical termination. The reverse effects are expected for monomers of lower water solubility. Lastly, the monomer water solubility is expected to affect the partitioning of the monomer during the microemulsion polymerization, due to the change in the microemulsion phase boundary.[5]

In this chapter, the effect of the monomer aqueous solubility is investigated. The RAFT microemulsion polymerization of a lower solubility monomer, styrene (St), and a higher solubility monomer, ethyl acrylate (EA), are studied and compared to the results of the moderately soluble BA monomer from the previous chapter (see **Table 5.1.1**). Besides aqueous solubility, there are other important chemical and physical factors that come into effect; such as the polarity and the monomer's interaction with the polymer. The polarity, for instance, affects

the degree of water solvation at the micelle/particle interface with the aqueous medium. The BA and EA have polarities similar to water, hence a good degree of solvation is expected.

Table 5.1.1: Physical properties of the monomers and their polymers; solubility in water, Hildebrand's solubility parameter (δ) of the monomer and polymer, and the Flory-Huggins interaction parameter (χ) between the monomer and polymer.

	Styrene (St)	Butyl Acrylate (BA)	Ethyl Acrylate (EA)
Aq. Solubility (mM)	2.9 [ref 8]	10.9 [ref 8]	150 [ref 8]
Polarity (Debye)	0.13 [ref 8]	1.72 [ref 9]	2.0 [ref 8]
δ mon ($cal^{0.5}/cm^{1.5}$)	9.30 [ref 10]	8.68 [ref 10]	8.60 [ref 10]
δ poly ($cal^{0.5}/cm^{1.5}$)	9.29 [ref 11]	8.8 [ref 11]	9.43 [ref 12]
χ mon-poly[a] ($\times 10^{-3}$)	0.02	3.50	127

[a] $\chi = Vr(\delta mon - \delta poly)/R.T$, where Vr is the molar volume, R is the gas constant, and T is the temperature (298 K).

The relative solubility of the monomer in the polymer and surfactant tails determines the monomer concentration at the locus of polymerization. The monomer-polymer interactions can be qualitatively assessed using the Flory-Huggins interaction parameter (χ) calculated from the experimental solubility parameters (δ) as shown in **Table 5.1.1**. It worth noting that the EA-Poly(EA) has the highest difference in the solubility parameter leading to the highest χ. Hence, EA is expected to have a higher concentration in the corona during the polymerization.

The RAFT microemulsion polymerizations are performed with the surface-active CTA, B11T, as well as the traditional hydrophobic CTA, B11C. Remarkably, both the St and EA polymerizations produce polymers of lower molecular weight polydispersity than the BA polymerizations for B11T/micelle ratio greater than 1. Moreover, the surface-active CTA, B11T, further demonstrates better RAFT control than B11C with both monomers.

5.2 Materials and Methods

The polymerizations of EA and St were carried out in microemulsion stabilized by DTAB surfactant. An α=5.0% and γ=12.0% were used for EA microemulsion, where $\alpha = mass_{monomer}/(mass_{monomer} + mass_{water}) \times 100$ and $\gamma = mass_{surfactant}/(mass_{surfactant} + mass_{monomer} + mass_{water}) \times 100$, while St microemulsion was composed of an α=4.0% and γ=12.0%. A lower α was chosen for St to be good margin from the phase boundary ($\alpha_{boundary}$~6%). The polymerizations were performed at 45°C and were started by adding 1ml of purged water containing VA044 initiator for a VA044 concentration of 2 wt% with respect to monomer. Reaction calorimetry was used to measure the monomer conversion along with sampling over time to check for gravimetric conversion and perform molecular weight analysis. The RAFT microemulsion polymerizations of EA were done at the following CTA per micelle ratios: 0.3, 1.1, 3.5, while the RAFT microemulsion polymerizations of St were done at the following CTA per micelle ratios: 0.3, 0.6, 1.1, 2.3, 3.5.

5.3 Results and Discussion

5.3.1 Uncontrolled Microemulsion Polymerization

In order to make a valid comparison between St, BA and EA in RAFT microemulsion polymerization, the uncontrolled microemulsion polymerization kinetics should be first understood. The BA and EA microemulsion polymerization reaches full conversion in couple minutes, while St microemulsion polymerization reaches 94% conversion after an hour (**Figure 5.3.1-left**).

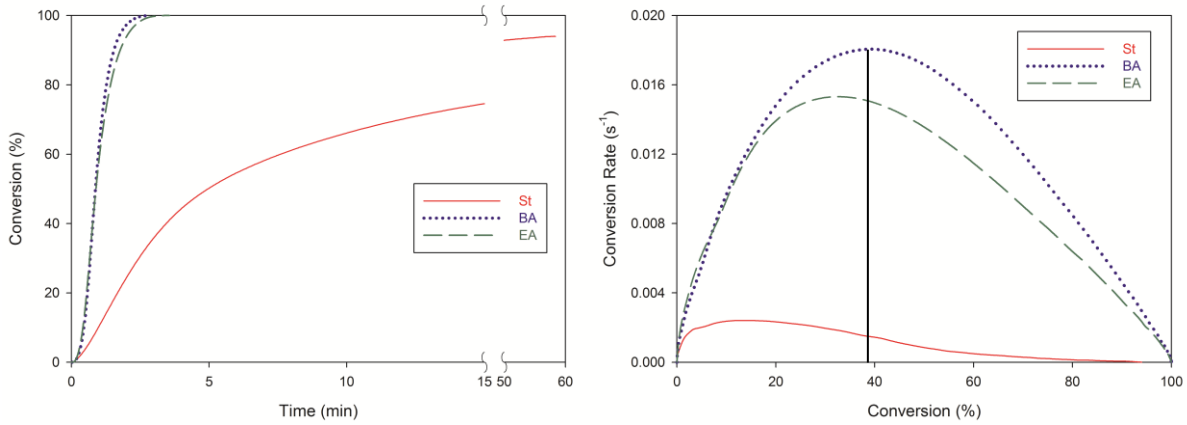

Figure 5.3.1: Left: Conversion of St, BA and EA as a function of time for uncontrolled microemulsion polymerization. Right: Rate of conversion of St, BA and EA as a function of conversion for uncontrolled microemulsion polymerization. The vertical line indicates the location of rate maximum predicted for microemulsion polymerization by the Morgan model.

The observed slower rate in St microemulsion polymerization is mainly due to the lower free-radical polymerization propagation constant (k_p) of styrene ($k_{p,St}$~10^2 $M^{-1}s^{-1}$)[13] which is two order of magnitude less than that of BA and EA ($k_{p,BA}$~$k_{p,EA}$~10^4 $M^{-1}s^{-1}$)[14, 15]. Moreover, poly(St) chain growth may experience diffusion limitations to further propagation within the polymer particle as conversion increases, since the reaction temperature is well below the glass transition temperature of poly(St) ($T_{g,poly(St)}$~100°C).[5] This could also explain the incomplete conversion in St microemulsion polymerization.

As shown in **Figure 5.3.1-right**, the maximum rate of conversion of BA microemulsion polymerization is reached at around 39% in agreement with the Morgan model prediction. On the other hand, the EA and St microemulsion polymerizations show a shift in the location of rate maxima to lower conversions (33% and 15%, respectively). According to the Morgan model, deviations from the predicted location of the rate maximum can be attributed to biradical termination and/or non-linear monomer diffusion.[16]

De Vries et al.[5] have argued the reasons for the observed location of rate maximum at lower conversions in St microemulsion polymerization. Using monomer partitioning data from SANS, which showed a nearly linear decrease in the concentration of monomer in the particle, they inferred that non-linearity by itself cannot justify the shift in the location of rate maximum, hence, biradical termination cannot be dismissed. Moreover, the effects of diffusion limitations to further propagation, which could slow the monomer consumption rate at higher conversions, could not be independently confirmed.

EA microemulsion polymerization shows a slight shift in the location of the rate maximum to 33% conversion. Due to the high water solubility of EA, the monomer/oligomer radical would enter and exit more number of micelles and particles before nucleating a micelle; hence, biradical termination from particle entry become more significant.[5] A SANS monomer partitioning study would be needed to identify if non-linearity in partitioning of monomer occurs.

The polymer nanoparticle size shows a strong proportional relationship with the monomer solubility (**Table 5.3.1**), which is in accordance with the literature for microemulsion polymerization.[1, 6] The ratio of the number of particles to the initial number of monomer-swollen micelles ($N_{part,f}/N_{micelle,i}$) is calculated for each monomer to estimate the ratio of initiated micelles. (See Appendix B for the calculation of $N_{part,f}/N_{micelle,i}$)

Table 5.3.1: Volume-average polymer nanoparticle diameter for the uncontrolled microemulsion polymerization obtained using dynamic light scattering, and the ratio of polymer particles to monomer-swollen micelles $N_{part,f}/N_{micelle,i}$.

	Particle Diameter (nm)	$N_{part,f}/N_{micelle,i}$
St	28	1:830
BA	38	1:1500
EA	69	1:9000

Comparing the acrylate monomers (BA and EA), which have a similar rate of polymerization constant, the poly(EA) particles are much larger in size and the fraction of initiated EA-swollen micelles is much lower. This indicates that the higher water solubility monomer EA partitions rapidly to the locus of polymerization causing the rapid depletion of the micelles and swelling of the polymer particles earlier in the polymerization.

5.3.2 RAFT Microemulsion Polymerization

5.3.2.1 Polymer nanoparticle size

Both of the St and BA RAFT microemulsion polymerizations produce smaller latex size compared to their corresponding uncontrolled polymerization (**Figure 5.3.2**), which is expected. On the other hand, the EA RAFT microemulsion polymerizations produce latex size higher or similar to the particles size from the uncontrolled polymerization.

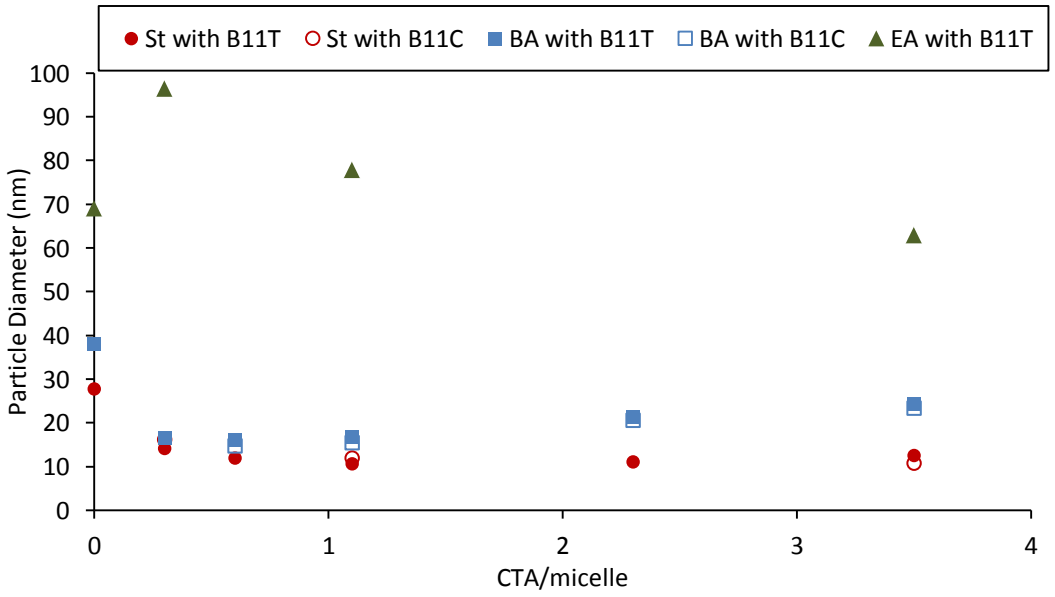

Figure 5.3.2: Volume-average latex particle diameter of poly(St), poly(BA) and poly(EA) as a function of CTA/micelle, measured by dynamic light scattering.

As discussed in the previous chapter, the polymer particle size is expected to decrease with longer polymerizations (i.e. as CTA/micelle increases) due to the initiation of more monomer-swollen micelles with the continuous thermal dissociation of the initiator. The RAFT microemulsion polymerization of the lower solubility monomers, St and BA, follow such expectation by producing smaller latex size in the controlled polymerization compared to the uncontrolled. However, the poly(BA) particles increase in diameter as the CTA/micelle ratio increases. The extended polymerization time at higher CTA/micelle ratios facilitates coalescence between the polymer particles and the high concentration of monomer-swollen micelles. The poly(St) particles, on the other hand, decrease in size as the CTA/micelle ratio increases from 0.3 to 1.1 and above CTA/micelle ratio of 1.1 the poly(St) particle size does not change. Examination of the ratio of the number of poly(St) particles to the initial number of monomer-swollen micelles ($N_{part,f}/N_{micelle,i} \cong 1:40$) at B11T/micelle ratio of 3.5 (**Table 5.3.2**) indicates that the possible number of monomer-micelle initiations is reaching its limit. The coalescence in St RAFT microemulsion polymerization is limited compared to BA RAFT microemulsion, since St is more hydrophobic and has much lower polarity compared to BA, so St tends to be more partitioned to the core of the polymer particle while the BA may partition closer to the surface.

Table 5.3.2: The ratio of final polymer particles to initial monomer-swollen micelles, $N_{part,f}/N_{micelle,i}$ at B11T/micelle ratio of 3.5.

	$N_{part,f}/N_{micelle,i}$
St	1:40
BA	1:350
EA	1:7000

The fact that poly(EA) particles produced from RAFT microemulsion polymerization are not smaller in size compared to the poly(EA) produced from the uncontrolled polymerization indicates that micelle initiation does not increase with time. Moreover, the ratio of the final number of poly(EA) particles to the initial number of monomer-swollen micelles $N_{part,f}/N_{micelle,i}$ is less than 1:7000 for all the EA polymerization, which means that only a few of the micelle are initiated. This indicates that the EA monomer either depletes rapidly from uninitiated micelles early in the polymerization and swells the polymer particles or coalescence becomes dominant. EA has the highest water solubility and polarity compared to the other monomers studied. Moreover, EA has the lowest solubility in its polymer compared to the other monomers. Hence, the hydrophobic poly(EA) is likely to partition to the core of the polymer particle, while EA partitions closer to the surface forming a soft shell that facilitates coalescence.

5.3.2.2 Polymerization Kinetics

In this section, the change in kinetics profiles for the lower solubility monomer St and higher solubility monomer EA are presented and compared against the trends predictions by O'Donnell Model for RAFT microemulsion polymerization.[17]

Similar to the BA RAFT microemulsion polymerization in Chapter 4, the St and EA RAFT microemulsion polymerizations experience increase rate retardation as the CTA/micelle ratio increases (**Figure 5.3.3**). All of the St and EA RAFT microemulsion polymerizations reached 100%.

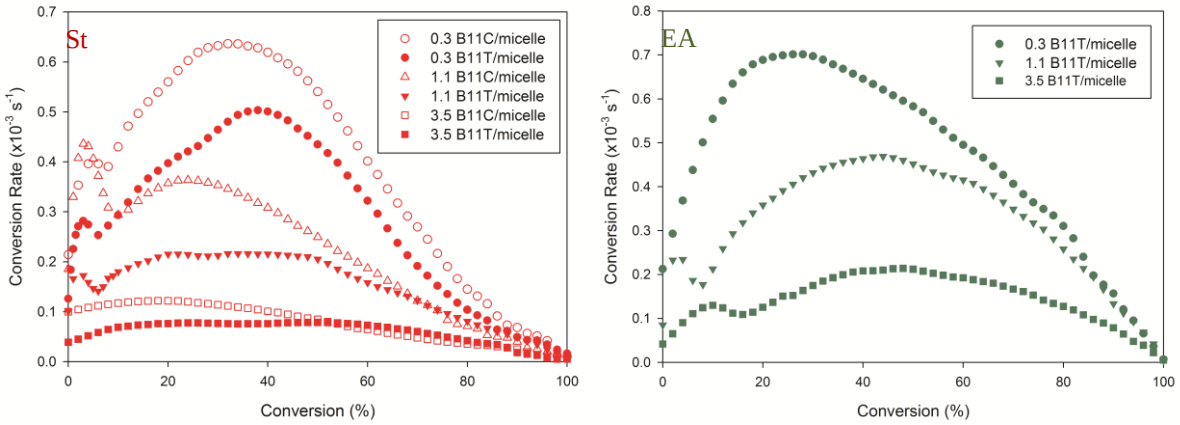

Figure 5.3.3: Rate of conversion as a function of conversion for RAFT microemulsion polymerization of styrene (left) and ethyl acrylate (right).

The small rate peaks observed at lower conversions (<10%) is believed to be artificial from the calorimeter response to the injection of the initiator solution. Such peak was not observed in the RAFT microemulsion polymerization of BA, since BA microemulsion polymerization had higher heat release rates than St and EA.

The monomer conversion rates of St RAFT microemulsion polymerizations with the surface-active CTA, B11T, are lower than the monomer conversion rates from the polymerizations with the traditional CTA, B11C (**Figure 5.3.3-left)**. The conversion rate is proportional to the monomer concentration at the locus of polymerization. The B11C is very hydrophobic and is likely to partition to the core of a poly(St) particle where the St concentration is higher compared to the corona. The location of rate maxima in the RAFT microemulsion polymerization with B11C shifts from 32% to 20% conversions as the B11C/micelle ratio increases from 0.3 to 3.5. The O'Donnell model demonstrates that a shift in the rate maxima to lower conversions as the CTA/micelle increases would be observed when the CTA diffuses from micelles to the locus of polymerization,[17] which was experimentally observed in the BA RAFT

microemulsion polymerization with a traditional chain transfer agent MOEP.[18] The continuous diffusion of CTA to polymer particles increases the CTA per particle ratio over time and, consequently, the active radical propagation rate decreases with conversion.

The polymerizations with the surface-active CTA B11T show two rate regions similar to the observations seen in BA RAFT microemulsion polymerization with B11T (**Section 4.3.2**). Overall, a shift in the location of rate maxima cannot be inferred from the data due to nearly constant rate at higher CTA/micelle ratios. Discussion about the polymerization rate kinetics and CTA activation for all the polymerizations are presented in **CHAPTER 6**.

EA RAFT microemulsion polymerizations with the surface-active CTA show an upward shift in the location of rate maxima from 26% to 49% conversion as the B11T/micelle increases from 0.3 to 3.5 (**Figure 5.3.3-right**). The O'Donnell model predicts that an upward shift would only occur when the CTA activation is reaction rate limited. This is very plausible for the EA microemulsion polymerization, since the EA forms much larger polymer nanoparticles compared to the BA and St, and the monomer partitions rapidly to the polymer particle; hence the polymerization and CTA activation is localized in the polymer growing particles earlier in the polymerization.

The EA RAFT microemulsion polymerizations with the traditional chain transfer agent B11C were unsuccessful. The microemulsion polymerizations with low B11C/micelle have shown uncontrolled kinetics behavior (rapid heat release) and multimodal molecular weight distribution, while the microemulsion polymerizations with the highest B11C/micelle ratio of 3.5 have shown phase separation as seen in the formation of yellow precipitate during the polymerization. The analysis of the precipitate shows it is rich with the B11C and low molecular weight polymer chains.

Degree of rate retardation:

The degree of rate retardation is assessed by normalizing the RAFT retarded maximum rate to the maximum rate obtained in the uncontrolled polymerization of the same monomer (**Figure 5.3.4**). Hence, a decrease in the normalized maximum rate of conversion would indicate an increase in the rate retardation. Since the maximum rate is normalized, the effects of the intrinsic monomer propagation rate constants are eliminated.

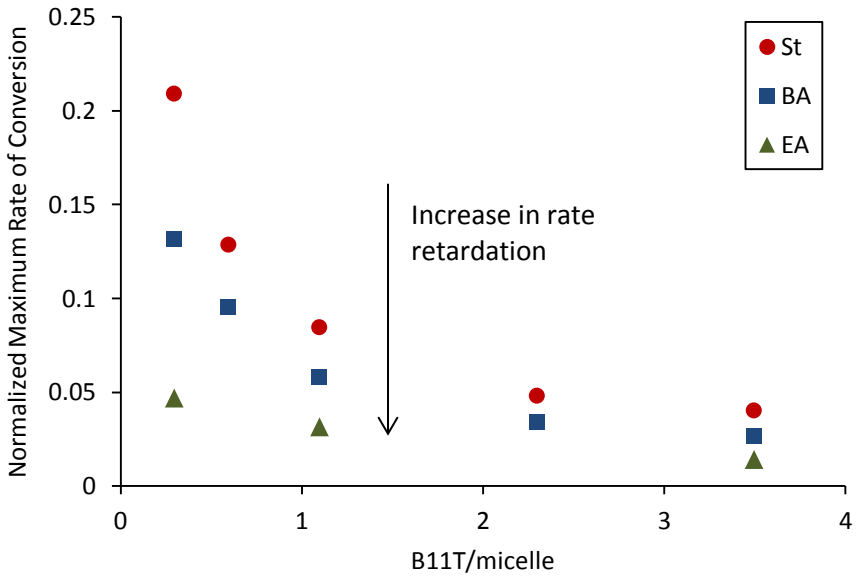

Figure 5.3.4: The change in the normalized maximum rate of conversion as the surface-active CTA B11T/micelle ratio increases for St, BA and EA RAFT microemulsion polymerizations. The decrease in the maximum rate indicates higher rate retardation.

The degree of rate retardation increases significantly as CTA/micelle ratio increases for all the monomers. As discussed in the previous chapter, the rate retardation is expected to increase as the CTA/micelle increase due to the higher number of CTAs at the locus of polymerization. Interestingly, the data shows a direct relationship between the degree of rate retardation and the monomer water solubility. The O'Donnell model shows that the rate

retardation is directly proportional to the CTA/particle ratio. In the case of the high water solubility monomer EA, this implicates that there is more CTA in the poly(EA) particles and/or less number of poly(EA) particles compared to the poly(BA). The molecular weight analysis (**Section 5.3.2.3**) indicates a similar degree of B11T activation between EA and BA polymerizations, whereas the final poly(EA) particle size is three times higher than poly(BA) (**Section 5.3.2.1**); thus, the higher rate of retardation in EA polymerizations is due to a higher CTA/particle ratio in poly(EA) particles.

5.3.2.3 Molecular Weight and Polydispersity

Both of the RAFT micromulsion polymerizations of low and high water solubility monomers, St and EA, with the surface-active chain transfer agen B11T show linear increase in the number average molecular weight (M_N) as a function of conversion (**Figure 5.3.5**). The linearity of M_N is an indication of RAFT control according to equation 2.1.

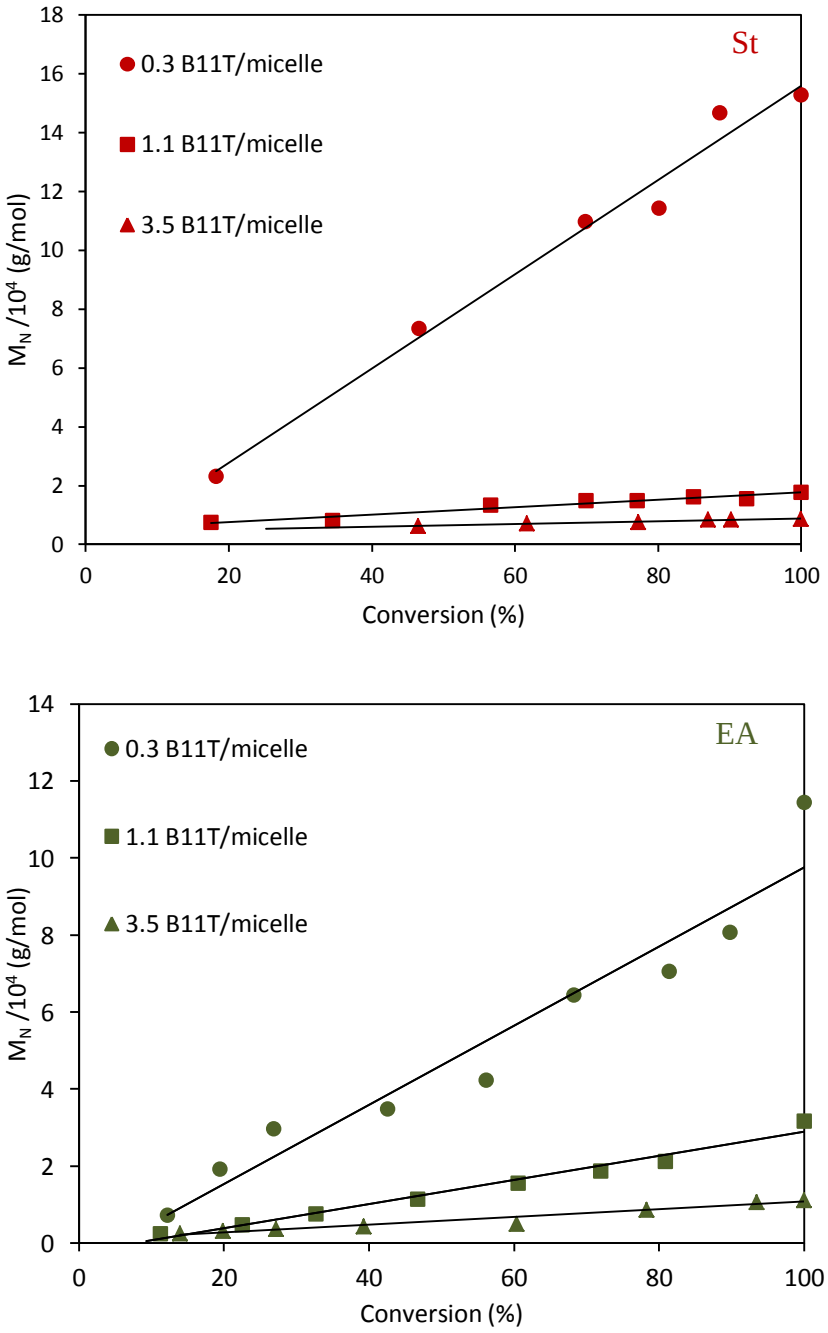

Figure 5.3.5: Number average molecular weight (M_N) of poly(St) (top) and poly(EA) (bottom) from RAFT microemulsion polymerization with surface-active CTA B11T. The lines are least-squares linear fits to the data.

Similar to BA RAFT microemulsion polymerization, the St and EA RAFT microemulsion polymerizations achieve final M_N values higher than the prediction (**Figure 5.3.6**), which indicates partial activation of the CTA.

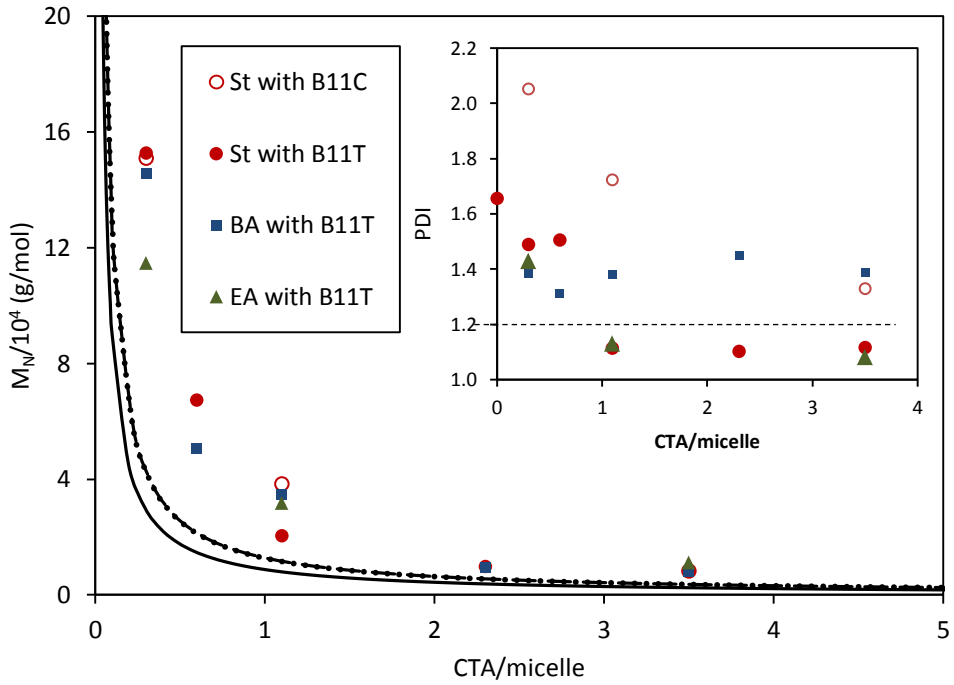

Figure 5.3.6: Number average molecular weight (M_N) and polydispersity index (PDI=M_W/M_N) (inset) of Poly(St), poly(BA) and poly(EA) at full conversion. The lines are the predictions from equation 2.1, solid line for St, dashed line for BA, and dotted for EA.

The polydispersity index (PDI) of all the polymers, except for poly(BA), shows a decreasing trend with increasing the CTA/micelle ratio, which is expected since there is a higher probability that a propagating radical would activate a CTA upon entry to a particle as the CTA/micelle ratio increases. At CTA/micelle ratio ≥1.1, the poly(EA) and Poly(St) from the polymerizations with the B11T achieve a desired low PDI~1.1.

The St microemulsion polymerizations with B11C show higher PDI values than those obtained from St polymerizations with B11T. Moreover, the PDI values at 0.3 and 1.1 B11C/micelle (PDI = 2.1 and 1.73, respectively) are even higher than the PDI from uncontrolled St microemulsion polymerization (PDI = 1.66). As discussed in the previous chapter, the diffusion of B11C over the polymerization time to the locus of polymerization leads to broad molecular weight distribution.

Degree of surface-active chain transfer agent activation:

All of the RAFT microemulsion polymerizations show partial activation of the surface-active chain transfer agent B11T (**Figure 5.3.7**), which indicates that the B11T remains partitioned between uninitiated micelles and polymer particles regardless of the monomer aqueous solubility.

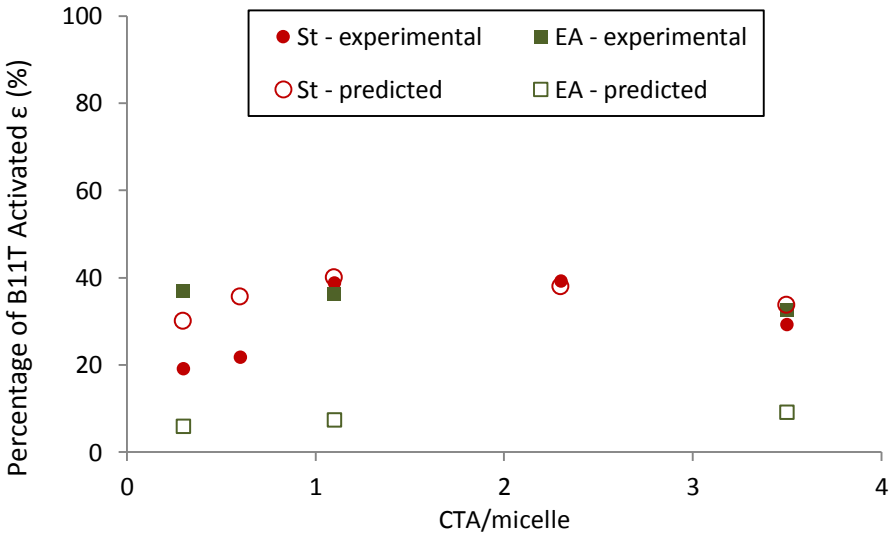

Figure 5.3.7: Percentage of surface-active CTA B11T activated (ε) for the St and EA RAFT microemulsion polymerizations. The experimental value is obtained from eq 4.2, and the predicted value is obtained from eq 4.3.

There is a very close match between the experimental B11T activated fraction (ε^{exp}), that is based on the final molecular weight (eq 4.3), and the predicted ($\varepsilon^{predicted}$), that is based on the fraction of initiated micelles and surface area growth (eq 4.3), for St RAFT microemulsion polymerization at CTA/micelle ratios ≥ 1.1. This indicates that the activation of the surface-active chain transfer agent in St polymerizations is directly dependent on the fraction of initiated micelles and adsorption of more surface-active CTA due to surface area growth. However, in the case of EA RAFT microemulsion polymerization, the ε^{exp} is significantly higher than $\varepsilon^{predicted}$. The $\varepsilon^{predicted}$ (eq 4.3) depends on the actual fraction of initiated micelles as estimated by the ratio of final number of polymer particles to the initial number of micelles ($N_{part,f}/N_{micelle,i}$). Coalescence between initiated micelles reduces the number of final particles; hence, $\varepsilon^{predicted}$ would be under estimated. Consequently, this suggests significant coalescence in EA RAFT microemulsion polymerization.

5.4 Conclusions

The water solubility of the monomer significantly impacts the nanoparticle size and polymerization kinetics in RAFT microemulsion polymerization. The size of the polymer particle increases as the water solubility of the monomer increases, indicating a decrease in the number density of polymer particles. Coalescence occurs extensively in monomers of high water solubility and polarity, which decreases the number of particles and leads to formation of larger particles. As a results, the number of CTA per particle increases with water solubility of the monomer and leads to an increase in the degree of rate retardation.

The surface-active chain transfer agent B11T in all of the RAFT microemulsion polymerizations have shown successful molecular weight control, whereas the traditional chain transfer agent have shown poor control in all of the polymerizations. The desired low

polydispersity (PDI~1.1) is achieved in the lower water solubility monomer St and higher water solubility monomer EA RAFT microemulsion polymerizations. Hence, monomer solubility dose not adversely affect the polymerization control of the surface-active CTA. All of the RAFT microemulsion polymerizations with the surface-active chain transfer agent B11T show partial CTA activation, indicating that B11T remains partitioned between micelles and polymer particles.

5.5 Bibliography

1. Arellano, J.; Flores, J.; Zuluaga, F.; Mendizabal, E.; Katime, I. *J. Polym. Sci. Pol. Chem.* **2011,** 49, (14), 3014-3019.

2. Bhawal, S.; Sanghvi, P. G.; Devi, S. *European Polymer Journal* **2003,** 39, (2), 389-396.

3. Co, C. C.; de Vries, R.; Kaler, E. W. *Macromolecules* **2001,** 34, (10), 3224-3232.

4. Co, C. C.; Cotts, P.; Burauer, S.; de Vries, R.; Kaler, E. W. *Macromolecules* **2001,** 34, (10), 3245-3254.

5. de Vries, R.; Co, C. C.; Kaler, E. W. *Macromolecules* **2001,** 34, (10), 3233-3244.

6. O'Donnell, J. M. Reversible addition-fragmentation chain transfer in microemulsion polymerizations. Dissertation, University of Delaware, Newark, Delaware, 2007.

7. O'Donnell, J.; Kaler, E. W. *Macromolecular Rapid Communications* **2007,** 28, (14), 1445-1454.

8. Lange, N. A.; Dean, J. A., *Lange's Handbook of chemistry*. McGraw-Hill: 1979.

9. Os, N. M.; Haak, J. R.; Rupert, L. A. M., *Physico-chemical properties of selected anionic, cationic, and nonionic surfactants*. Elsevier: 1993.

10. Belmares, M.; Blanco, M.; Goddard, W. A.; Ross, R. B.; Caldwell, G.; Chou, S. H.; Pham, J.; Olofson, P. M.; Thomas, C. *J Comput Chem* **2004,** 25, (15), 1814-1826.

11. Wohlfarth, C., Solubility Parameters of Selected Polymers. In *CRC Handbook of Chemistry and Physics*, 92 ed.; Haynes, W. M., Ed. Taylor & Francis: Boca Raton, FL, 2011.

12. Mark, J. E., *Polymer data handbook*. Oxford University Press: New York, 1999; p xi, 1018 p.

13. Kamachi, M.; Yamada, B., Propagation and Termination Constants in Free Radical Polymerization. In *Polymer Handbook*, Fourth ed.; Brandup, J.; Immergut, E. H.; GRULKE, E. A., Eds. JOHN WlLEY & SONS, INC.: 1999.

14. Kock, J. B. L. d. Chain-Length Dependent Bimolecular Termination in Free-Radical Polymerization. Technical University of Eindhoven, Eindhoven, The Netherlands, 1999.

15. Asua, J. M.; Beuermann, S.; Buback, M.; Castignolles, P.; Charleux, B.; Gilbert, R. G.; Hutchinson, R. A.; Leiza, J. R.; Nikitin, A. N.; Vairon, J.-P.; van Herk, A. M. *Macromolecular Chemistry and Physics* **2004,** 205, (16), 2151-2160.

16. Morgan, J. D.; Lusvardi, K. M.; Kaler, E. W. *Macromolecules* **1997,** 30, (7), 1897-1905.

17. O'Donnell, J. M.; Kaler, E. W. *Journal of Polymer Science Part A: Polymer Chemistry* **2010,** 48, (3), 604-613.

18. O'Donnell, J.; Kaler, E. W. *Macromolecules* **2010,** 43, (4), 1730-1738.

CHAPTER 6. KINETIC ANALYSIS OF RAFT MICROEMULSION POLYMERIZATION

6.1 Introduction

As shown in Chapter 4 and 5, the polymerization rate in RAFT microemulsion polymerization decreases with increasing CTA/micelle ratio. O'Donnell and Kaler developed a kinetic model, based on the simple Morgan model, for the RAFT microemulsion polymerization (described in **Section 2.3**) which was able to quantitatively capture the kinetic data of the RAFT microemulsion polymerizations of butyl acrylate with methyl-2-(O-ethylxanthyl)propionate (MOEP) as a function of the MOEP/micelle ratio.[1] The increase in rate retardation with increasing CTA/micelle ratio was shown to result from slow fragmentation of the intermediate macroRAFT radical (P•XP). The O'Donnell model captures the average polymerization kinetics and facilitates the analysis of the magnitude of both the fragmentation rate constant (k_f) and CTA activation rate constant (k_{tr}). The comparison of k_{tr} to the addition rate constant (k_{add}) determines if CTA activation is reaction- or diffusion- limited. These results can be qualitatively compared to the fraction of CTA activated, which was calculated in **Section 4.3.1 and 5.3.2.3**.

Schematic 6.1.1: Simplified RAFT polymerization reactions

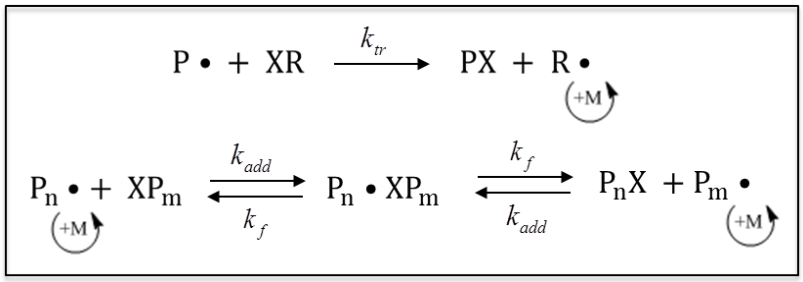

The selection of the monomer parameters required to fit the kinetic data with the O'Donnell model are described in **Section 6.2.1**. The determination of the RAFT addition rate constant (k_{add}) for the traditional CTA *benzyl undecyl carbonotrithioate* (B11C) and surface-active CTA *2-((11-(((benzylthio)carbonothioyl)thio)undecanoyl)oxy)-N,N,N-trimethylammonium iodide* (B11T) is described in **Section 6.2.2**. The reaction rate data for the n-butyl acrylate (BA) and styrene (St) RAFT microemulsion polymerization with the traditional chain transfer agent B11C are used to determine the respective k_f and k_{tr} values (**Section 6.3.1**). The k_f values are then used in assessing the k_{tr} value for the RAFT microemulsion polymerizations with the surface-active chain transfer agent B11T (**Section 6.3.2**).

6.2 Model Parameters

6.2.1 Selection of Monomer Parameters

The Morgan model[2] for uncontrolled microemulsion polymerization provides a simple tool for studying microemulsion polymerization kinetics and assessing deviations due to biradical termination and nonlinear monomer partitioning (described in **Section 2.2**). The radical concentration as a function of thermal decomposition of initiator, transfer and termination reactions was derived by de Vries and coworkers by assuming that instantaneous polymer particle termination occurs when an aqueous phase radical enters an active polymer particle.[3] The source of the aqueous phase radical can be either initiator-derived or monomer radicals derived from chain transfer to monomer. The probability of polymer particle termination is inversely proportional to the characteristic residence time (τ_{res}) of a typical aqueous phase radical in a micelle, which is approximated by:[3]

$$\tau_{res} \approx q \frac{{R_{mic}}^2}{3D_{aq}^{mon}} \qquad \text{(eq 6.1)}$$

where R_{mic} is the micelle radius (~3 nm), D_{aq}^{mon} is the diffusivity of the monomer in the aqueous phase (~10^{-9} m^2/s), and q is the partition coefficient of the monomer between the micelle and aqueous phases:

$$q = \frac{C_{mon}^{(mic)}}{C_{mon}^{(aq)}} \quad \text{(eq 6.2)}$$

where $C_{mon}^{(mic)}$ is the monomer concentration in the hydrophobic core of the monomer swollen micelles, and $C_{mon}^{(aq)}$ is the monomer aqueous solubility.

The monomer concentration at the locus of polymerization ($C_{mon}^{(part)}$) can be evaluated from in-situ small-angle neutron scattering (SANS) data. de Vries and coworkers have empirically accounted for deviation from linear monomer partitioning by introducing the exponent b to the function:[3, 4]

$$C_{mon}^{(part)} = C_{mon,0}^{(part)}(1 - f)^b \quad \text{(eq 6.3)}$$

where $C_{mon,0}^{(part)}$ is the initial monomer concentration at the locus of polymerization. BA monomer partitioning in the RAFT microemulsion polymerization with MOEP is found to be nearly linear with slight positive deviation (b = 1 - 0.8)[5], whereas St has been shown to have a b value of 1.4[3, 4] in microemulsion polymerization.

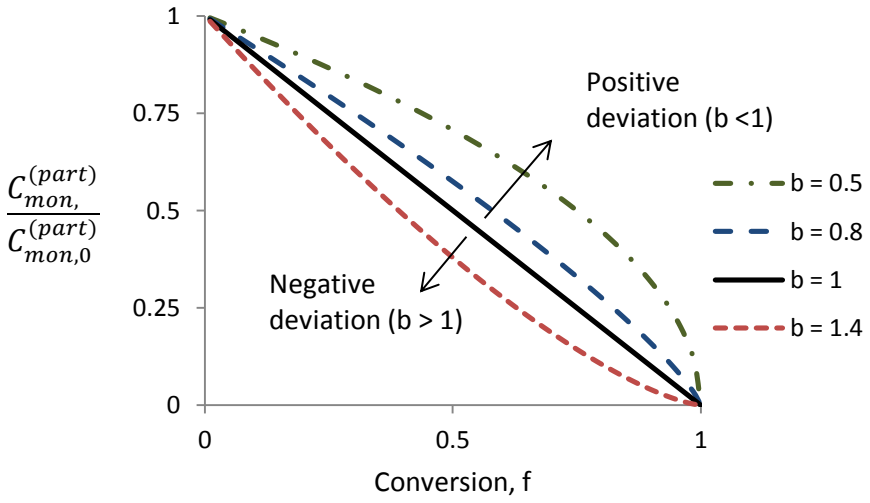

Figure 6.2.1: Illustration of the deviations from linear monomer partitioning, using eq. 6.3.

Ethyl Acrylate Parameters from Microemulsion Polymerization Kinetic Data:

Since the ethyl acrylate (EA) monomer partitioning in microemulsion polymerization has not been studied, the uncontrolled microemulsion polymerization data is used to deduce the partitioning parameter. The EA uncontrolled microemulsion polymerization kinetic data shows a rate maximum at 33% conversion (**Section 5.3.2.2**) which deviates from the Morgan model prediction of 39% conversion for linear monomer partitioning and negligible biradical terminations. Termination reactions in EA microemulsion polymerization are not likely to be negligible because its τ_{res} is much lower than τ_{res} for St and BA. Moreover, EA is expected to positively deviate from linearity (b < 1) due to significant particle coalescence, which increases the monomer concentration at the locus of polymerization.

The EA uncontrolled microemulsion polymerization data is used to obtain the value of b that captures the location of the rate maximum (**Figure 6.2.2**). Moreover, the value of k_p is selected to capture the magnitude of the rate maximum.

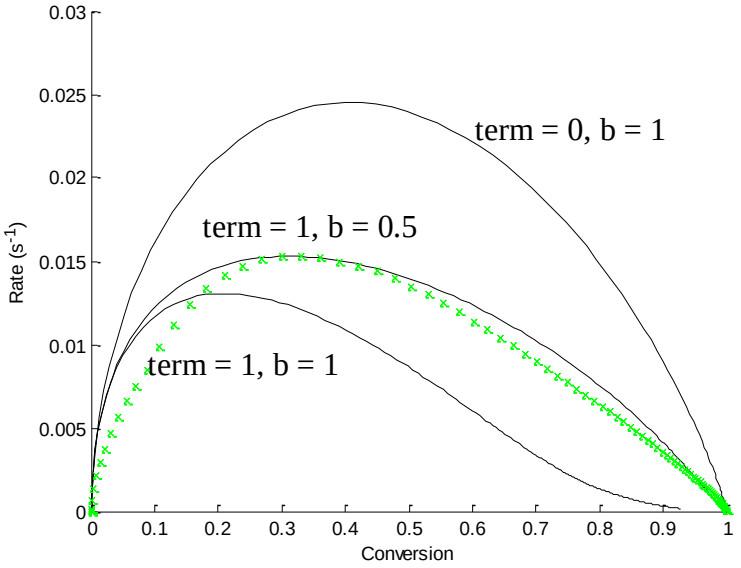

Figure 6.2.2: Rate of uncontrolled ethyl acrylate microemulsion polymerization as a function of conversion. (x) Experiment, (-) Morgan model predictions (term = 0, b = 1), model prediction with biradical termination (term = 1, b = 1) and model prediction with biradical termination and non-linear monomer termination (term = 1, b = 0.5). The propagation rate constant used is k_p = 2,500 M^{-1} s^{-1}.

Only when non-linear monomer partitioning is considered (b = 0.5), can the model capture the location of the rate maximum with biradical terminations. The polymerization rate constant k_p of EA (2,500 M^{-1} s^{-1}) that is obtained from the fitted EA microemulsion polymerization (**Figure 6.2.2**) is on the same order of magnitude of k_p for BA (**Table 6.2.1**) and that of a reported k_p for EA (k_p = 4,700 M^{-1} s^{-1})[6].

Table 6.2.1: Summary of the monomer properties used in the kinetic model for RAFT microemulsion polymerization; propagation rate constant k_p at 45ºC, initial monomer concentration at the locus of polymerization $C_{mon,0}^{(part)}$, linear/non-linear correlation factor b, chain transfer to monomer rate constant k_{tr}^{mon}, and monomer characteristic residence time τ_{res}.

Monomer	k_p (x 10^2 M^{-1} s^{-1})	$C_{mon,0}^{(part)}$	b	k_{tr}^{mon} (M^{-1} s^{-1})	τ_{res} (s)
St	2 [ref 7]	3.8 [a]	1.4 [ref 4]	0.02 [ref 3, 8]	8.3×10^{-6} [b]
BA	16.6 [ref 1]	2.9 [ref 1]	1-0.8 [ref 1]	0.0025 [ref 1]	1.2×10^{-6} [ref 1]
EA	25 [c]	3.3 [d]	0.5 [c]	~0.0025 [e]	6.7×10^{-8} [b]

[a] From ref [4]; interpolated at α = 4% from SANS data provided for α = 3% and 5%.
[b] Evaluated using eq. 6.1, EA is assumed to swell the surfactant tails, while St is assumed to reside in the core.
[c] Obtained from microemulsion polymerization best fit, Fig. 6.2.2
[d] Estimated from monomer swelling the surfactant tails $C_{mon,0}^{(part)} \cong \frac{n_{mon}}{V_{surf\ tails}+V_{mon}}$
[e] Assumed same as BA.

6.2.2 Chain Transfer Agent Addition Rate Constant k_{add}

Kubo et al.[9] have determined the k_{add} value for styrene (St) and methyl methacrylate (MMA) with a macroRAFT molecule S=C(CH3)S-Polymer (**Table 6.2.2**). The chain transfer agents (B11C & B11T) used in this research have a similar alkyl Z-group. Computational studies of RAFT polymerization have shown that a methyl Z-group has similar fragmentation efficiency to those of S-methyl and S-ethyl.[10] Hence the k_{add} for St with B11C and B11T can be fairly assumed to be similar to the experimentally determined k_{add} for St with S=C(CH3)S-Poly(St).

Table 6.2.2: Chain transfer agent addition rate constants used in the kinetic model for RAFT microemulsion polymerization.

Monomer	CTA	k_{add} ($\times 10^4$ M^{-1} s^{-1})	Used for
St	S=C(CH_3)S-Poly(St)	8.6 [a]	St w/ B11C & B11T
MMA	S=C(CH_3)S-Poly(MMA)	4.5 [a]	-
BA	B11C: S=C(S-(CH_2)$_{10}$-CH_3)S-CH_2Ph	2 [b]	BA w/ B11C & B11T EA w/ B11T

[a] From ref [9], at 45°C
[b] Determined using eq. 6.4

A reported k_{add} value for BA with a similar CTA could not be found. Instead, the k_{add} value for BA with B11C is approximated from the RAFT solution polymerization experimental data using a method described by Barner-Kowollik and coworkers which uses molecular weight to deduce the rate constant value:[11]

$$k_{add} = \frac{k_p[Mon]_0}{(DP^{inst}-1)[CTA]_0 0.5} \qquad \text{(eq 6.4)}$$

where $[Mon]_0$ and $[CTA]_0$ are the initial monomer and chain transfer agent concentrations, respectively, and DP^{inst} is the instantaneous degree of polymerization, determined from the linear fit of the number-average molecular weight versus conversion, as shown in **Figure 6.2.3**.

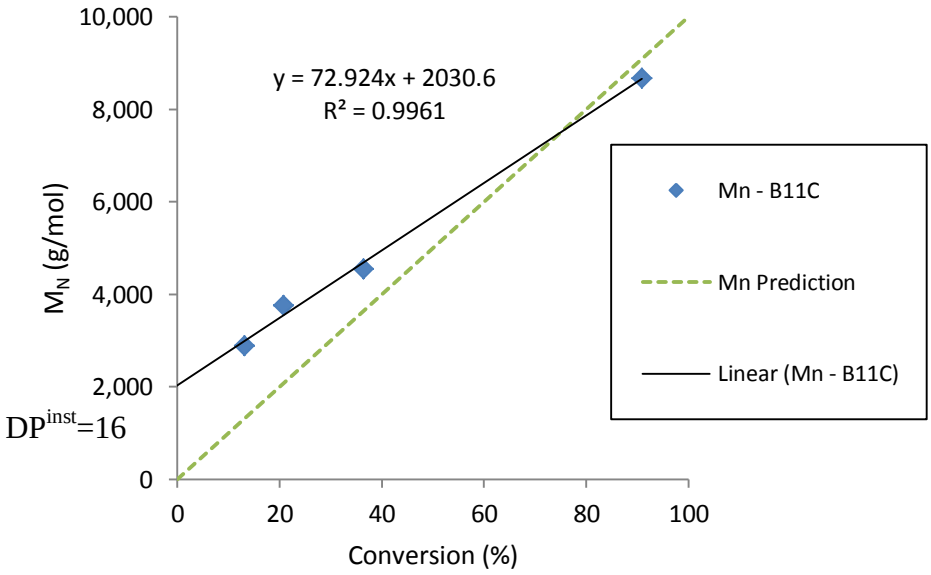

Figure 6.2.3: Number-average molecular weight (M_N) as a function conversion for poly(BA) from solution RAFT polymerization with B11C. Extrapolation of the linear least-square fit to the data to zero conversion yields the instantaneous molecular weight.

The k_{add} value (2×10^4 M^{-1} s^{-1}) for BA with B11C from eq. 6.4 is similar to the values calculated for St and MMA with the similar chain transfer agent. The same k_{add} value is used for the BA and EA with B11T chain transfer agent.

6.3 Results and Discussions

6.3.1 Model Fitting RAFT Microemulsion Polymerizations with the Traditional CTA B11C

The average volume of a single particle in which the polymerization occurs $\langle V_{part} \rangle$ (used in eq. 2.12 in **Section 2.3**) depends on the partitioning of the monomer within the polymer particle. For BA microemulsion polymerization, the polymerization occurs in the corona formed by the surfactant tails surrounding the polymer core,[5, 12] and V_{part} is approximated from the radius of the polymer core (r_{poly}) and the length of the surfactant tail (l_{tail} ~ 1.67 nm for DTAB) as:[1]

$$\langle V_{part} \rangle = \frac{4}{3}\pi \left[\left(\langle r_{poly} \rangle + l_{tail} \right)^3 - \langle r_{poly} \rangle^3 \right] \qquad \text{(eq 6.5)}$$

and the average radius of polymer core is calculated from the average concentration of polymer in a particle:[1]

$$\left\langle r_{poly} \right\rangle = \left(\frac{3 f M_o MW_{mono}}{4\pi \left[Particles \right] N_A \rho_{mono}} \right)^{1/3} \qquad \text{(eq 6.6)}$$

where ρ_{mono} is the density of the monomer.

On the other hand, the St polymerization is expected to occur within the polymer particle core, since St is very hydrophobic and the monomer-polymer interaction parameter χ is low (i.e. good monomer swelling). Hence, V_{part} for St is approximated as:

$$\langle V_{part} \rangle = \frac{4}{3}\pi \langle r_{poly} \rangle^3 \qquad \text{(eq 6.7)}$$

In the literature, values of the fragmentation rate constant vary over a wide range (from 10^{-2} to 10^{6} s^{-1})[13, 14] because of difference in mechanistic interpretations of the rate retardation, i.e. slow fragmentation[13] versus cross-termination[14] of the macroRAFT radical.

The characteristic activation time of the CTA, based on k_{add} and average CTA concentration at the locus of polymerization, is ~10^{-3} s and ~10^{-4} s for BA and St RAFT microemulsion polymerizations, respectively. The characteristic diffusion time of the CTA to the locus of polymerization, approximated by $\tau_{res,CTA} \times (\frac{N_{mic}}{N_{part}})_{avg}$,[15] is ~$10^{-1}$ s. Consequently, the rate of CTA activation is likely diffusion-limited and the diffusion-limited k_{tr} value would be less than the reaction-limited k_{tr} value by up to a factor of 10^{-2} and 10^{-3} for BA and St RAFT microemulsion polymerizations, respectively. The reaction-limited k_{tr} value has a theoretical upper limit of k_{add}; hence, the diffusion-limited k_{tr} value can be as low as 0.02 $\times 10^4$ M^{-1} s^{-1} for BA and 0.0086 $\times 10^4$ M^{-1} s^{-1} for St.

The experimental rate data of BA and St RAFT microemulsion polymerization with B11C is fitted with the RAFT microemulsion polymerization model within the above mentioned k_f and k_{tr} ranges to obtain the best fit, as shown in **Figure 6.3.1**.

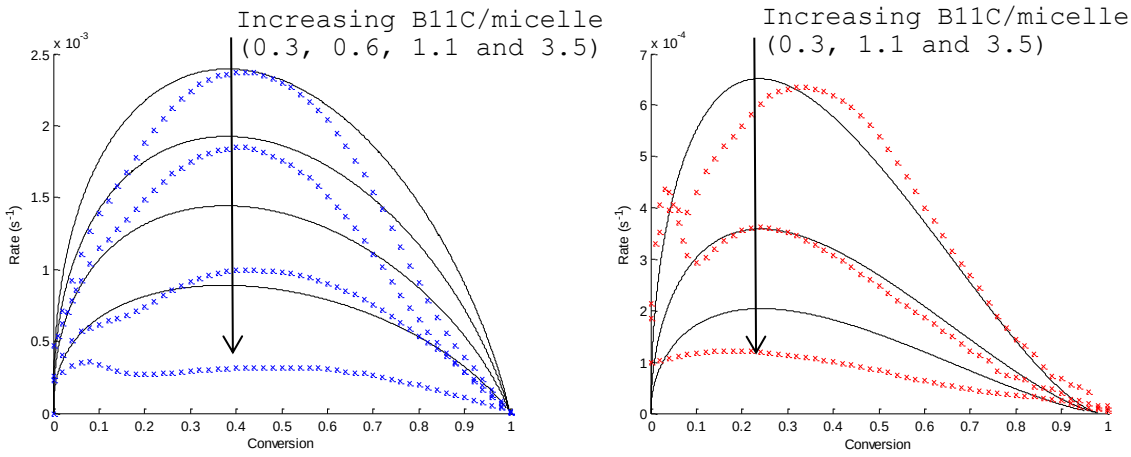

Figure 6.3.1: Comparison of (-) model predicted rate of polymerization and (x) experimental rate of polymerization; (left) for BA with B11C ($k_f = 10^{0.41}$, $k_{tr} = 0.8 \times 10^4$, $k_{add} = 2 \times 10^4$, b = 0.8), (right) for St with B11C ($k_f = 10^0$, $k_{tr} = 0.01 \times 10^4$, $k_{add} = 8.6 \times 10^4$, b = 1.4). Monomer properties are given in Table 6.2.1.

The experimental rate of polymerization for BA with B11C is qualitatively captured by the model when $k_f = 10^{0.41}$, $k_{tr} = 0.8 \times 10^4$ and b = 0.8 (**Figure 6.3.1-left**). As the CTA/micelle ratio increases, the model overestimates the experimental rate. It is known that coalescence increases with increasing CTA/micelle ratio due to longer reaction times (**Section 4.3.3** and **5.3.2.1**). Particle-particle coalescence would lead to an increase in the probability of biradical termination as well as an increase in the number of CTA per particle, and, as a result, both effects would lead to a decrease in the overall experimental conversion rate.

For St RAFT microemulsion polymerization with B11C, the rate of polymerization predicted by the model shows good agreement with the experimental rate of polymerization when $k_f = 10^0$, $k_{tr} = 0.01 \times 10^4$ and b = 1.4 (**Figure 6.3.1-right**). Compared to the BA RAFT microemulsion polymerization with B11C, the model for the St microemulsion polymerization with B11C better captures the data trend, which can be attributed to lower degree of coalescence in the St RAFT microemulsion polymerization.

The RAFT microemulsion polymerization model has shown that slow fragmentation ($k_f \sim 10^3$ for BA with MOEP) is the main source of rate retardation.[1] The fragmentation rate model fit values obtained for both BA and St with B11C ($10^{0.41}$ and 10^0 s^{-1}, respectively) support the slow fragmentation interpretation. Furthermore, the obtained k_f values correspond with computational studies that have shown that the fragmentation efficiencies of a trithiocarbonate CTA with an alkyl Z-group (as in B11C & B11T) is much less than a xanthate CTA with O-ethyl Z-group (as in MOEP).[10] It is also expected that St would have a slower fragmentation rate than BA, since St is more stable due to higher resonance, and poly(St) is a stiffer chain.

Both k_{tr} values for BA and St with B11C (0.8×10^4 M^{-1} s^{-1} and 0.01×10^4 M^{-1} s^{-1}, respectively) are lower than their respective k_{add} values of 2×10^4 and 8.6×10^4, which means B11C activation is diffusion-limited.

6.3.2 Model Fitting RAFT Microemulsion Polymerizations with the Surface-Active CTA B11T

In this section, the kinetic model is solved using the k_f values determined from the model fitting of the RAFT microemulsion polymerization with the traditional chain transfer agent B11C (**Section 6.3.1**). Increasing the k_{tr} value decreases the rate maximum at each value of CTA/micelle ratio and maintains relatively the same location with respect to conversion. Hence, the secondary peaks observed in BA and St RAFT microemulsion polymerization with B11T cannot be attributed to a change in k_{tr}. The experimental rate of polymerization for BA with B11T is best fitted with the same model parameters used for BA with B11C (**Figure 6.3.1-left**), as shown in **Figure 6.3.2-left**. Whereas, the St with B11T data is best fit with a k_{tr} value of 0.03 $\times 10^4$ M^{-1} s^{-1}, as shown in **Figure 6.3.2-right.**

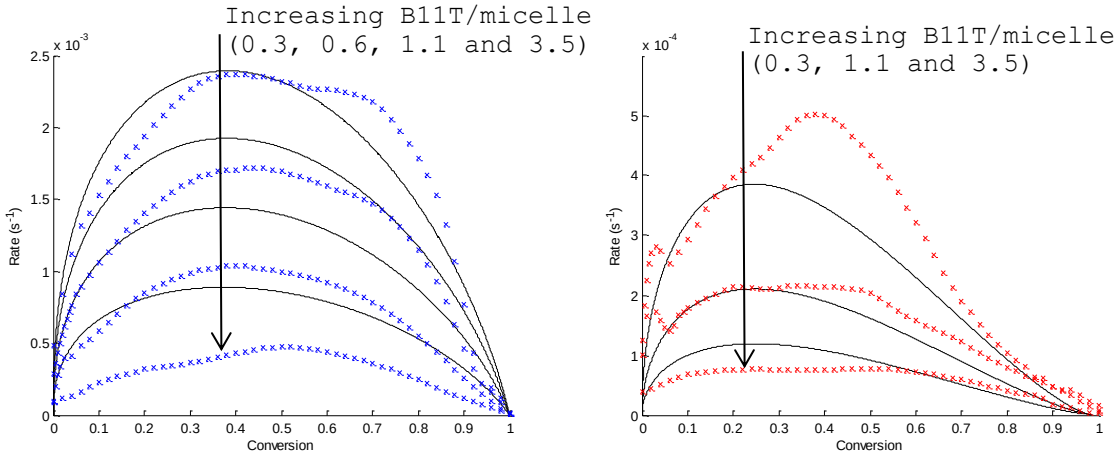

Figure 6.3.2: Comparison of (-) model predicted rate of and (x) experimental rate of polymerization; (left) for BA with B11T ($k_f = 10^{0.41}$, $k_{tr} = 0.8 \times 10^4$, $k_{add} = 2 \times 10^4$, b =

0.8), (right) for St with B11T ($k_f = 10^0$, $k_{tr} = 0.03 \times 10^4$, $k_{add} = 8.6 \times 10^4$, b = 1.4). Monomer properties are given in Table 6.2.1.

Due to the significant increase in the surface area of the polymer particle during the microemulsion polymerization, and the fact that activated CTA cannot exchange between particles and micelles while surfactant can, the concentration of the surface-active CTA on the particle surface is expected to decrease. As a result, the reaction of the active propagating chain with the surface-attached dormant chain (macroRAFT) can become diffusion-limited (i.e. decrease in effective k_{add}) over the course of polymerization. This would allow more time for propagation reactions compared to reactions with the macroRAFT, thus leading to a higher rate if monomer conversion. In order to test such hypothesis, the k_{add} is adjusted in the model beyond a certain conversion (f_c) to decrease with conversion as a power function with constant β:

$$k_{add}^{app} = k_{add} * 10^{-\beta*(f-f_c)} \quad \text{(eq 6.8)}$$

The secondary peak locations are best captured with f_c of 0.55 and β of 0.4 for BA with B11T (**Figure 6.3.3-left**), and f_c of 0.25 and β of 0.6 for St with B11T (**Figure 6.3.3-right**). The St monomer partitions closer to the polymer particle core, hence it is reasonable to see diffusion limitation effects with the surface-active CTA at earlier conversions and higher factor compared to BA with B11T.

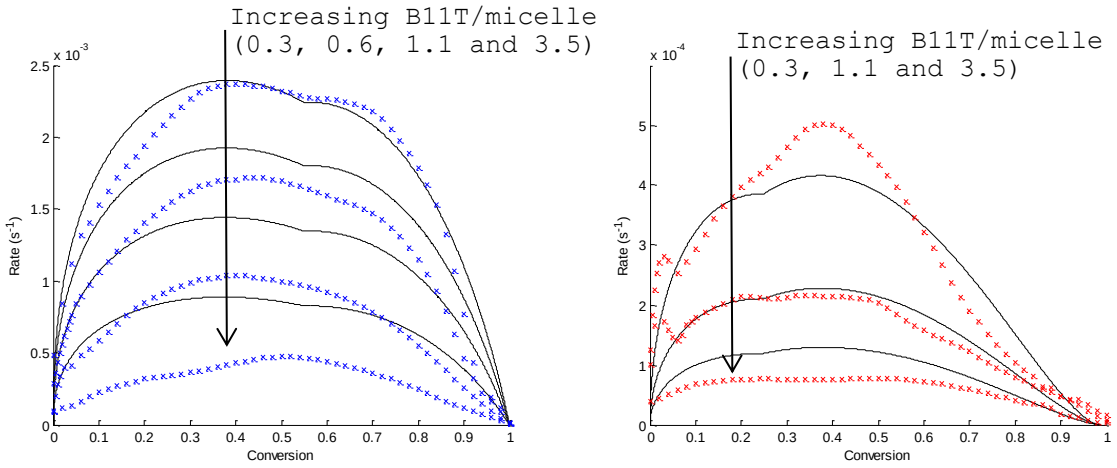

Figure 6.3.3: Comparison of (-) model predicted rate of polymerization including diffusion-limitation (eq. 6.8) and (x) experimental rate of polymerization; (left) for BA with B11T ($f_c = 0.55$, $\beta = 0.4$, $k_f = 10^{0.41}$, $k_{tr} = 0.8 \times 10^4$, $k_{add} = 2 \times 10^4$, $b = 0.8$), (right) for St with B11T ($f_c = 0.25$, $\beta = 0.6$, $k_f = 10^0$, $k_{tr} = 0.03 \times 10^4$, $k_{add} = 8.6 \times 10^4$, $b = 1.4$). Monomer properties are given in Table 6.2.1.

The model fits show that as the CTA/micelle ratio increases the secondary peak becomes less pronounced (**Figure 6.3.3**), which is similarly observed in the experimental rate, with the exception of BA with B11T at CTA/micelle ratio of 3.5. The BA RAFT microemulsion polymerizations with B11T experiences higher coalescence at higher CTA/micelle ratios, which would lead to an increase in the particle size at earlier conversions. Using a lower f_c of 0.25 and same β of 0.4 can capture the trend and location of rate maxima for the CTA/micelle ratio of 3.5, and the ratio of the primary to secondary peaks is similar between the data and the model.

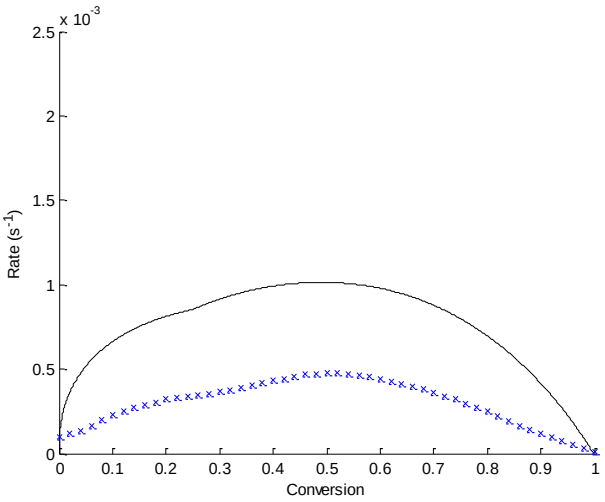

Figure 6.3.4: Comparison of (-) model predicted rate of polymerization including diffusion-limitation (eq. 6.8) and (x) experimental rate of polymerization for BA with B11T at CTA/micelle of 3.5 ($f_d = 0.25$, $\beta = 0.4$, $k_f = 10^{0.41}$, $k_{tr} = 0.8 \times 10^4$, $k_{add} = 2 \times 10^4$, $b = 0.8$). Monomer properties are given in Table 6.2.1. k_{add} rate constant is given in Table 6.3.1.

Even though diffusion limitation modification (eq. 6.8) can account for the observed secondary peaks, a careful measurement of the particle size growth is required to fully verify the hypothesis, wherein the diffusion limitation to the rate constant needs to be correlated with particle growth and other physical parameters. Another proposition for the observed secondary peaks is that particles that are initiated later in the microemulsion polymerization have less available surface-active chain transfer agents, which can be similarly expressed as a lower effective k_{add} at higher conversions.

Solving the rate equation for the consumption of the chain transfer agent (eq. 2.14 in **Section 2.3**), the concentration of the chain transfer agent [XR] can be obtained as a function of conversion. Interestingly, both BA and St with B11T model fits show partial activation of the chain transfer agent (**Figure 6.3.5**), which corresponds with the partial B11T activation inferred from the experimental molecular weight analysis (**Section 4.3.1 and 5.3.2.3**). Moreover, the

predictions show qualitative agreement with the experimental fraction of B11T activation (ε), as the BA RAFT microemulsion polymerizations have a higher ε compared to St RAFT microemulsion polymerizations.

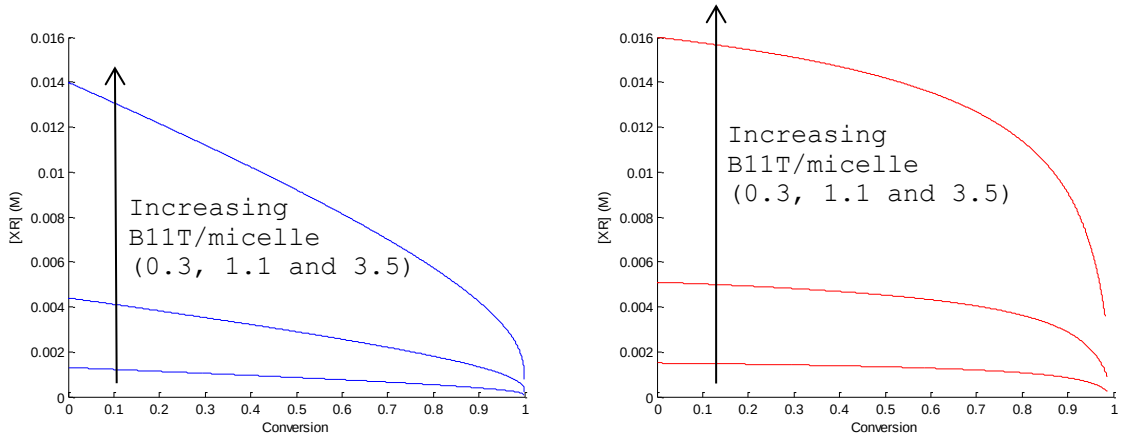

Figure 6.3.5: Predicted B11T chain transfer agent concentration [XR], from model fits in Figure 6.3.3, as a function of conversion of (left) BA and (right) St.

The EA/B11T data (**Figure 6.3.6**) are fitted with the fragmentation rate constant obtained from BA with B11C since the EA RAFT microemulsion polymerizations with B11C were unsuccessful. The model fit for EA with B11T was only able to capture the data trend at the lowest CTA/micelle ratio, and the magnitude of the rate of polymerization is overestimated even at the highest k_{tr} theoretical value ($k_{tr} = k_{add} = 2 \times 10^4$), as shown in **Figure 6.3.6**. Decreasing the k_{tr} value only increases the magnitude of the rate of polymerization while the location of the rate maximum remains at similar conversions.

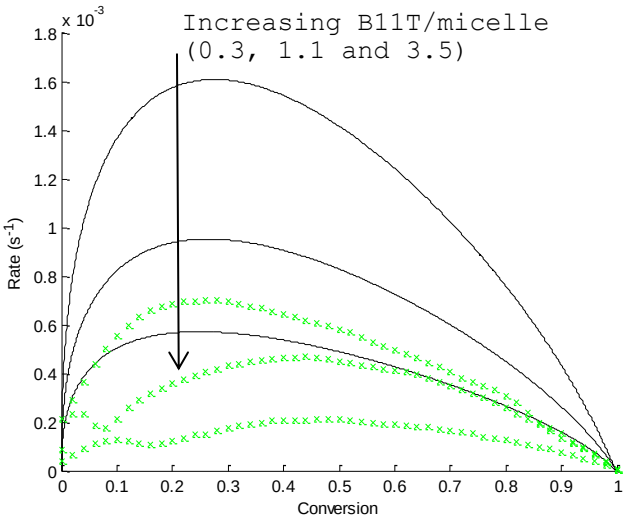

Figure 6.3.6: Comparison of (-) model predicted rate of polymerization and (x) experimental rate of polymerization for EA with B11T ($k_f = 10^{0.41}$, $k_{tr} = 2 \times 10^4$, $k_{add} = 2 \times 10^4$, b = 0.5). Monomer properties are given in Table 6.2.1.

Overestimation of the rate by the model is attributed to the high degree of coalescence seen in the EA RAFT microemulsion polymerization (**Section 5.3.2.1**). As discussed earlier, coalescence has a direct effect on increasing the CTA/particle and rate of biradical termination, which decreases the conversion rate. Coalescence should be incorporated into the RAFT microemulsion model to calculate the respective concentration of polymer particles ([Particles]) and change in termination reactions by introducing a coalescence term into the termination effect equation:

$$\frac{dN^*}{dt} = 2\gamma k_d I_o \left(\frac{1 - p_{term}/p_{prop}}{1 + p_{term}/p_{prop}} \right) - 2\left(k_{tr}^{mono} C_{mon}^{(part)} + k_{tr} C_{XR}^{(part)}\right) N^* x_{act} \left(\frac{p_{term}/p_{prop}}{1 + p_{term}/p_{prop}} \right) + \text{"Coalescence term"} \quad \text{(eq 6.9)}$$

Hence, a quantification of coalescence and model adjustment is needed to fit the data and obtain a correct k_{tr} value.

6.4 Conclusions

The kinetic model for RAFT microemulsion polymerization[1] was used to fit the experimental data from the RAFT microemulsion polymerizations of St, BA and EA. The model captures the decrease in the rate of polymerization with increasing CTA/micelle under slow fragmentation of the macroRAFT radical. Moreover, the model fits for St and BA with the surface-active chain transfer agent B11T shows partial activation of the chain transfer agent, which agrees with the experiments in Chapter 4 and 5. Lastly, the model have shown an overestimation of polymerization rate when coalescence occurs.

6.5 Bibliography

1. O'Donnell, J. M.; Kaler, E. W. *Journal of Polymer Science Part A: Polymer Chemistry* **2010,** 48, (3), 604-613.

2. Morgan, J. D.; Lusvardi, K. M.; Kaler, E. W. *Macromolecules* **1997,** 30, (7), 1897-1905.

3. de Vries, R.; Co, C. C.; Kaler, E. W. *Macromolecules* **2001,** 34, (10), 3233-3244.

4. Co, C. C.; de Vries, R.; Kaler, E. W. *Macromolecules* **2001,** 34, (10), 3224-3232.

5. O'Donnell, J.; Kaler, E. W. *Macromolecules* **2008,** 41, (16), 6094-6099.

6. Fukuda, T.; Ide, N.; Ma, Y. D. *Macromol Symp* **1996,** 111, 305-315.

7. Gilbert, R. G. *Pure and Applied Chemistry* **1996,** 68, (7), 1491-1494.

8. Berger, K. C.; Meyerhoff, G., In *Polymer Handbook*, Third ed.; Brandup, J.; Immergut, E. H., Eds. Wiley Interscience: 1989.

9. Kubo, K.; Goto, A.; Sato, K.; Kwak, Y.; Fukuda, T. *Polymer* **2005,** 46, (23), 9762-9768.

10. Coote, M. L.; Krenske, E. H.; Izgorodina, E. I. *Macromolecular Rapid Communications* **2006,** 27, (7), 473-497.

11. Theis, A.; Feldermann, A.; Charton, N.; Stenzel, M. H.; Davis, T. P.; Barner-Kowollik, C. *Macromolecules* **2005,** 38, (7), 2595-2605.

12. O'Donnell, J.; Kaler, E. W. *Macromolecular Rapid Communications* **2007,** 28, (14), 1445-1454.

13. Barner-Kowollik, C.; Quinn, J. F.; Morsley, D. R.; Davis, T. P. *J. Polym. Sci. Pol. Chem.* **2001,** 39, (9), 1353-1365.

14. Wang, A. R.; Zhu, S. *Journal of Polymer Science Part A: Polymer Chemistry* **2003,** 41, (11), 1553-1566.

15. O'Donnell, J. M. Reversible addition-fragmentation chain transfer in microemulsion polymerizations. Dissertation, University of Delaware, Newark, Delaware, 2007.

CHAPTER 7. CORE/SHELL POLYMER NANOARTICLE SYNTHSIS

7.1 Introduction

The synthesis of well-defined and uniform structures is a key step towards the full utilization of nanoparticles in advanced applications. The core/shell (CS) morphology provides the advantage of producing particles that can be tailored for multiple chemical and physical properties depending on the desired function. Using microemulsion polymerization, CS polymer nanoparticles can be produced using multiple addition or semi-continuous microemulsion polymerization.[1-4] This chapter aims to study the kinetics of semi-continuous microemulsion polymerization (SCMEP) to examine the requirements for core/shell formation, and to implement RAFT in SCMEP with the surface-active chain transfer agent B11T in an attempt to produce well defined CS morphology and low polydispersity.

In addition to the RAFT benefit in controlling the SCMEP, the surface-active CTA has the advantage of forming block copolymer shell. For instance, the added monomer reacts with the pre-activated CTA linked to the first block (macro-RAFT) to form an additional block. Moreover, since the surface-active CTA is constrained to the corona of the particle, this localizes the polymer chain growth at the particle's surface and forces the direction of particle growth outward, which in turn kinetically traps the added monomer to form a shell.

SCMEP is composed of two stage polymerizations; (i) first-stage seed microemulsion polymerization, (ii) and second-stage continuous feed of the second monomer. One of the main challenges in the second-stage polymerization of SCMEP is the formation of new particles (secondary nucleation) instead of shell formation in existing seed particles. The factors effecting secondary nucleation have been studied for semi-continuous emulsion polymerization (seeded

emulsion polymerization).[5] In order to suppress secondary particle formation, the seed particle size should be minimized (higher surface area), the latex solid content should be maximized (higher particle number density), and monomer should be fed under starved conditions. In this respect, microemulsion polymerization has the advantage of producing smaller particles than those made from emulsion polymerization. Xu et al. investigated SCMEP for the purpose of increasing the latex solid content, and have shown that the feed of added monomer must be slower than the rate of consumption of monomer.[6] If the feed of monomer is greater than the rate of consumption of monomer, then the empty micelles swell with monomer and this causes nucleation of new particles. Hence, the feeding rate becomes even more important for the RAFT SCMEP due to rate retardation of the polymerization. Moreover, the RAFT introduces additional complication to the SCMEP due to the partitioning of the chain transfer agent between polymer particles and micelles. Secondary nucleation is expected to activate chain transfer agents that were not consumed in the seed polymerization. As a result, bimodal distributions of polymer molecular weight and particle size are expected in the case of secondary nucleation.

In this chapter, the formation of core/shell polymer nanoparticles using uncontrolled and RAFT SCMEP is investigated for styrene (St) and butyl acrylate (BA) monomers. In the uncontrolled SCMEP, the effect of the polymerization sequence (i.e. St/BA vs BA/St) on the polymerization kinetics and core/shell structure is studied. The polymerization rate is found to be dependent on the polymerization sequence, whereas the final core/shell structure is independent of the polymerization sequence. For the RAFT SCMEP, the effect of the BA feed duration (t_{feed}) is investigated for the St/BA RAFT SCMEP. Two BA monomer feed duration were studied. The first feeding duration results in secondary nucleation, while the longer feeding duration indicates starved feed conditions with no secondary nucleation.

7.2 Materials and Methods

The seed polymerizations were carried out in microemulsion stabilized by DTAB surfactant. An α_{St}=4.0% for St seed polymerization, α_{BA}=5.0% for BA seed polymerization, and γ=12.0% were used, where $\alpha = mass_{monomer}/(mass_{monomer} + mass_{water}) \times 100$ and $\gamma = mass_{surfactant}/(mass_{surfactant} + mass_{monomer} + mass_{water}) \times 100$. A CTA per micelle ratio of 3.5 was used for the RAFT experiments. The polymerizations were performed at 45°C and were started by adding 1ml of purged water containing VA044 initiator for a VA044 concentration of 2 wt% with respect to monomer. Reaction calorimetry was used to measure the monomer conversion. When the heat evolved from the seed polymerization reached baseline (~1hr for uncontrolled, and ~8hrs for RAFT), purged and heated BA or St is semi-continuously fed using a syringe pump over a specified duration and until a St:BA ratio of 50:50 is reached. When samples are taken during the semi-continuous feed, the feeding rate is decreased by the percentage of mass decrease of the reaction mixture. After the polymerization reaction ended, the heat capacity of the latex was measured. The monomer conversion as a function of time was calculated with standard RC1e software, and the final conversion was confirmed gravimetrically.

7.3 Results and Discussion

7.3.1 Uncontrolled Semi-continuous Microemulsion Polymerization

In semi-continuous microemulsion polymerization (SCMEP), the monomer conversion rate (df/dt) is calculated as the ratio of the rate of monomer consumption to the total number of monomer moles added (n_T):

$$\frac{df}{dt} = \frac{Rate\ of\ Polymerizaton}{n_T} \qquad \text{(eq 6.1)}$$

The total number of monomer moles added is calculated as:

$$n_T = \dot{n}_{in} t_{feed} \qquad \text{(eq 6.2)}$$

where $\dot{n}_{in}$ is the monomer molar feed rate into the microemulsion, and t_{feed} is the monomer feed duration. At steady state (S.S.), the rate of polymerization is equal to the feed rate, hence:

$$\left(\frac{\mathrm{df}}{\mathrm{dt}}\right)_{S.S.} = \frac{\dot{n}_{in}}{\dot{n}_{in} t_{feed}} = 1/t_{feed} \qquad \text{(eq 6.3)}$$

Equation 6.3 is simple and useful in assessing steady state in semi-continuous microemulsion polymerization, since its value is irrespective of the monomer type and polymerization rate.

Figure 7.3.1 shows the effect of second monomer feed duration (t_{feed}) on the rate of polymerization in BA/St and St/BA uncontrolled semi-continuous microemulsion polymerization. All of the polymerizations reach the predicted S.S. monomer conversion rate, which is inversely proportional to t_{feed}.

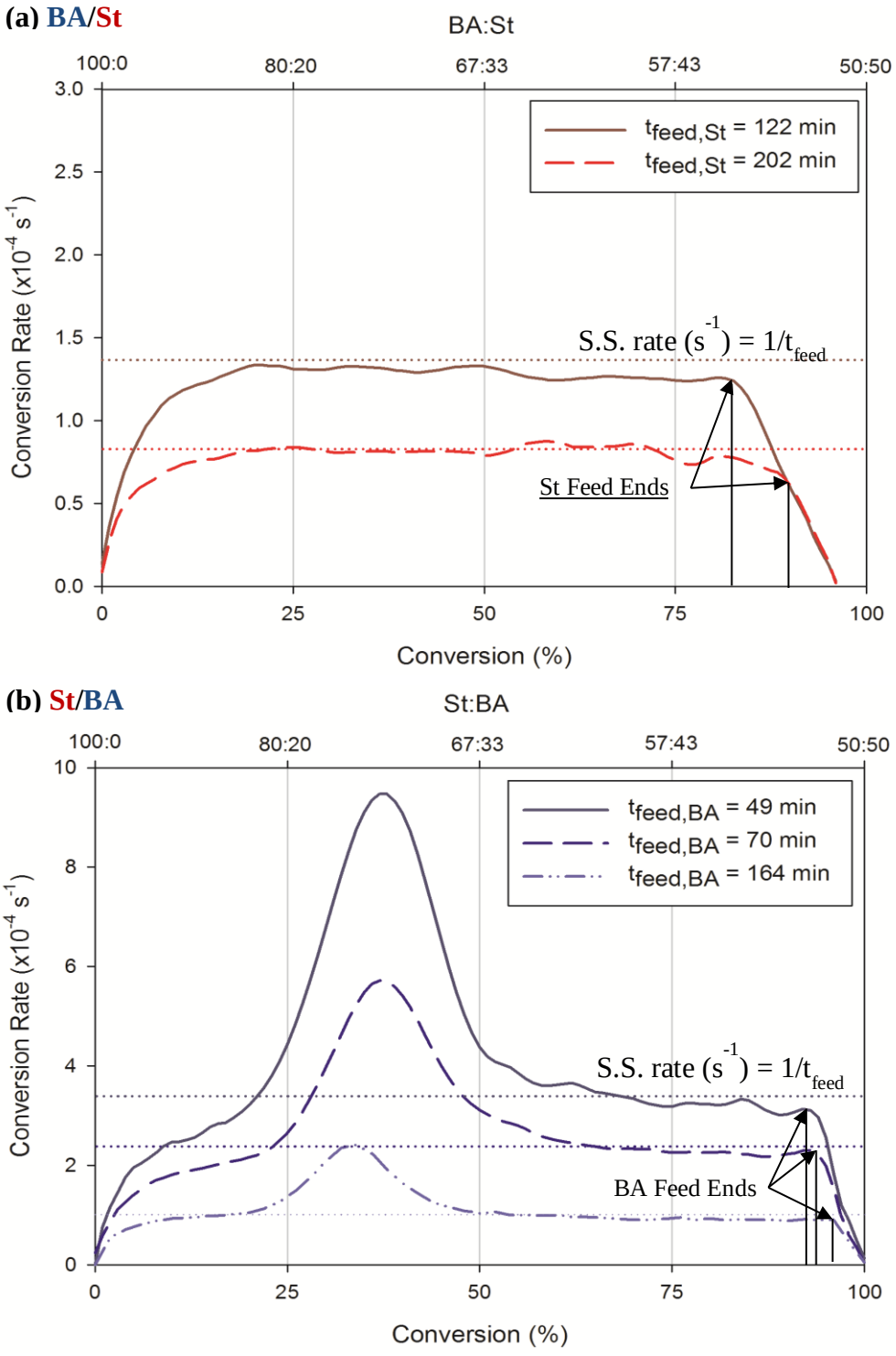

Figure 7.3.1: Conversion rate during second monomer feed in (a) St/BA and (b) BA/St RAFT semi-continuous microemulsion polymerization. The horizontal dotted lines indicate steady state (S.S.) rate prediction from eq 6.3. The vertical lines indicate when the second monomer feed ends.

The rate of St polymerization in BA/St SCMEP (**Figure 7.3.1-a**) increases upon St feed until reaching steady state at around 20% conversion and matches the predicted conversion rate prediction from eq 6.3. At steady state the monomer consumption rate is equal to the monomer feed rate. When the St feed ends, the conversion rate decreases to zero and the polymerization reaches a maximum of 96% St conversion.

The rate of BA polymerization in St/BA SCMEP (**Figure 7.3.1-b**) also increases upon BA feed. However, as the rate reaches steady state it further increases to reach a rate maximum between 33% and 37% conversion. The rate then decreases to reach steady state until the BA monomer feed is stopped, and the rate rapidly decreases to zero.

As expected, all of the conversion rates reach the predicted steady state value, which confirms that the monomer does not continue to accumulate. However, it was not expected to see a rate peak at intermediate conversions in St/BA SCMEP. The increase in the rate of polymerization is likely caused by an increase in the monomer concentration at the locus of polymerization. As the BA monomer is fed, the BA is solubilized into the poly(St) particles, hence the poly(BA) propagation will be limited by the solubility and diffusivity of BA in the poly(St) particle core. Once a critical volume fraction is reached, the poly(BA) chains are likely to separate from the poly(St) core and forms a shell since it thermodynamically favors partitioning to the shell of a of St/BA polymer nanoparticle.[7] Formation of a poly(BA) shell phase would increase the monomer concentration at the locus of polymerization due to its close proximity to the particle-water interface. Hence, the BA polymerization rate is expected to increase upon phase separation. As the polymerization proceeds the rate would decrease because the monomer consumption rate is higher than the monomer feed rate. The fact that the observed

rate peak occurs at relatively the same conversion range for the different $t_{feed,BA}$ experiments, would support the phase separation hypothesis.

The core/shell latex was imaged by TEM (**Figure 7.3.2**). Due to positive staining with ruthenium tetroxide, the poly(St) region becomes electron dense and shows as a dark region in the micrograph. Poly(BA), on the other hand, is not effected by the ruthenium oxide staining and remains bright. This allows for the visual contrast between poly(BA) and poly(St). The TEM micrographs verify core/shell formation with poly(St) in the core and poly(BA) in the shell for both St/BA and BA/St SCMEP. This is consistent with the results obtained by Huo et al. for BA/St semi-continuous emulsion polymerization.[7] Huo et al. have shown that the poly(St)-core/poly(BA)-shell structure is the thermodynamic equilibrium morphology based on minimizing the interfacial surface tension between Poly(St), Poly(BA), and Water.

The TEM images also shows the presence of individual poly(St) and poly(BA) in both polymerization sequences. The apparent polymer nanoparticle size seen in the micrographs is in on the same order of the DLS measured diameter of 47 and 33 nm for BA/St and St/BA SCMEP, respectively.

(a) BA/St

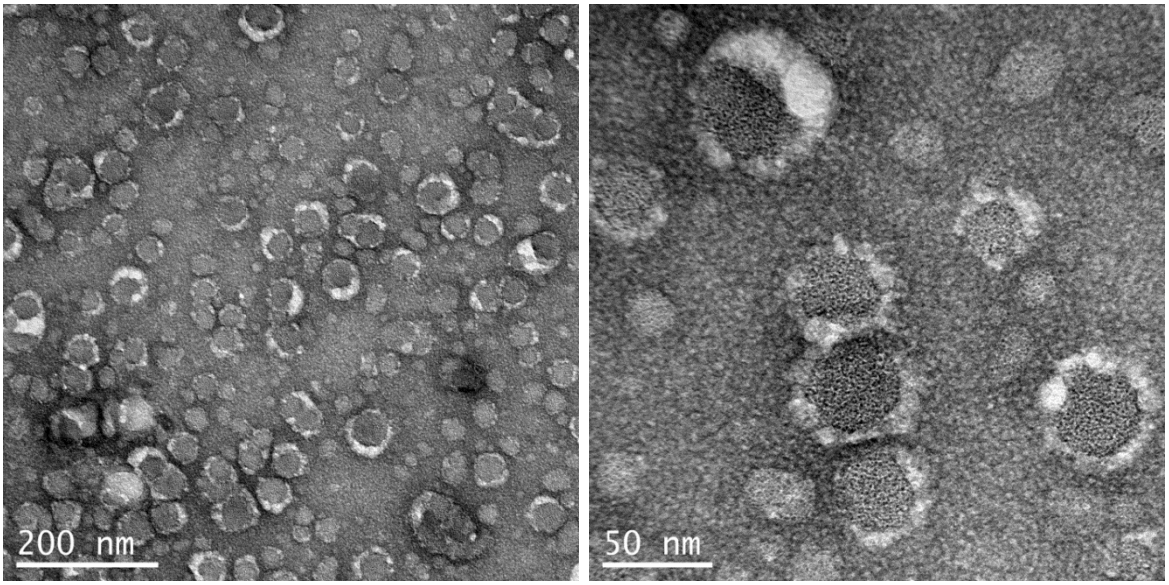

(b) St/BA

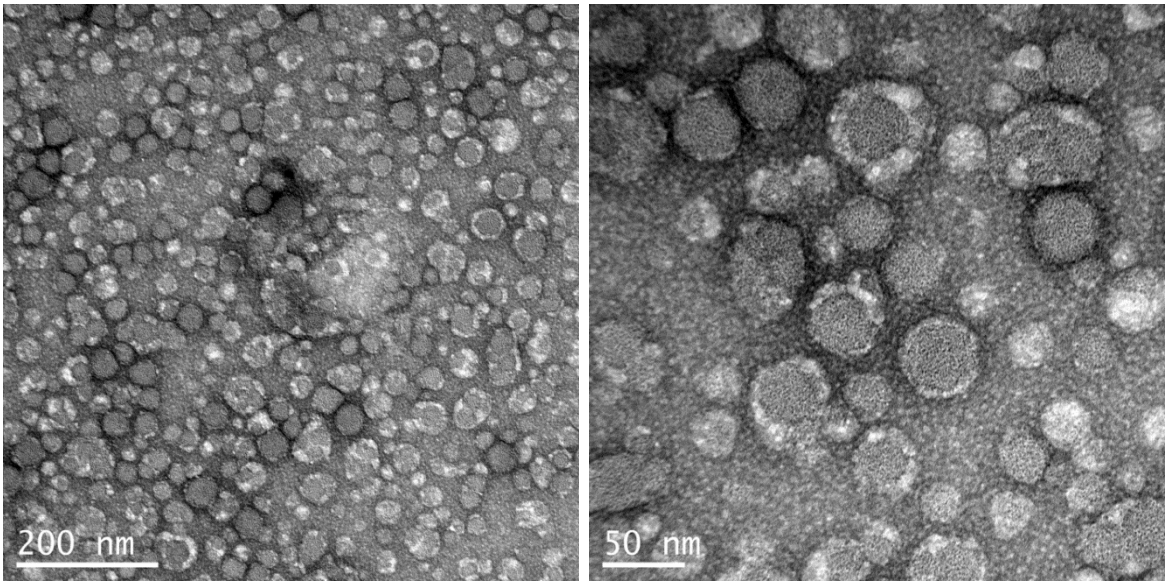

Figure 7.3.2: Transmission electric microscopy (TEM) images of the polymer nanoparticle formed from the (a) BA/St and (b) St/BA uncontrolled semi-continuous microemulsion polymerization. St feed duration is 202min and BA feed duration is 164 min. Negative staining with uranyl acetate, and positive staining with ruthenium tetroxide Dark regions are Poly(St); lighter regions are Poly(BA).

7.3.2 St/BA RAFT Semi-continuous Microemulsion Polymerization

In this section, the St/BA RAFT SCMEP with surface-active chain transfer agent B11T is performed at two BA feed durations ($t_{feed,BA}$) of 164 and 320 minutes. **Figure 7.3.3** shows that at the lower $t_{feed,BA}$ of 164 minutes the conversion rate of BA steadily increases until the feed stops. On the other hand, for the higher $t_{feed,BA}$ of 320 minutes, the conversion rate of BA steadies after ~35% conversion. After the feed stops, both polymerizations show a steady decrease in the conversion rate. A continuous increase in the conversion rate indicates higher monomer concentration at the locus of polymerization and/or higher number of active propagating radicals. Reaching a steady state in the conversion rate indicates a match between the monomer feeding rate and consumption rate. After the feed stops, the conversion rate decreases because the concentration of monomer at the locus of polymerization decreases.

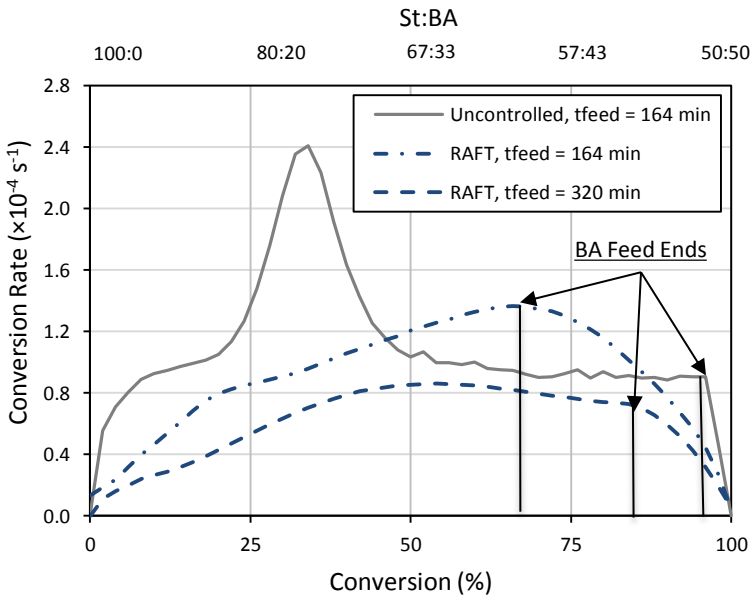

Figure 7.3.3: Conversion rate during second-stage uncontrolled SCMEP and RAFT SCMEP with surface-active CTA B11T. The rate of BA conversion is measured for BA feeding durations of 164 and 320 minutes.

The rate of increase in the polymerization rate during BA feed in RAFT is slower than the uncontrolled, which is expected due to the chain transfer agent rate retardation effect. Both of the RAFT semi-continuous microemulsion polymerizations do not show rapid increase in the conversion rate as seen in the uncontrolled polymerization.

Samples were taken before, during, and after the BA feeding, and were analyzed using size exclusion chromatography (**Figure 7.3.4)**. At the lower $t_{feed,BA}$ of 164 minutes (**Figure 7.3.4-a**) the molecular weight distribution shows a shift in the initial poly(St) seed peak to higher molecular weight (i.e. shift to lower elution time) accompanied by emerging peak at lower molecular weight (elution times 21-23min). This indicates that the added BA partitions between forming a block copolymer with the poly(St) and creating separate chains. The SEC data alone cannot verify whether the separate poly(BA) chains are formed in the existing poly(St) seed particles or as new particles. On the other hand, the experiment with the longer $t_{feed,BA}$ of 320 min (**Figure 7.3.4-b**), shows only a progression of a the initial St seed peak from lower to higher molecular weight as the BA conversion increases, which indicates that the added BA only forms shell block copolymer with the existing poly(St) seed.

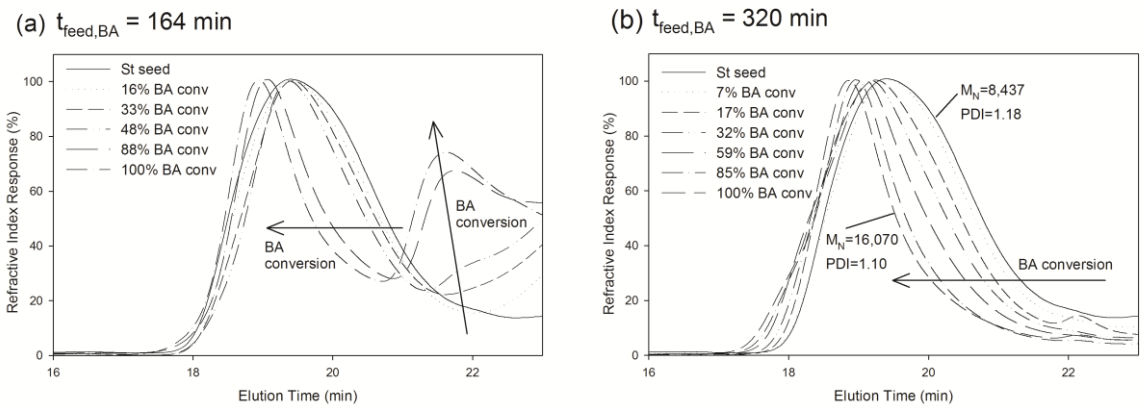

Figure 7.3.4: The change in polymer molecular weight distribution, obtained using SEC, during the second-stage polymerization of BA in the St/BA RAFT semi-continuous microemulsion polymerizations with surface-active CTA B11T. The number-average molecular weight (M_N), in g/mol, and molecular weight polydispersity (PDI) are displayed for the St seed polymer nanoparticle and the final core/shell in (b).

The analysis of number-average molecular weight (M_N) for the longer BA feeding duration of 320 min shows a linear increase over BA conversion (**Figure 7.3.5**), which indicates that RAFT control/"livingness" is maintained.

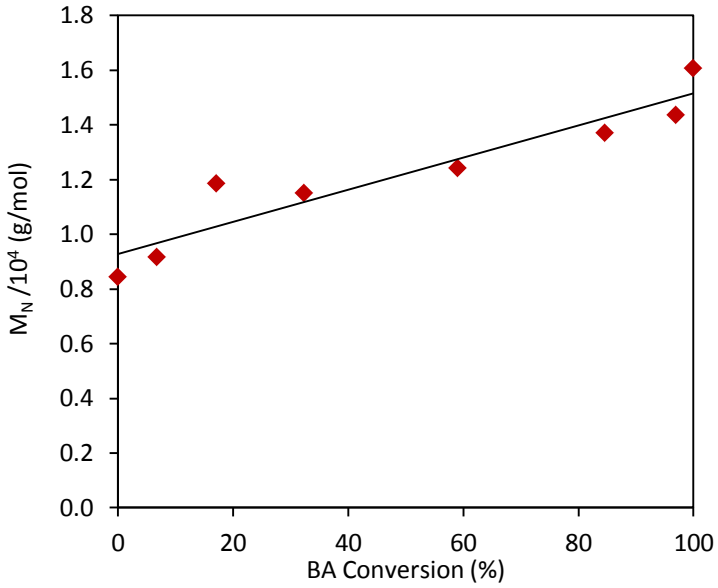

Figure 7.3.5: Number-average molecular weight (M_N) of poly(St-b-BA) vs. BA conversion for the second-stage RAFT SCMEP with B11T at $t_{feed,BA}$ =320 minutes. The dn/dc numbers used to calculate M_N are estimated from the weight average of poly(BA) and poly(St) dn/dc numbers. The lines are least-squares linear fits to the data.

The final M_N (16,070 kg/mol) is in close match to the predicted M_N of 15,300 kg/mol. Such evidences directly indicates that the BA monomer grows as a block copolymer within the St seed particles when the BA monomer is fed under starved conditions ($t_{feed,BA}$ of 320min). The TEM micrographs verify the formation of polymer nanoparticles and provide meaningful analysis of the final polymer particles composition and size (**Figure 7.3.6**).

(a) $t_{feed.BA}$= 164 min

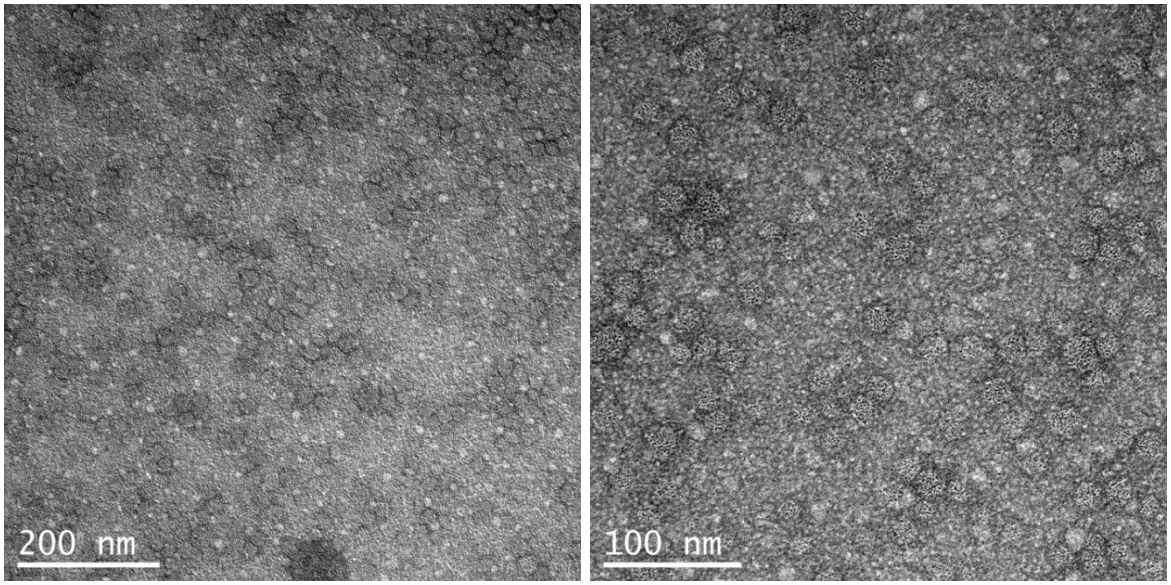

(b) $t_{feed.BA}$= 320 min

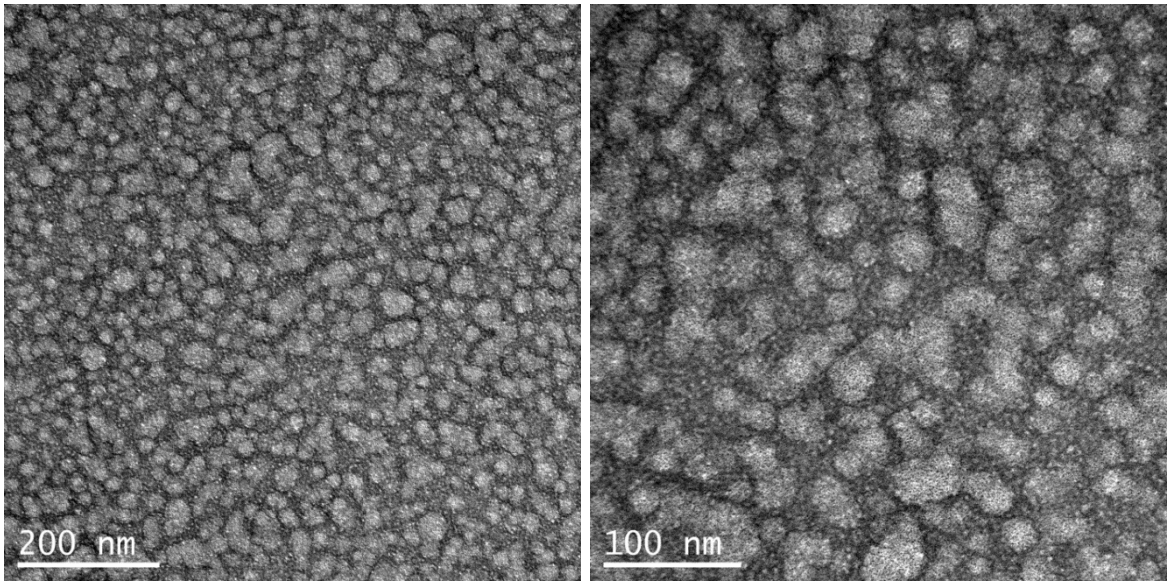

Figure 7.3.6: Representative transmission electric microscopy (TEM) images of the polymer nanoparticle formed from the St/BA RAFT semi-continuous microemulsion polymerizations with surface-active CTA B11T. BA feed duration is (a) 164 min, and (b) 320 min. Dark regions are Poly(St); lighter regions are Poly(BA).

The micrographs for the shorter BA feeding time (**Figure 7.3.6-a)** clearly verifies the formation of secondary poly(BA) particles (bright particles). The poly(BA) particles are much

smaller in size compared to the poly(St) particles. On the other hand, the polymerization with the longer BA feeding time shows consistent particles (**Figure 7.3.6-b**). The contrast of such particles is transient between bright and dark, hence it is difficult to distinguish between core and shell regions in the particle. At this length scale and limited TEM resolving power, it would be challenging to establish good staining contrast between the core and shell. Even though the micrographs shows some non-spherical particles, this may not be true representative of the solution sample as the poly(BA) is above its glass transition temperature at room temperature which would result in a film formation capability when dried.[8]

7.4 Conclusion

The polymerization rate in the BA/St and St/BA uncontrolled semi-continuous microemulsion polymerization (SCMEP) is dependent on the polymerization sequence. The poly(St) partitions to the core, while the poly(BA) partitions to the shell in the final core/shell morphology, irrespective of the polymerization sequence.

Semi-continuous RAFT microemulsion polymerization with surface-active chain transfer agent is successful in producing core/shell polymer nanoparticles. However, careful selection of the monomer feed is required to achieve starved feed conditions. Calorimetry is demonstrated as a viable tool to assess the reaction rate that satisfies starved monomer conditions. The RAFT SCMEP with the surface-active CTA is a facile approach to produce uniform sized polymer nanoparticles with very low molecular weight PDI and may be used for synthesizing a variety of core-shell or multi-layered polymer nanoparticles.

7.5 Bibliography

1. Perez-Carrillo, L. A.; Puca, M.; Rabelero, M.; Meza, K. E.; Puig, J. E.; Mendizabal, E.; Lopez-Serrano, F.; Lopez, R. G. *Polymer* **2007,** 48, (5), 1212-1218.

2. Aguiar, A.; Gonzalez-Villegas, S.; Rabelero, M.; Mendizabal, E.; Puig, J. E.; Dominguez, J. M.; Katime, I. *Macromolecules* **1999,** 32, (20), 6767-6771.

3. Rabelero, M.; Lopez-Cuenca, S.; Puca, M.; Mendizabal, E.; Esquena, J.; Solans, C.; Lopez, R. G.; Puig, J. E. *Polymer* **2005,** 46, (16), 6182-6191.

4. Okubo, M. In *Control of Particle Morphology in Emulsion Polymerization*, 2nd International Symp on Copolymerization and Copolymers in Dispersed Media, Lyon, France, Apr 03-07, 1989; Lyon, France, 1989; pp 307-325.

5. Ferguson, C. J.; Russell, G. T.; Gilbert, R. G. *Polymer* **2002,** 43, (17), 4557-4570.

6. Xu, X. J.; Chew, C. H.; Siow, K. S.; Wong, M. K.; Gan, L. M. *Langmuir* **1999,** 15, (23), 8067-8071.

7. Huo, D.; Liu, D. *Polymer International* **2002,** 51, (7), 585-593.

8. Ferguson, C. J.; Russell, G. T.; Gilbert, R. G. *Polymer* **2002,** 43, (24), 6371-6382.

CHAPTER 8. FUTURE WORK

8.1 High polydispersity in BA RAFT microemulsion polymerization

As shown in Chapter 4 and 5, the CTA diffusion from micelles to the locus of polymerization is minimized by using a surface-active CTA. As a result, the poly(St) and poly(EA) have shown improved polydispersities as low as 1.1, whereas the polydispersity of poly(BA) remained around 1.4. The reasons behind the higher PDI in poly(BA) needs to be further examined. There are two hypothesis proposed in this section. Coalescence during the BA RAFT microemulsion polymerization could be a leading to the increased poly(BA) polydispersity. Testing this hypothesis can be approached by studying a monomer of similar aqueous solubility to BA but with much lower polarity.

Another hypothesis is that BA polymerization in microemulsion undergoes branching which increases the molecular weight polydispersity. The free-radical polymerization of BA is found to experience branching due to chain transfer to polymer, as seen in bulk polymerization[1], and emulsion polymerization[2]. In this research, low poly(BA) PDI (~1.1) have been obtained in the RAFT solution polymerization with the traditional CTA B11C. However, the RAFT microemulsion polymerization is closer to a bulk polymerization than a solution polymerization due to the higher monomer concentration at the locus of polymerization. This hypothesis can be tested by performing a RAFT bulk polymerization of BA with the traditional CTA.

Minimizing the concentration of BA in the polymer particles is expected to minimize the effects of both coalescence and branching. Hence, a modified synthesis approach is proposed to achieve lower polydispersities. The approach involves starting with a microemulsion

polymerization with a lower concentration of BA, and then followed by starved BA feed to achieve desired particle size and solid content.

8.2 Core/shell synthesis

The core/shell synthesis using uncontrolled semi-continuous RAFT microemulsion polymerizations (SCMEP) have shown that the polymerization kinetics of St/BA and BA/St depends on the polymerization sequence. An increase in the rate of polymerization is observed in St/BA uncontrolled SCMEP during the BA continuous feed after 22% BA conversion. The change in locus of polymerization from core to shell has been postulated as a potential reason for the observed increase in polymerization rate. This requires further investigation using in-situ small-angle neutron scattering to identify the concentration of the monomer at the locus of polymerization as well as morphology changes during polymerization.

The RAFT SCMEP presented in Chapter 6 laid out the groundwork for the synthesis of well-defined core/shell polymer nanoparticles. Further investigation of different monomer types and combinations is suggested to fully understand the synthesis requirements and limitations. The starved monomer feed rate requirement depends on the monomer's partitioning into seed polymer particles and its reactivity with the chain transfer agent. A fundamental study of the reaction kinetics during the SCMEP is hence recommended.

8.3 Bibliography

1. Dube, M. A.; Rilling, K.; Penlidis, A. *J. Appl. Polym. Sci.* **1991,** 43, (11), 2137-2145.

2. Ahmad, N. M.; Heatley, F.; Britton, D.; Lovell, P. A. *Macromol Symp* **1999,** 143, (1), 231-241.

APPENDIX A. CALCULATION OF CTA/MICELLE RATIO

This calculation procedure is adopted from O'Donnell's work. [1]

Assumption:

All monomer and surfactant form monodisperse micelles at the initial microemulsion.

Calculations:

Total micelle volume (V_T): $V_T = n_{surfactant} N_A V_{tail} + \frac{m_{monomer}}{\rho_{monomer}}$

Total micelle area (A_T): $A_T = n_{surfactant} N_A A_{head}$

Surface Area of a single micelle (A): $A = 4\pi r^2 = 4\pi \left(\frac{3V_T}{A_T}\right)^2$

Aggregation number (N_{agg}): $N_{agg} = \frac{\mathrm{A}}{A_{head}}$

Micelle number ($N_{micelle}$): $N_{micelle} = \frac{n_{surfactant} N_A}{N_{agg}}$

$$CTA/micelle = \frac{\mathrm{n}_{CTA} N_A}{N_{micelle}}$$

Definitions:

$n_{surfactant}$: The total moles of surfactant in the microemulsion

N_A: Avogadro's number

V_{tail}: The volume of a single surfactant tail ($V_{tail,DTAB}$ = 0.3502 nm^3)[2]

A_{head}: The surface area of the head group ($A_{head,DTAB}$=0.68 nm^2)[2]

$m_{monomer}$: The total mass of the monomer

$\rho_{monomer}$: The density of the monomer

n_{CTA}: The number of moles of the chain transfer agent

BIBLIOGRAPHY

1. O'Donnell, J. M. Reversible addition-fragmentation chain transfer in microemulsion polymerizations. Dissertation, University of Delaware, Newark, Delaware, 2007.

2. Os, N. M.; Haak, J. R.; Rupert, L. A. M., *Physico-chemical properties of selected anionic, cationic, and nonionic surfactants*. Elsevier: 1993.

APPENDIX B. CALCULATION OF RATIO OF PARTICLES TO MICELLES

Calculations:

Volume-average nanoparticle diameter from DLS: d_{part}

Single Particle Volume: $V_{part} = \frac{4\pi}{3}(\frac{d_{part}}{2})^3$

Total Particle Volume: $V_{Tpart} = \frac{m_{monomer}}{\rho_{monomer}}$

Number of Particles: $N_{part} = \frac{V_{Tpart}}{V_{part}}$

Ratio of particles to micelles: $\frac{N_{part}}{N_{micelle}}$

Definitions:

$m_{monomer}$: The total mass of the monomer

$\rho_{monomer}$: The density of the monomer

$N_{micelles}$: The micelle number calculated from Appendix A.